THE INFLUENCE OF LIMESTONE CALCINATION ON THE UTILIZATION OF THE SULFUR-SORBENT IN ATMOSPHERIC PRESSURE FLUID-BED COMBUSTORS

EPRI FP-426
(Research Project 720-1)

Final Report

August 1977

Prepared by

WESTINGHOUSE ELECTRIC CORPORATION
Research & Development Center
Beulah Road
Pittsburgh, Pennsylvania 15235

PRINCIPAL INVESTIGATORS
N. H. Ulerich
E. P. O'Neill
D. L. Keairns

Prepared for

Electric Power Research Institute
3412 Hillview Avenue
Palo Alto, California 94304

EPRI Project Managers
Dr. M. Maaghoul
T. E. Lund

LEGAL NOTICE

This report was prepared by Westinghouse Electric Corporation (Westinghouse), as an account of work sponsored by the Electric Power Research Institute, Inc. (EPRI). Neither EPRI, members of EPRI, Westinghouse, nor any person acting on behalf of either: (a) makes any warranty or representation, express or implied, with respect to the accuracy, completeness, or usefulness of the information contained in this report, or that the use of any information, apparatus, method, or process disclosed in this report may not infringe privately owned rights; or (b) assumes any liabilities with respect to the use of, or for damages resulting from the use of, any information, apparatus, method, or process disclosed in this report.

ABSTRACT

Fluidized bed combustion for electric power generation is a direct combustion process for coal with the potential for improved thermal conversion efficiency, reduced costs, and acceptable environmental impact. Using limestone to capture the sulfur in the combustion bed, current EPA new source performance standards (NSPS) for SO_x emissions can be met, but the process as currently practiced requires a >3/1 mole ratio of calcium to sulfur, instead of the theoretical limiting value of 0.9/1. In this study, a method for improving the limestone capacity using a controlled calcination technique was investigated. It was demonstrated, in laboratory scale studies, that retarded calcination of the sorbent in carbon dioxide rich atmospheres creates a superior pore-volume distribution in sorbents, so that their capacity for reacting with sulfur dioxide is effectively doubled. With this technique, sulfur penetrates further into lime particles and further into the individual grains of the lime particles. Projected limestone savings and reduction in the quantities of spent sorbent for disposal could be $>2 \times 10^5$ tons per annum for a 600 MW plant. An outline is given of application of the technique to an atmospheric pressure fluidized bed combustor. It is recommended that the technique be tested in a continuous pilot plant, of sufficient scale to develop detailed cost information.

ACKNOWLEDGMENTS

Apart from the many people who assisted in the work described here, the following made major contributions:

Mr. W. F. Kittle
Mr. R. E. Brinza
Mrs. Catherine Hill
Mr. Wayne Beck
Mr. Art Fellers
Mr. George Blann
Mr. R. W. Palmquist
Mr. R. M. Garretson

Our colleagues, Dr. Walter Vaux and Mrs. C. C. Sun provided invaluable advice.

The authors wish to acknowledge the assistance provided by the late Dr. M. Maaghoul of EPRI. They are also greatly appreciative of the manner in which Mr. T. Lund assumed responsibility for the project and encouraged its completion.

TABLE OF CONTENTS

LIST OF ILLUSTRATIONS

LIST OF ILLUSTRATIONS (Continued)

LIST OF ILLUSTRATIONS (Continued)

LIST OF ILLUSTRATIONS (Continued)

LIST OF ILLUSTRATIONS (Continued)

LIST OF TABLES

Section 1

INTRODUCTION AND SUMMARY OF RESULTS

1.1 INTRODUCTION

The objective of this program was to develop techniques for reducing the quantities of limestone required to lower the sulfur dioxide emissions from atmospheric pressure fluidized bed combustors (afbc). At present, fluidized bed combustors which operate at atmospheric pressure require at least a 3/1 calcium to sulfur mole ratio in the feedstock to lower the sulfur emissions from combustion of a high sulfur coal by 90%. The theoretical limit of 0.9/1 Ca/S mole ratio would result in a three-fold lowering of limestone consumption and a reduction by a factor of 2 in the weight of spent sulfated sorbent produced.

Previous research has indicated that the rate at which lime sulfates depends on the calcination conditions under which the lime is produced. The primary objective of the current research program was to determine the optimum conditions for calcining limestone which result in rapid sulfation even when the stone sorbent is already highly sulfated (greater than 30% sulfated). The results are to be used to specify operational techniques for calcining limestone in an atmospheric pressure fluidized bed combustor so that afbc sulfur dioxide emission can be controlled at acceptable Ca/S molar ratios. Specific program objectives were:

- Provide information on the kinetics of limestone utilization in afbc
- Determine the mechanism of SO_2 absorption by limestone in fluidized-bed combustion
- Develop means of improving limestone utilization

1.2 SUMMARY OF EXPERIMENTAL RESULTS

1.2.1 Basic Thesis of the Project

In an atmospheric pressure fluidized bed coal combustor, limestone in the bed calcines to form calcium oxide (lime), a porous material which then reacts with sulfur dioxide and air to form calcium sulfate. The sulfur dioxide liberated

during coal combustion must be trapped as the gas passes through the fluidized particles of sorbent. To maintain a high efficiency of sulfur capture, the reaction rate between sulfur dioxide and the lime must remain fast. As sulfur builds up in the sorbent, the reaction rate decreases so that sulfur capture becomes less efficient. To maintain a satisfactory level of sulfur capture, fresh limestone must be added to the bed. The rate at which fresh limestone must be added depends on how much sulfur is captured by the sorbent, before its reactivity declines. This decrease in reactivity depends on how porous the sorbent is, and on the type of pores present in the sorbent. The dependence of rate on the type of pores is conceptually illustrated in Figure 1-1. Sorbent A has wide-mouthed pores, so that formation of calcium sulfate near the pore mouth does not block access by the sulfur gas to the inner core of the sorbent. Sorbent B has more pores and more pore volume than sorbent A, but these pores have narrow mouths. To gain access to the inner core of sorbent, the gases must diffuse through the layer of product calcium sulfate which is blocking the pore entrances.

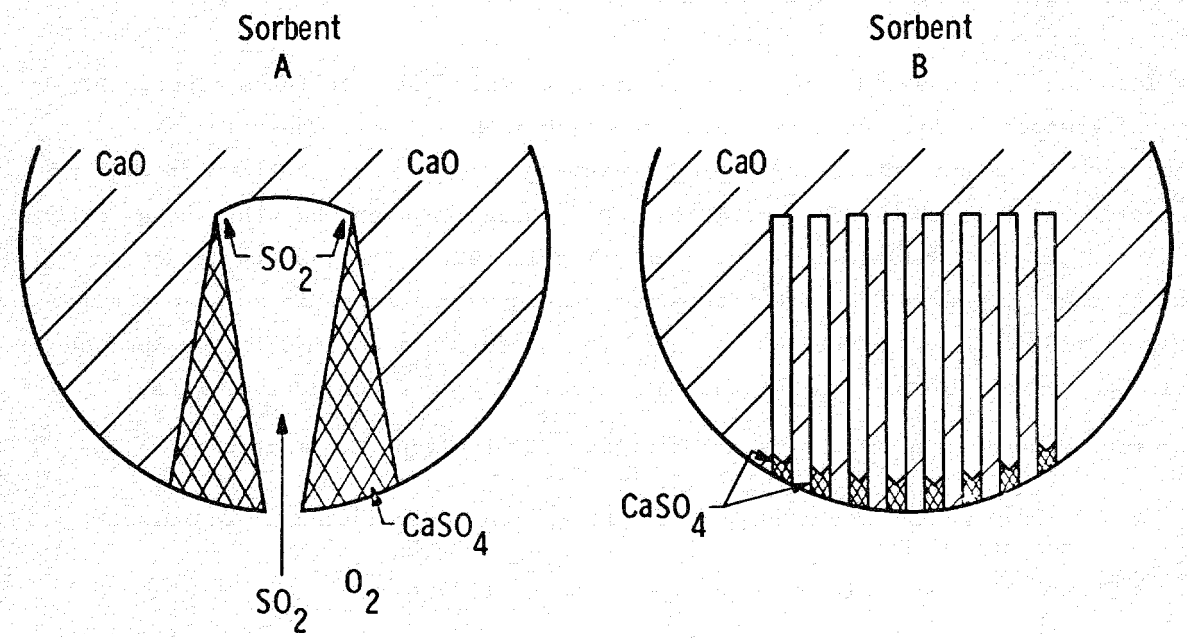

Figure 1-1. The Pore-Volume/Size Distribution Hypothesis

The premise on which this work is based is that the pores in the sorbent are formed during the calcination process. By controlling the calcination process to favor the formation of wide-mouthed pores (diameter in the range ∿0.1 → 2.0 microns) an improved sorbent, with greater sulfation capacity (i.e., greater utilization), is formed.

A detailed discussion of sulfur removal in afbc systems is included in a separate report, for a parallel EPRI contract, "Criteria for the Selection of SO_2 Sorbents for Atmospheric Pressure Fluid Bed Combustors - Task 1 Report," RP NO 721. At this point, it should be noted that other mechanisms such as ash build-up on the sorbent outer surfaces may also prevent limestone from reaching its ultimate sulfation potential.

The four calcium-based natural mineral sorbents tested, were chosen to represent a range of limestone types, and also because they will be used, or have been used in fbc pilot plant operations such as those outlined in Table 1-1.

A standard reactivity test was established: <20 mg of the calcined sample was sulfated in 0.5% SO_2, 4% O_2/N_2 in a modified thermogravimetric apparatus (TG) at 815°C. Sulfation was continued until the rate of sulfation of the sorbent fell below 0.1% Ca reacting per minute. The basis for this choice is outlined in Section 2.1, but it should be noted that the sulfation data may be used for most models of desulfurization, and the utility of the data presented is not in general constrained by this choice of cut-off rate.

Calcined stones were prepared either by calcination in the TG apparatus, or by calcination in a batch loaded fluidized bed unit (3.8 cm diameter). The purpose of the latter tests was to verify that fluid bed calcinations yielded products with the same capacities for SO_2 as those prepared under similar conditions in the small scale TG apparatus. In addition, the large samples (∿30 g) prepared in the fluidized bed unit yielded sufficient material for characterization of the sorbent structure by surface area and pore size distribution measurement. Sulfur distribution in the product sulfate was determined by the electron microprobe.

1.2.2 The Effect of Calcination Conditions

Calcination conditions may be used to improve the utilization in sulfation of all the sorbents tested. In Figure 1-2 the sulfation history of (1000-1180) micron diameter Greer limestone is shown for two calcination environments. Calcination

Table 1-1

USE OF SORBENTS IN PILOT PLANT TESTS OF THE FLUIDIZED BED COMBUSTION PROCESS

Sorbent	Origin	Previous Tests: Laboratory Scale	Previous Tests: Pilot Plant Scale	Chief Characteristics
Limestone 1359	Virginia	(W) TVA NCB	NCB ANL PER EXXON	High purity, high calcium limestone
Greer Limestone	West Virginia		PER ANL*	Impure limestone: candidate for use on the ERDA-Rivesville facility
"Lowellville Limestone"	Eastern Ohio		B&W*	Fairly pure limestone: candidate for use on the 6' x 6' combustor (EPRI-B&W) at Alliance
Dolomite 1337	Western Ohio	(W)	NCB ANL EXXON	Pure dolomite desulfurizes at Ca/S = 1.2/1 in pressurized systems

*Concurrent with this study

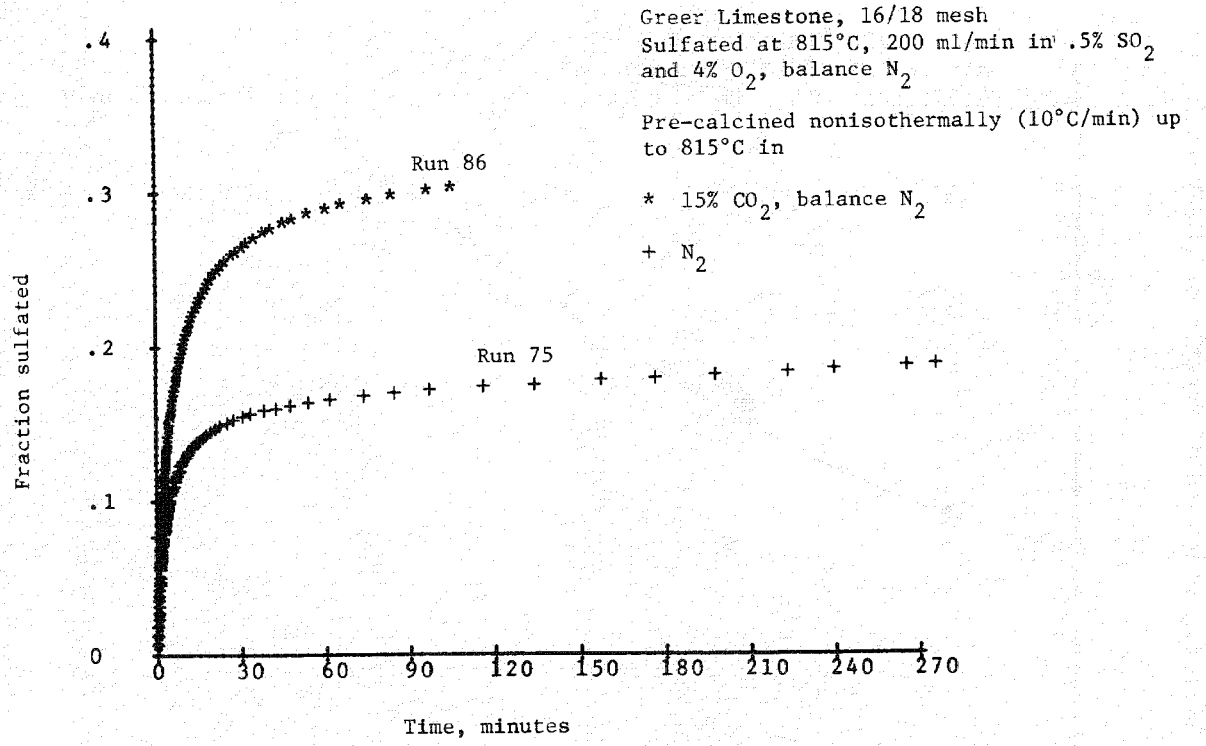

Figure 1-2. The Effect of Calcination Atmosphere on the Sulfation of Greer Limestone

in 15% CO_2 improves the calcium utilization from 17% to 30%. For "Lowellville" stone, the utilization (based on the reaction rate limitation of >0.1% Ca/minute) is shown as a function of the CO_2 content of the calcination atmosphere in Figure 1-3. It may be noted that the range of utilization varies from <20% in 15% CO_2 (typical of an afbc), to more than 40% in 0.8 atm of CO_2. The current results from the Babcock and Wilcox 3' x 3' unit (EPRI Project RP 719) indicate about 20% utilization of this sorbent when calcined "in situ" at less than 15% CO_2.

1.2.3 The Effect of Calcination Temperature

The temperature of calcination is also extremely important in governing the sorbent capacity. Contrary to some expectations (see Appendix 2), heating the Lowellville stone to higher temperatures in calcination improved sorbent utilization at 815°C (Figure 1.4). The limiting utilization is close to 50% and this corresponds to the utilization which must be achieved, if the bed material is to be fed at a Ca/S molar ratio of 1.8 to achieve 90% sulfur removal (see Table 1-2).

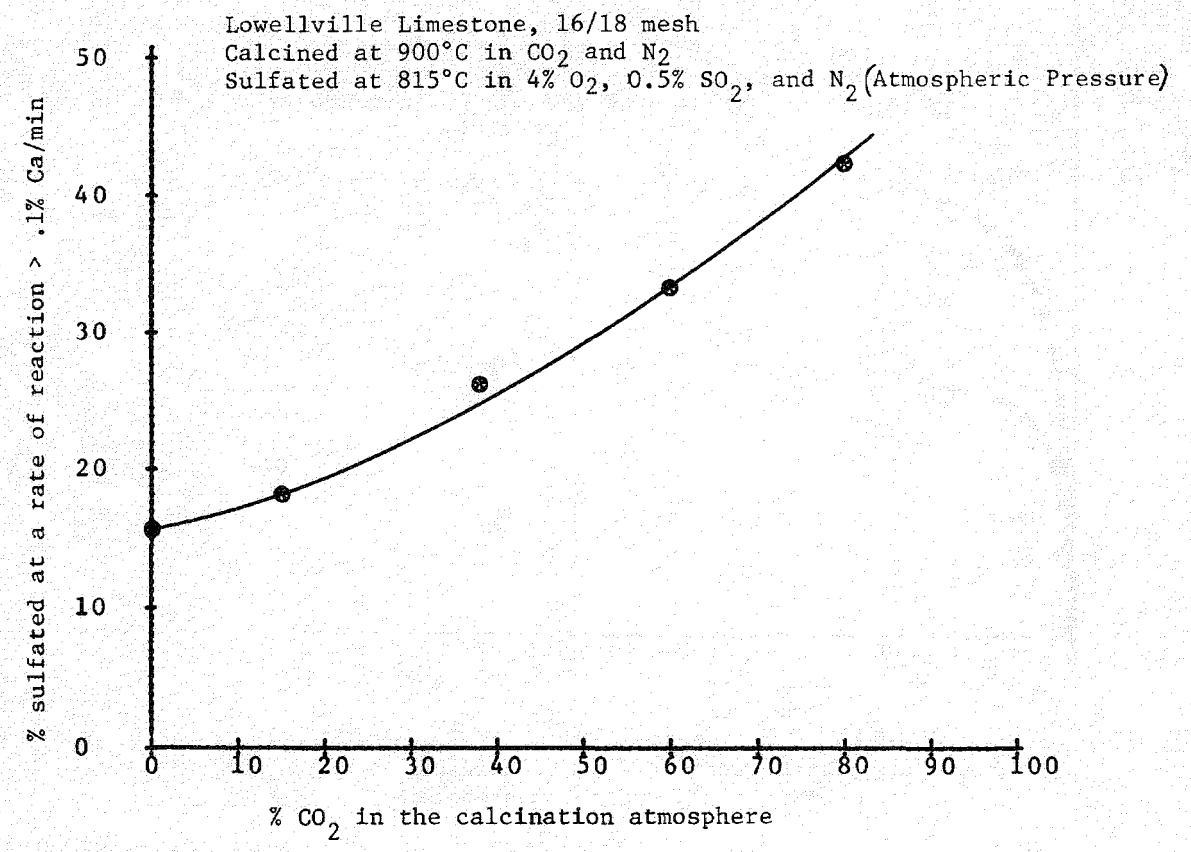

Figure 1-3. The Effect of Calcination Atmosphere on the Sulfation of Lowellville Limestone

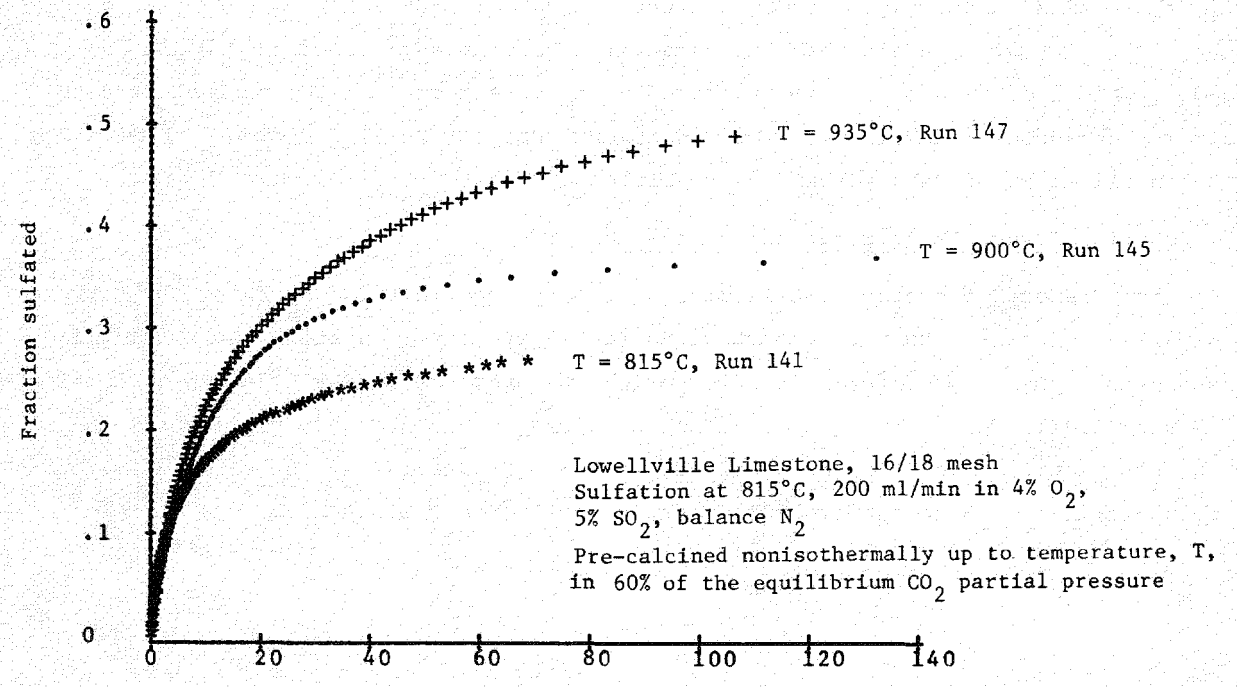

Figure 1-4. The Effect of Calcination Temperature on Lowellville Limestone Sulfation

Table 1-2

Ca/S MOLAR RATIOS AS A FUNCTION OF LIMESTONE UTILIZATION AND DESULFURIZATION

u % utilization of limestone $\left\{\frac{\text{moles of sulfur reacted with CaO}}{\text{moles of Ca input}} \times 100\right\}$	F = R/u Ca/S molar ratio $\left\{\frac{\text{moles of Ca input}}{\text{moles of sulfur input}}\right\}$	
	R = 90%*	R = 75%*
10	9.0	7.5
25	3.6	3.0
50	1.8	1.5
100	0.9	0.75

*R is % sulfur removal

$$R = \frac{\text{moles of sulfur reacted with CaO}}{\text{moles of sulfur input}} \times 100$$

1.2.4 Comparison of Fluid-Bed and TG Calcines

Comparison of the extent of sulfation of TG calcines with similar fluid-bed calcines revealed good correspondence. In most cases, the fluid-bed calcines were marginally superior, indicating that TG samples somewhat underestimate the potential of the sorbent. Typical comparisons are illustrated in Section 3.2.1.

The repeatability of sulfation curves on two batches of the same sample was excellent, as Figure 1-5 illustrates. The average coefficient of variation of the limiting utilization was 4.5%.

It was concluded that TG calcines are adequate simulations of fluid-bed calcines, provided that sorbent residence times at temperature are controlled.

1.2.5 The Effect of Sorbent Residence Time at Elevated Temperature, After Calcination, but Before Sulfation

Holding calcined samples at high temperature 815-900°C after calcination, before sulfation, produced varied effects. For Greer stone, this effect is illustrated in Figure 1-6. In run 119, holding the sample at 900°C for two hours after calcination doubled the sorbent utilization in the subsequent sulfation. However this technique was not as effective as precalcination at 900°C in 60% CO_2-(run 87).

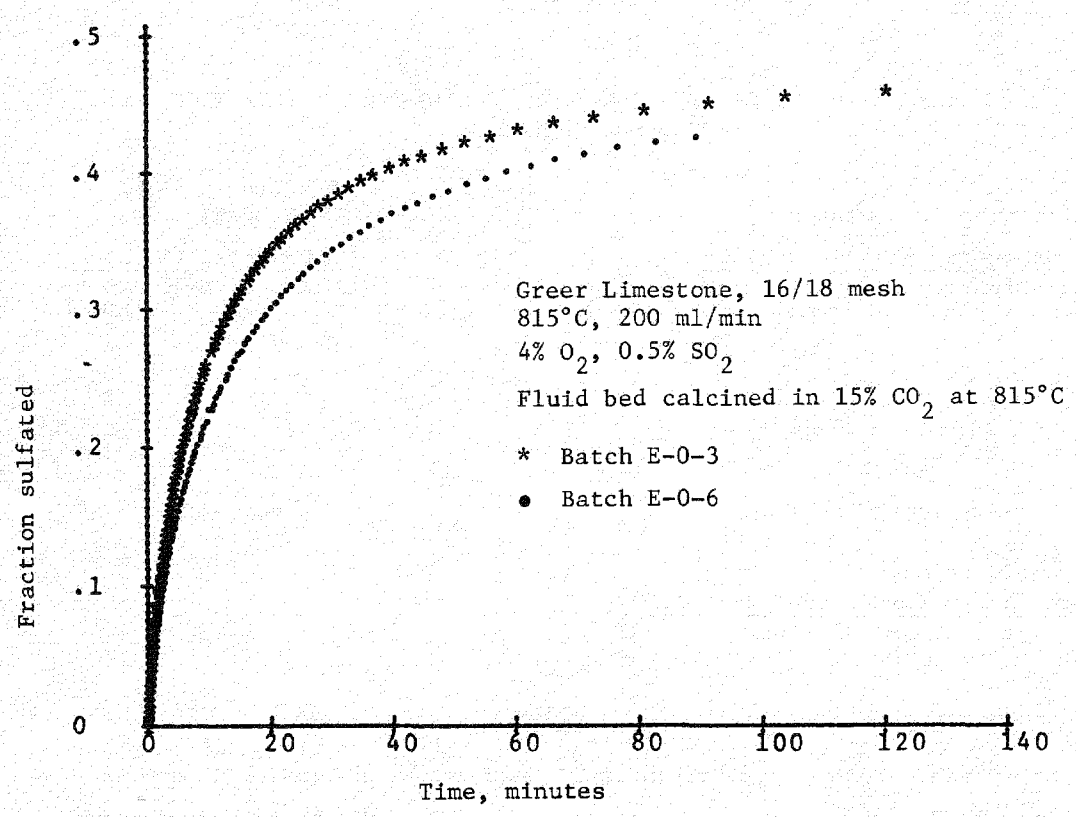

Figure 1-5. Repeatability of the Sulfation of Calcines (Typical)

When the Lowellville stone was held for 2.5 hours at 900°C, its subsequent utilization in sulfation fell from 38% to 25%.

Although this effect was not investigated in depth, it is clear that there is an optimum time/temperature history for each sorbent in producing the most highly sulfated sorbent.

1.2.6 The Effect of Sulfation Temperature on Calcines with High Utilization

In order to demonstrate that the improved utilization resulting from controlled calcination is not limited to sulfation temperatures of 815°C, two samples of Greer stone were additionally tested at 855°C and 895°C, for sulfation. The calcine prepared in N_2 at 815°C declined in utilization from 29% (815°C) through 25% (855°C) to 22% (895°C), in keeping with previous studies that indicate a temperature maximum for sulfation exists (800-850°C). However, an active calcine prepared at 900°C in 15% CO_2 improved with temperature from 57% at 815°C through 62% at 855°C to 67% at 895°C.

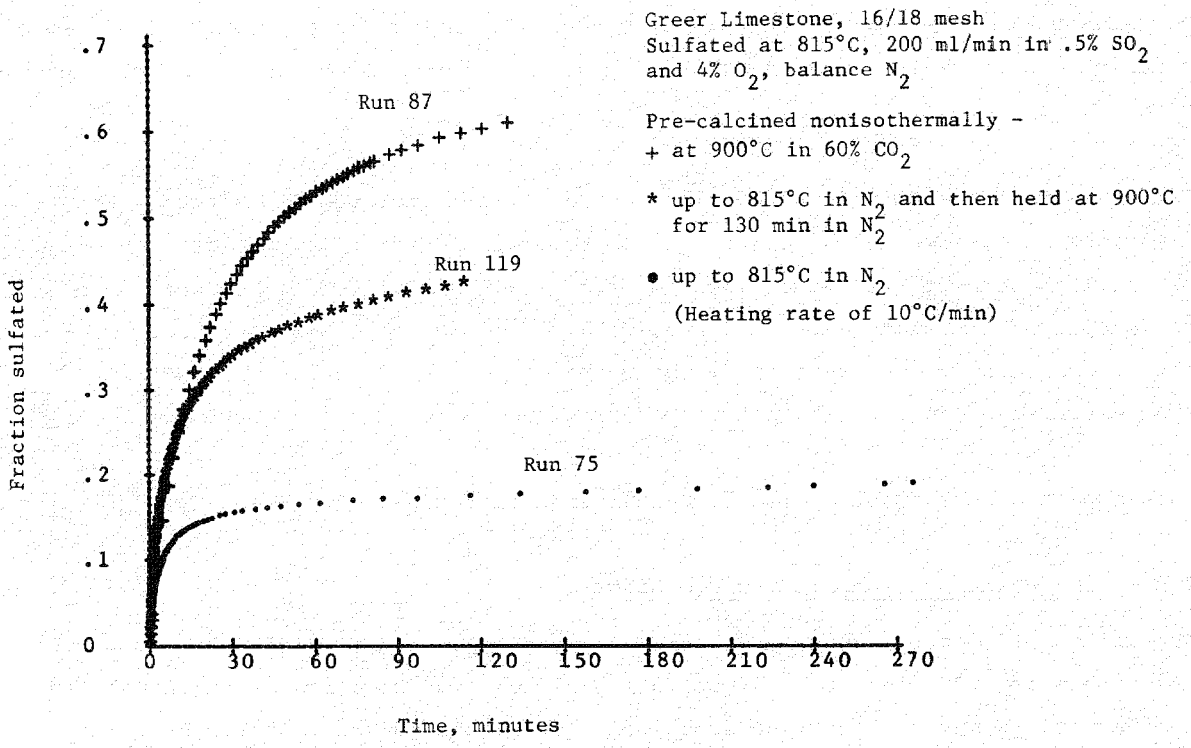

Figure 1-6. The Effect of Calcine Residence Time on the Utilization in Sulfation of Greer Limestone

1.2.7 The Effect of Sorbent Residence Time in Sulfation

Extended sorbent residence times were simulated on the TG by lowering the SO_2 concentration by a factor of 5, in order to prolong the elapsed time at temperatures necessary to reach a given level of sulfation. {Longer residence times at temperature in the fluidized bed will result from improved sorbent utilization.} For limestone 1359, the stone was much less active than first-order projections from the results at 0.5% SO_2 would indicate. This shows that a competing reaction to deactivate the stone parallels the sulfation reaction. It was demonstrated that this competing reaction could be simulated by holding the sorbent in nitrogen at temperature for 200 minutes before sulfating it in 0.5% SO_2 so that the total elapsed time at temperature was the same for experiments with 0.1% SO_2 and 0.5% SO_2.

A third type of experiment was carried out in which the stone was partially sulfated, held in nitrogen, and then resulfated so that the total elapsed time simulated an experiment at 0.1% SO_2. In this case, utilization was decreased in

comparison with the optimum sulfation, by a small factor. A partly sulfated stone apparently suffers less deactivation than an unsulfated stone over long residence times.

This aspect of the sulfation reaction has never been thoroughly explored. With limestone 1359, some of the benefit of improved calcination may be lost because of the long sorbent residence times in afbc (∿6-24 hrs).* The inhomogeneity of the sample of limestone 1359 used precludes definitive conclusions without further research. On the other hand, the work noted above with Greer stone showed that extended exposure at high temperature yields a more active sorbent.

This aspect of the problem clearly requires further research.

1.2.8 The Recarbonation of Calcined Sorbent

The extent of recarbonation, under fixed conditions, of six calcines was measured to compare it with the extent of sulfation. There was no correlation between the two values. Recarbonation is a function of surface area and probably of pores of fine radii.

1.2.9 Calcination in the afbc Environment

Preliminary calculations showed that the rate of calcination of limestone is significantly faster than the sulfation rate, at temperatures above 780°C in the carbon dioxide atmosphere generated by coal combustion. Experimental tests showed that calcination was slower than the calculated values but that the time required for calcination is not significant in terms of the long residence times of the sorbent (6-24 hours).* The course of calcination of 1000 micron diameter particles in 15% CO_2 at 815°C is shown in Figure 1-7.

1.2.10 Distribution of Sulfur in the Sulfated Products

The sulfur distribution in sulfated products was determined by analysis of characteristic X-rays in an electron microprobe analyzer.

---

*The anticipated range of sorbent residence times in a 30 MW module of a fluid bed combustor burning (2-6) % sulfur coal.

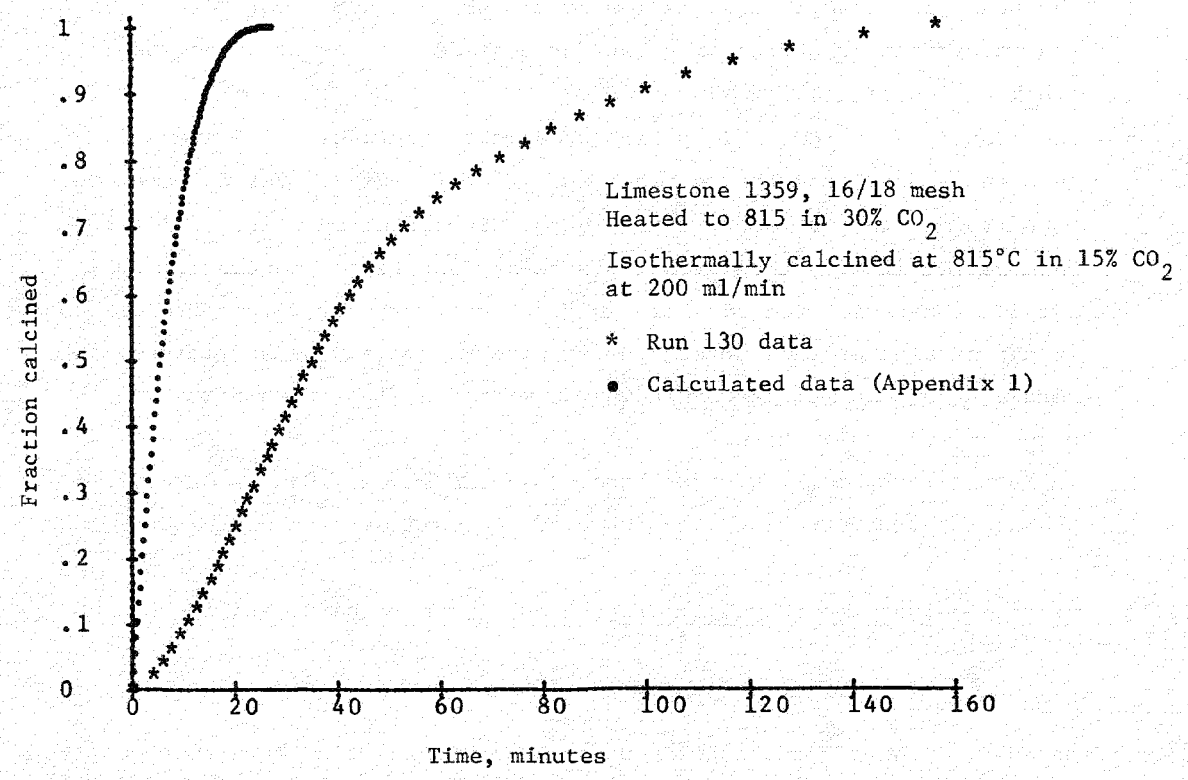

Figure 1-7. Calcination of Limestone 1359 at 815°C in 15% CO_2

The distribution of sulfur and calcium in the cross-section exposed is shown for each of the samples studied in Section 3.6. The results may be summarized as follows:

1. Sulfation can be either characterized by a sharp interface between reacted and unreacted sorbent, or by a diffuse distribution of sulfur into the center of the particle. In general, sorbents with low utilization have the sulfur concentrated at the edges of the particle.
2. The grain size of the parent limestone, as seen in an optical microscope (Figures 2-9 and 2-10), is important in determining sulfur distribution. With Lowellville (parent grain size ~40 micron diameter) penetration of sulfur towards the particle center was more obvious, since penetration into the large grains at the surface was slow.
3. Apart from distinguishing between slightly sulfated and heavily sulfated sorbents, estimation of the extent of sulfation from the sulfur mass is very inaccurate because of the odd particle shapes, uncertainty as to the exact cross-section, and the incomplete penetration of individual grains.

4. The scans indicate that sulfation models which account for both inter and intragranular diffusion of sulfur dioxide are essential to model the kinetics of the reaction.
5. The result of the CO_2 calcination treatment for Lowellville stone can be clearly seen from the photographs, (Figure 1-8). After calcination in nitrogen, the surface grains are not penetrated by sulfur. After calcination in CO_2, the surface grains are apparently completely sulfated. Apparently the porosity shift occurs actually within the grains. It can be assumed that intergranular pore volume may be sacrificed, as long as the pore volume within the 40 micron grains is shifting to pores of wider diameters.
6. In future work, the individual grains should be examined to determine the depth of penetration as a function of position of the grain.

1.2.11 Relation between the Physical Properties of the Sorbent, and its Potential Utilization in Sulfation

Surface Area

The surface area of the sorbent calcine does not increase with the sorbent capacity at the rate criterion. A sorbent may yield a lower surface area calcine on controlled calcination, yet have a higher capacity for sulfation.

Pore Volume/Pore Size Distribution

For the limestone studied, improved utilization upon controlled calcination was always accompanied by a shift in pore-volume distribution, unique to each stone. More pores were found in the pore-radius range (0.08 → 2 microns) with the active calcines, confirming the hypothesis as to why controlled calcination improves the sorbent's properties.

1.2.12 Application of Modified Calcination Conditions to Atmospheric Pressure Fluidized Bed Combustors

The integration of a separate, controlled sorbent calcination zone as part of an afbc process offers potential economic advantages. Although the overall economic impact has not been determined, the most favorable design alternatives appear to be: 1) precalcination in a separate bed which is connected to the combustor, or 2) precalcination in a separate zone within the combustor.

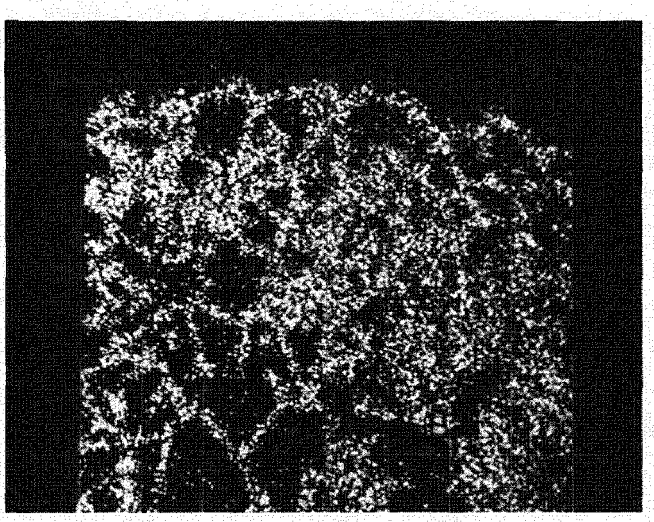

Run 114, Sulfated 23% in 200 minutes at 815°C in 4% O_2 and 0.5% SO_2 after calcination at 815°C in N_2 (X250)

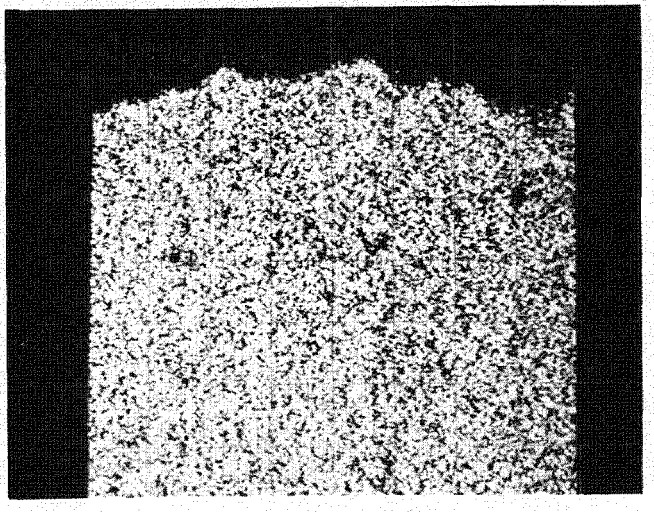

Run 116, Sulfated 40% in 100 minutes at 815°C in 4% O_2 and 0.5% SO_2 after controlled calcination at 900°C in 60% CO_2 and N_2 (X225)

Figure 1-8. Sulfur Scans of Lowellville Limestone, Edge Sections of 16/18 Mesh Particles

1.3 CONCLUSIONS

- Modified calcination techniques can reduce limestone consumption in atmospheric fluid bed coal combustors.
- The optimum design and operating conditions for a modified calcination system should be determined on a continuous fluid bed combustion system.
- The overall economic impact of a modified calcination system should be established.
- The impact of sorbent residence time at operating temperatures on utilization should be fully explored.

Section 2

PROJECT SCOPE AND METHODOLOGY

2.1 PRELIMINARY ASSESSMENT AND OBJECTIVES

2.1.1 Definition of Conditions of Interest

The current design conditions for atmospheric pressure fluidized-bed combustors were examined to determine the ranges of relevant parameters for the calcination and sulfation of limestone. The available information is summarized in Table 2-1.

From the design parameters listed it was possible to make some general definitions of the ranges of variables which should be studied in this program.

The gas residence time in the fluidized-bed will lie in the range 0.25 - 1.0 seconds (assuming a bed voidage of 0.5). The particle size of limestone used will tend to lie in the range-8+20 mesh (U.S.) or 840-2380 micron diameter. This is in general a larger particle size than used in our previous laboratory studies. (The use of finer particles with recycle is not ruled out but is the subject of a separate EPRI investigation.) It is widely believed that 815 to 870°C is the optimum temperature range for desulfurization. In general low excess oxygen values corresponding to 2-4% oxygen in the effluent are expected.

In order to translate the process design parameters into a criterion for the required rate of stone sulfation in the bed, a model of sulfur retention in fluidized-bed combustion derived previously was used.[1]

The model assumes that first order reaction occurs between gas and solid in the bed, that the solid is perfectly mixed, and that uniform sulfur dioxide generation occurs throughout the bed. The extent of sulfur retention in the fluid-bed is plotted in Figure 2-1 as a function of the mean first order reaction rate in the bed for different superficial velocities through the bed, and for a bed height of 4 ft. assuming pure limestone as the sorbent.

Table 2-1

ATMOSPHERIC PRESSURE FLUID-BED COMBUSTORS DESIGN
CONDITIONS RELEVANT TO DESULFURIZATION

Source	Particle Size	Superficial Velocity	Bed† Height	Excess Air	Sorbent	Ca/S Mole Ratio	Temperature
Pope, Evans and Robbins/Foster-Wheeler[2]	<1/4"	6-12 fps	4 ft	20%	Limestone	3/1	1500°F
General Electric[3] (Study)	<1/8"	2-10 fps	4 ft	20%		2/1	1480-1500°F
Westinghouse[4] (Study)	<1/4"	10-15 fps	3 ft			(*)	1400-1700°F
Babcock and Wilcox[5] (Planned Unit)	<1/4"	2-8 fps	4 ft	10%	Limestone		1450-1600°F

*Estimated as 5/1 at time of report (1971)
Now estimated as ∿3/1
†Bed height used with superficial velocity and voidage to obtain gas residence time.

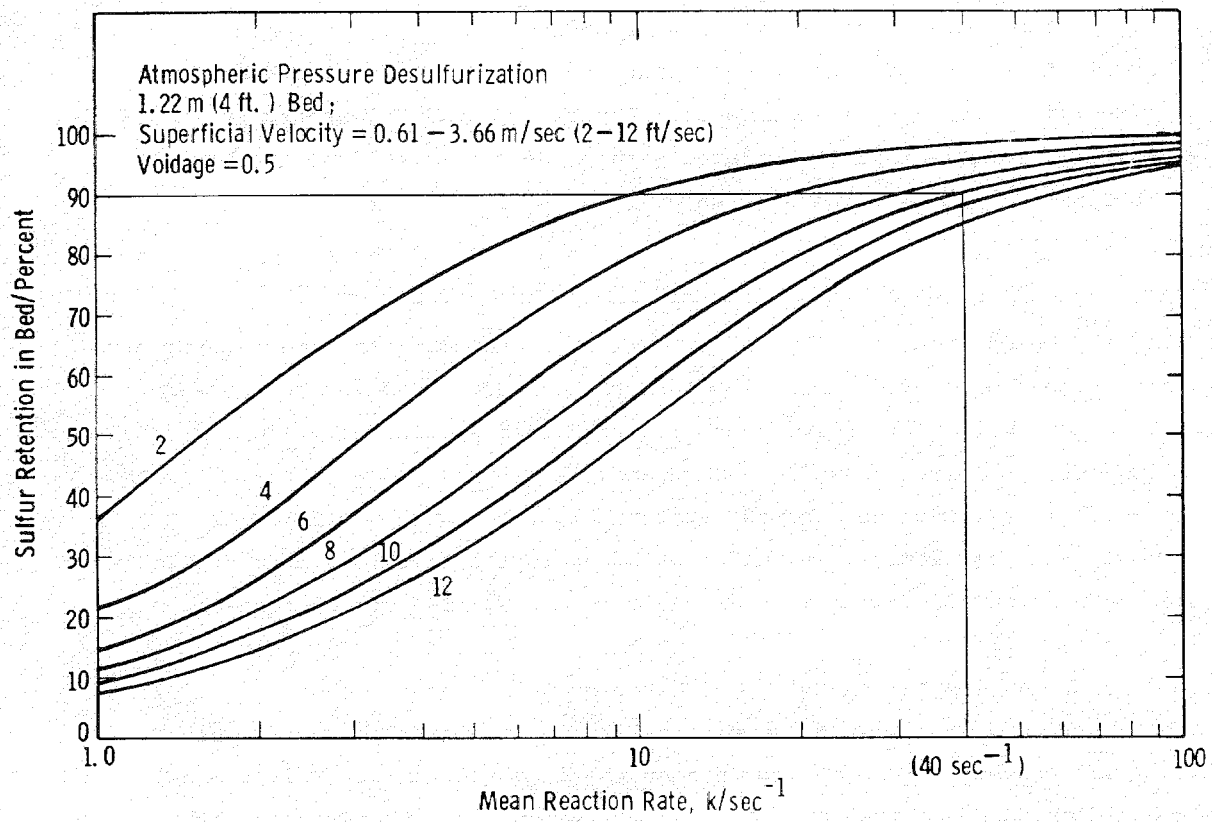

Figure 2-1. Sulfur Retention as a Function of Superficial Velocity, Mean Reaction Rate and Gas Residence Time

Mean Reaction Rate

It should be noted that estimation of the critical rate of reaction does not rely heavily on the particular model used. Typically, the rate of sulfation for 500 micron diameter particles of calcined limestone 1359 can change by half an order of magnitude within an increase of sulfation level of 5 molar percent. The utilization of the limestone in the bed with high sulfur retention cannot proceed past the point when this rapid change in rate takes place.

From Figure 2-1 it can be seen that to maintain 90% sulfur retention in the 4 ft. bed at 8 ft/sec, k should have a value of 40 sec^{-1}. A limestone particle should react at ~1% calcium sulfating per minute at 0.5% SO_2 in a typical TG experiment in order to meet this criterion. To achieve 80% sulfur removal in the bed, 0.5% of the calcium would have to react per minute. In this program, we should, therefore, determine the extent of sulfation at which the rate of calcium utilization falls from 1% (min^{-1}) to 0.1% (min^{-1}).

Since the limestone particles may have residence times in the combustor up to 24 hours the effect of long term exposure to very low partial pressures of sulfur dioxide will have to be investigated. Typically, in a TG experiment at 0.5% SO_2, 4% O_2, the stone is rapidly sulfated within 10-20 minutes, and the utilization changes minutely over periods of several hours after the rapid phase.

2.1.2 Assessment of the Relevant Rates of Limestone Calcination

Since the combustion of a typical coal will generate an atmosphere containing about 16% carbon dioxide in an atmospheric pressure fluidized bed, the calcination of limestone will be to some extent retarded. At sufficiently low temperatures, below 760°C, calcination will be slow enough to interfere with the sulfur removal process, since limestone does not appreciably react with sulfur dioxide until it has calcined. (Dolomite, on the other hand, is reactive to sulfur dioxide even under conditions where calcium carbonate is the stable form of the sorbent.)

In order to assess the extent of calcination which should occur in a typical atmospheric pressure system, some calculations were carried out in which the stone was assumed to calcine in an atmosphere containing one-half the exit gas carbon dioxide concentration. This is equivalent to the assumption that CO_2 is uniformly produced throughout the bed. The details of the calculation are shown in Appendix 1 (A1.2). Kinetic data obtained in previous studies were used, and are subject to modification in the light of experimental studies reported here. In particular, it was found in experiments described in Section 3.1 that calcination was more severely retarded by the presence of carbon dioxide, than was assumed for the purposes of these calculations. The results show that at temperatures above 1391°F (755°C), the carbon dioxide production in the bed should be insufficient to interfere with the sulfation reaction. Figure 2-2 illustrates the extent of calcination expected for a mean stone residence time of 12.5 hours, and different particle sizes of stone. (See calculations in Appendix 1). For 6,000 micron diameter stone, the extent of calcination would be just sufficient to permit 50% sulfation, and smaller particles would have a greater degree of calcination. However, if the stone residence time were lowered, as would occur at higher Ca/S molar feed ratios (i.e., lower calcium utilization), then the extent of calcination might interfere with desulfurization. Figure 2-3 illustrates the effect of longer stone residence times in increasing the extent of calcination.

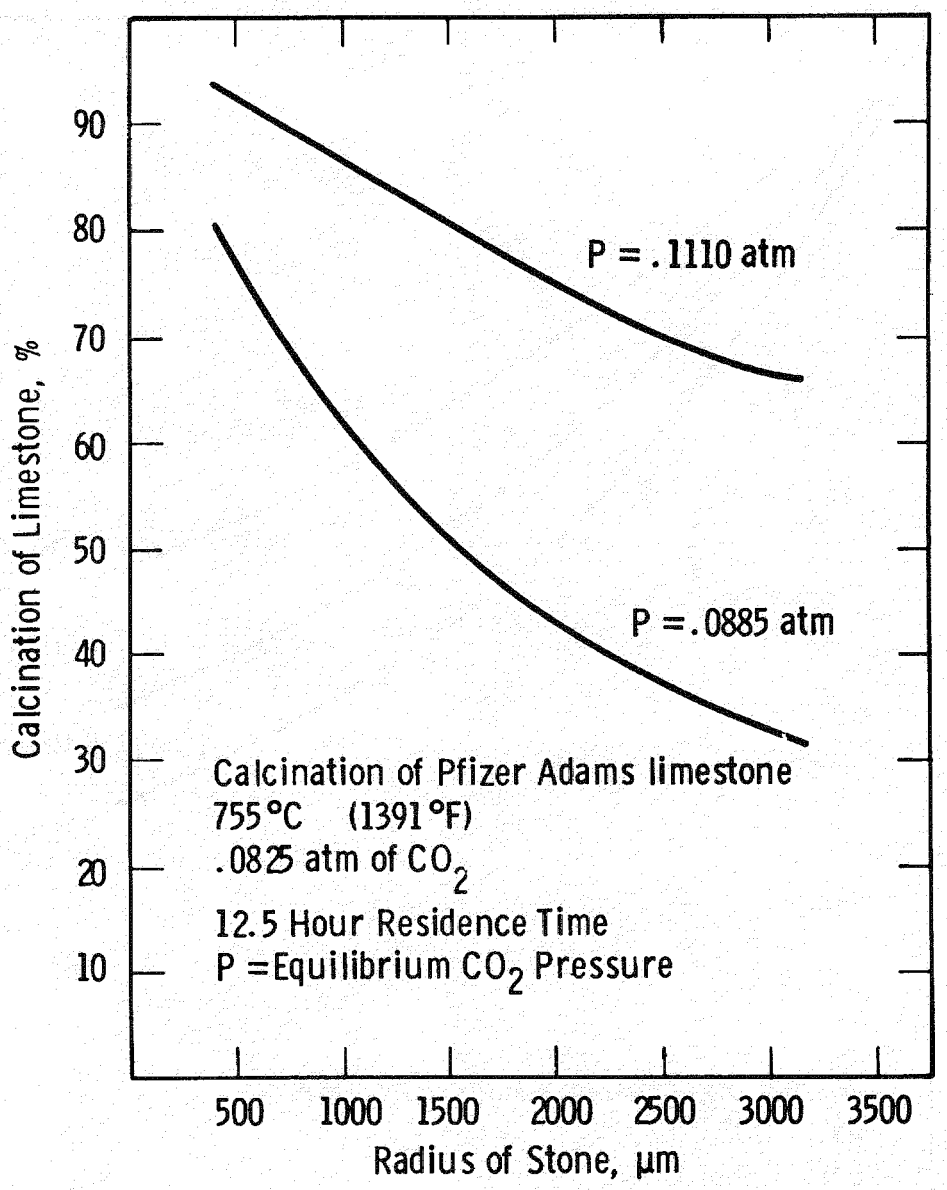

Figure 2-2. The Extent of Calcination of Spent Sorbent from a Fluidized Bed as a Function of Particle Size with Different Equilibrium CO_2 Pressures

It may be concluded that the overall extent of calcination should not directly prevent desulfurization above 750°C, unless the generation of CO_2 (coal combustion) occurs mostly in the lower part of the bed. In the worst case, the temperature limit at atmospheric pressure would be raised to about 790°C. It is necessary to consider how partial sulfation of the limestone may hinder calcination, thereby reducing the stone utilization. This is best assessed by experimental studies on the T.G.

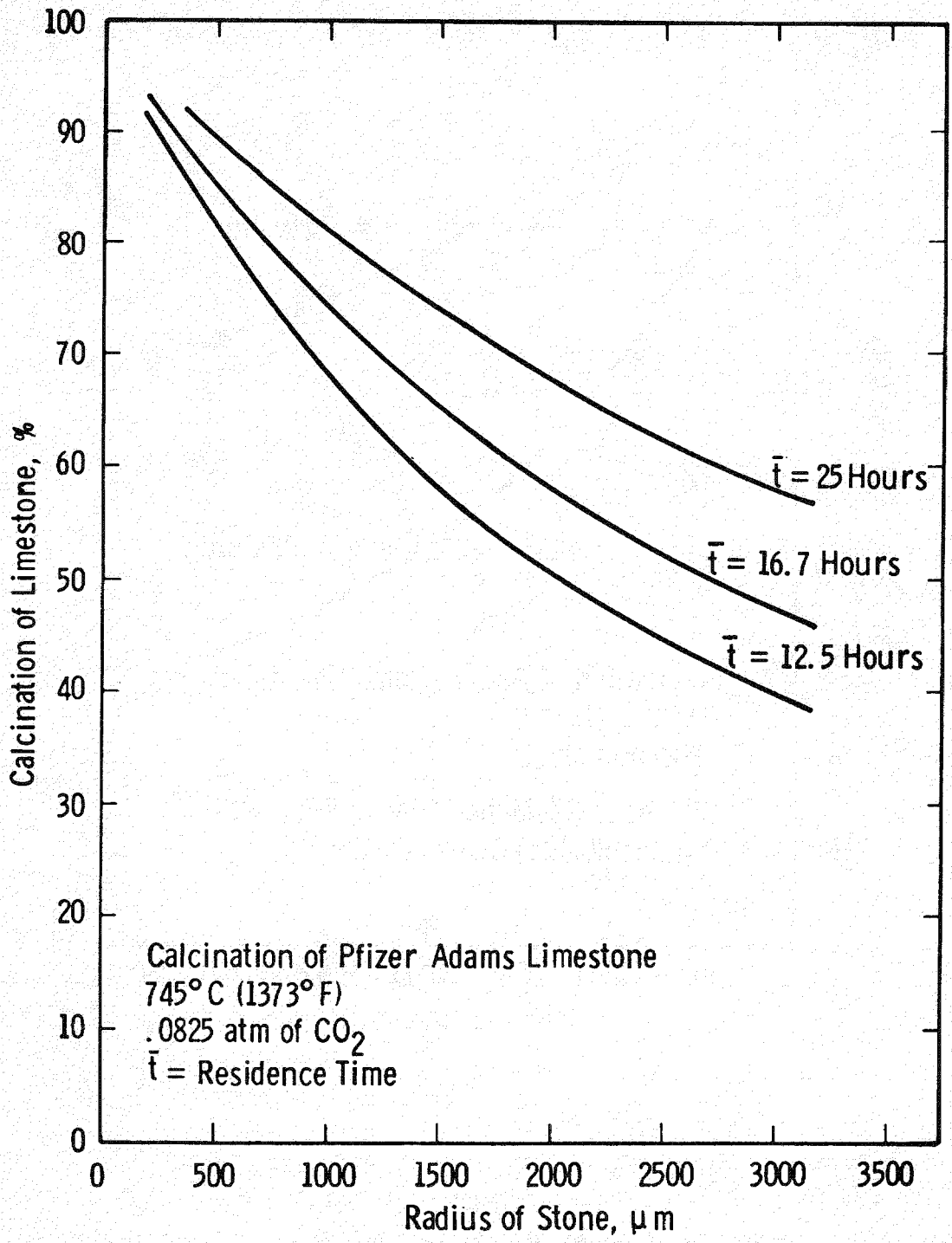

Figure 2-3. The Extent of Calcination of Spent Sorbent from a Fluidized Bed as a Function of Particle Size

The rate of calcination of limestone is discussed in Appendix 1.

2.1.3 Assessment of the Effect of Limestone Calcination Conditions on Stone Structure

The development of pore structure in calcined limestone is a critical factor in determining the suitability of a calcine as a sulfur removal sorbent in fluidized-bed combustion.[6,7] (It is also a critical factor in determining the capacity of other oxides to absorb sulfur dioxide.)[8] In attempting to improve calcium utilization during sulfation, some reactivity may be sacrificed. This loss of reactivity is caused by the coalescence of small pores to form large pores, and a corresponding reduction in internal surface (lowering the reaction rate), but an increase in the number of pores with sufficient volume to accommodate sulfate ions without hindering transport of reacting gases into the interior of the solid.

A general review of the effects of calcination conditions on the activity of CaO is given in Appendix 2. The principal factors which have been found to influence the reactivity of calcines are: heating rate before calcination, temperature of calcination, retention time at temperature after decomposition, and the presence of impurities in the stone. (Sodium is the only impurity reported to increase lime reactivity.)

There are some reports in the literature which have a direct bearing on this work. Although it has been known from D.T.A. studies that lattice rearrangement continues in calcined lime after all the carbon dioxide is expelled, Searcy has recently identified a metastable calcium oxide formed at the reaction interface.[9] The reaction kinetics determined by weight loss, or gas evolution measurements refer to the reaction which forms this metastable oxide as product. However, it is the rearrangement of this product to give the sorbent calcium oxide which probably determines the capacity of the sorbent in sulfation. The factors which control the conversion of the metastable oxide will be the critical factors for producing good sulfur dioxide sorbents. The rate at which the calcium carbonate interface recedes from this intermediate oxide may be critical in determining the crystallite size and porosity in the final oxide product.

Zawadzky has described the occurrence of false equilibria in reversible reactions such as calcium carbonate decomposition.[10]

He showed that decomposition rates could be much slower than expected at conditions near the equilibrium where the crystallite size of reactants and products might affect the equilibrium partial pressure of carbon dioxide. This effect appears to have been demonstrated by Cremer and Nitsch, who showed that increasing crystallite size in calcium carbonate could cause a deceleration of decomposition at temperatures of 850°C.[11]

It may be concluded that reaction conditions in calcination can profoundly influence the rate at which the product lime is formed, that the product lime may rearrange in the period immediately after calcination, and that further modification of the product lime due to sintering or the presence of impurities may occur at high temperatures.

2.1.4 Definition of Calcination Effects which Should be Investigated

This investigation has been based largely on our previous finding that calcination in carbon dioxide produces sulfur sorbents of greater capacity in fluidized bed combustion/desulfurization.[1] The major questions we wished to answer were

- what is the greatest utilization of calcium that can be achieved in afbc by varying the calcination conditions
- what is the mechanism by which calcination in carbon dioxide increases the capacity of the stone
- can the temperature range over which desulfurization can be achieved at low Ca/S ratios, be extended above 840°C.

Since the principal effect of calcining under carbon dioxide is to decrease the rate of calcination and enhance the subsequent sulfation reaction, it was decided to examine the structure produced in, and the sulfation properties of lime which has been produced at both fast and slow calcination rates. In addition, because a temperature of about 1500°F (816°C) has been found optimum for desulfurization in afbc, careful examination of the rates of calcination and sulfation, and the porosity of calcine produced in this temperature region, under partial pressures of carbon dioxide close to those produced in the fluidized bed by the combustion of coal, was required.

2.1.5 Conclusions

The calcination of limestone is to some extent retarded by carbon dioxide from the combustion of coal, at least up to 800°C. Since previous work has shown that

retarded calcination leads to improved calcium utilization in sulfation, the optimum conditions for enhancing this effect should be determined. One of the key elements is the rate at which limestone will calcine in the fluidized bed combustor. One of the first steps in establishing this link is the experimental determination of the rates at which limestone calcines in the carbon dioxide-containing atmosphere of the fluidized bed.

2.2 PROCEDURES AND MATERIALS

2.2.1 Experimental Details

Thermogravimetric Apparatus. The equipment used was a DuPont 951 thermogravimetric (TG) balance which, modified as described by Ruth,[12] was capable of operation in flowing gas containing sulfur dioxide at elevated temperatures. (See Figure 2-4.) The balance, controlled by a DuPont 990 console, sends out a continuous electric signal which provides a reading of the weight of the sample as a function of time. Occasional experiments were carried out using an older instrument - a DuPont 950 controlled by a model 900 console. All work was carried out at atmospheric pressure, 97 ± 6 kPa (28.7 ± 0.2 in. Hg) in Pittsburgh.

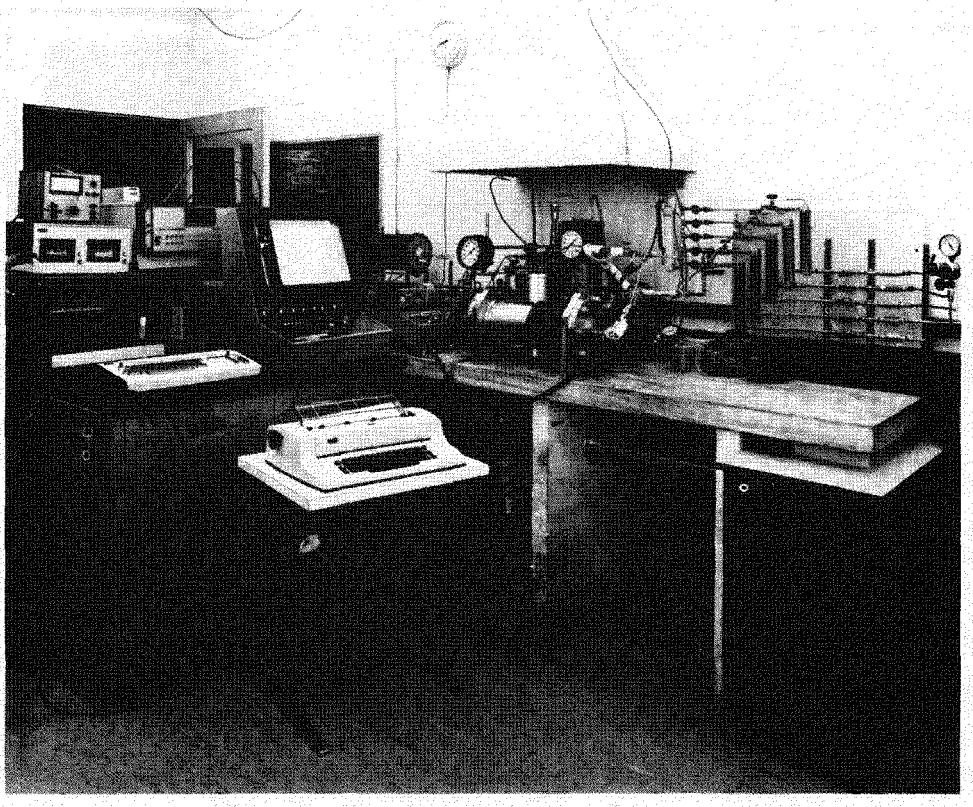

Figure 2-4. The Westinghouse Thermogravimetric Analysis System

The TG data were routinely stored on a cassette tape: reduction of the data was carried out by rereading the data into a Wang 2200 calculator. Each weight datum was read to ±5 μg which corresponds to 0.03% sulfation of a typical 10 mg sample of calcium oxide. The "noise" level of weight readings of a sample held at 871°C in flowing nitrogen typically yield a time average value for weight ±2 μg. The temperature was maintained constant during the sulfation reactions, with a standard deviation of 0.04 mv (1.1°C).

Data were stored on the cassette tape in the form of millivolt readings, every five seconds. A microprocessor, pre-programmed through the Wang calculator, controlled the data acquisition equipment, leaving the Wang free for analysis of previously recorded data. All the points read were not necessary for reduction and, if used, would overflow the memory of the Wang system. Therefore, about 100 data points were used. The points were selected at 1% weight change increments for each reaction. In calcinations and recarbonations, this increment was approximated using the initial weights and the percent weight drop as input. The percentage calcination was calculated assuming 100% reaction. The recarbonated fraction was calculated using the % weight drop in calcination. A 1% weight change in sulfation was found by inputing the initial and final weights as guides for reading the data. The percent sulfated was then calculated from the % Ca as determined by EDTA titration which was input to the program.

Occasional runs were recorded solely on the analog chart recorder.

It was noted that the rate curves had a high level of noise as the reaction slowed and sulfation approached 1% CaO sulfating per minute. This was due to limitations in weight readings produced from the balance in the A to D converter. Weight changes of 5-15 μg were being used to calculate reaction rates when the resolution of the readings was only 5 μg. The program for data reduction was changed to use larger increments in weight for a better time-averaged rate. The rate data was further improved by using every fifth point, increments of about 5% weight change, to calculate the rate. Figures 2-5 and 2-6 show how the "noise" level in the rate was dampened by using a larger fraction increment to compute the rate of sulfation.

Fluid Bed Calcination Apparatus and Procedure. Stone samples were crushed at room temperature, sieved into size fractions and a 50 gm charge placed in the reactor. The reactor was a 3.5 cm diameter Inconel 600 reactor with a distributor plate

Sulfation Rate of Lowellville Limestone

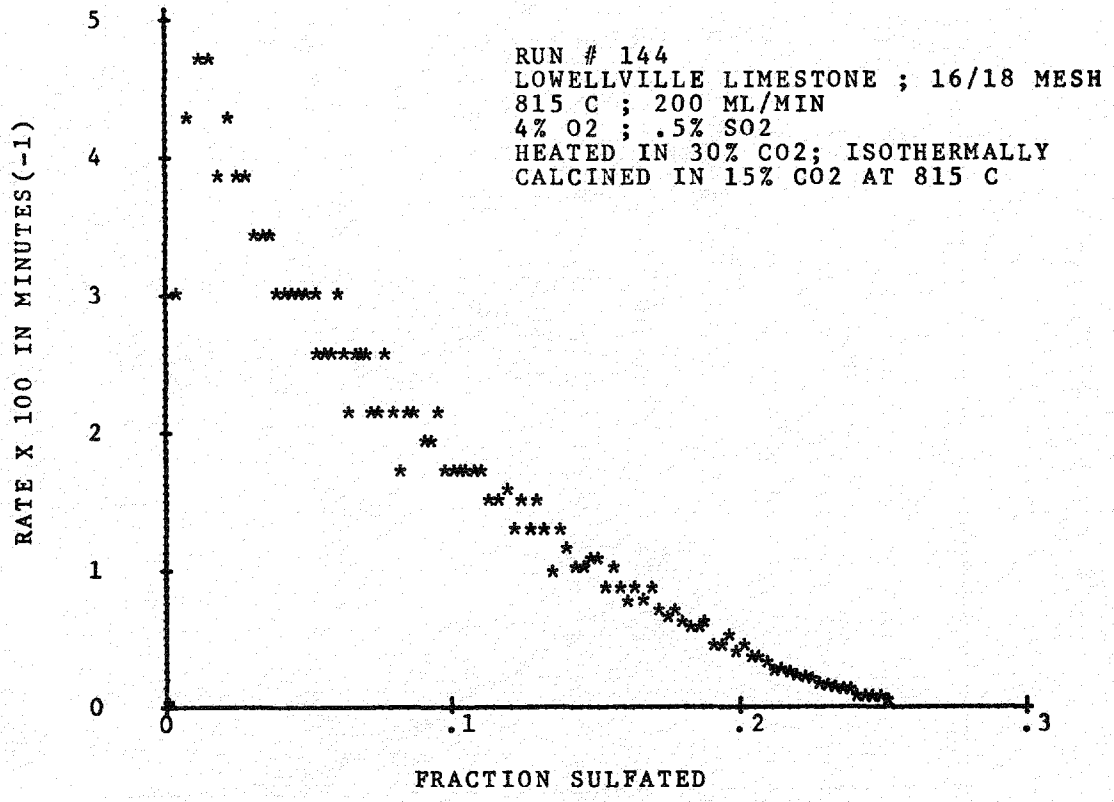

Figure 2-5. Rate Calculated with Points Chosen at Intervals of About 1% of the Total Weight Change in Sulfation

made of Inconel 600 through which 37 holes of 0.012 cm diameter were drilled (shown in Figure 2-7). The fluid bed was located in a shell furnace which could be pressurized to 10 atm. For these experiments, the shell was open to the atmosphere. Four electric heater coils were controlled by a Trendtrak programmer. A thermocouple entered the flanged lid of the reactor and extended down into the solids region. A set of solenoid valves in the effluent line lead to evacuated 75 ml steel cylinders. The solenoids could be opened at given time intervals by a mechanical programmer, or they could be fired manually. Pressure and temperature data were fed to a data acquisition system where they were printed on a teletype unit at selected time intervals. They could also be stored on cassette tapes.

In operation, the bed was brought to temperature, and then the fluidizing gas was switched on. A preheater coil in the incoming gas line wrapped around the outside

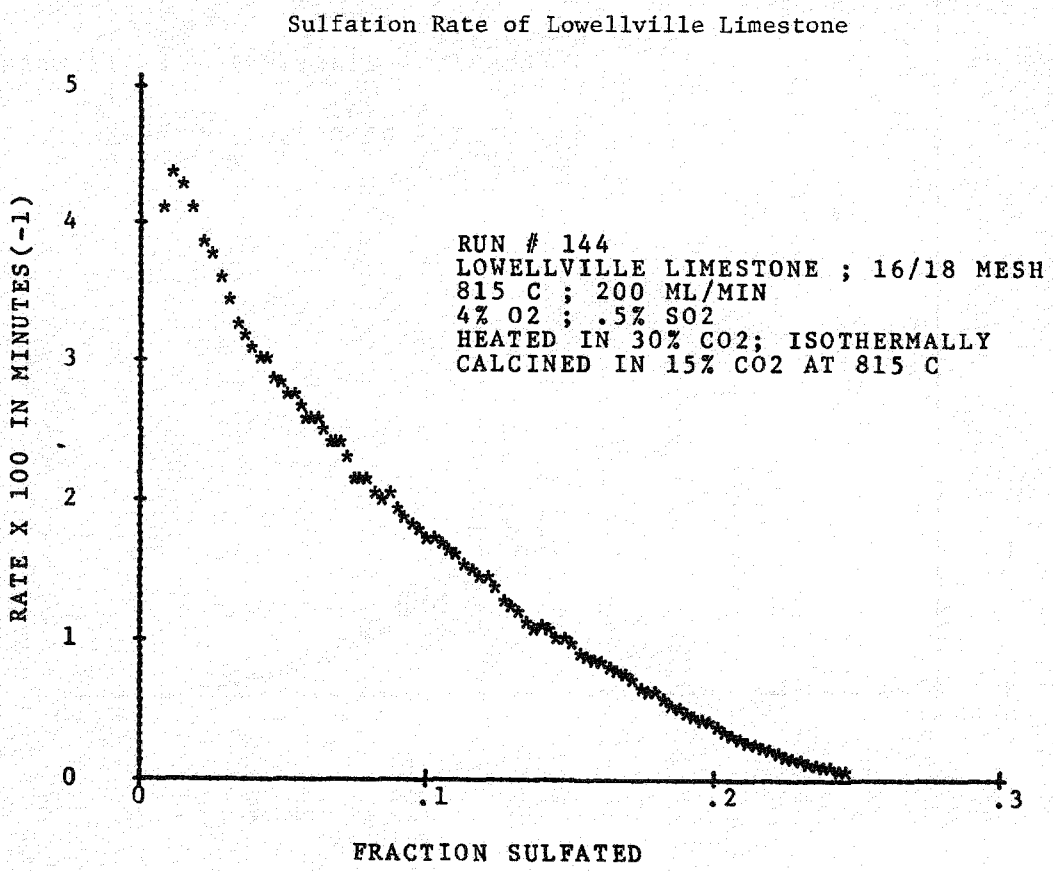

Figure 2-6. Rate Calculated with Fraction-Averaged Points Chosen at Intervals of about 5% of the Total Weight Change in Sulfation

of the reactor minimized the initial temperature drop. However, after run E-0-6, the preheater coil was removed when refabrication of the reactor was requested due to distributor damage. The temperature of the fluid bed after the coil was removed is shown in Figure 2-8. The accuracy of the setting was about ±4°C, from run to run, but the temperature was controlled to within 2°C after the initial temperature drop.

The gas samples were analyzed on a Carl chromatograph, using a Hewlett-Packard integrator. On the early runs, difficulty was experienced using automatic sampling valves with Teflon seats, and erratic CO_2 analyses were recorded. Subsequently the valve seats were replaced by Viton A material, and consistent gas analyses were obtained.

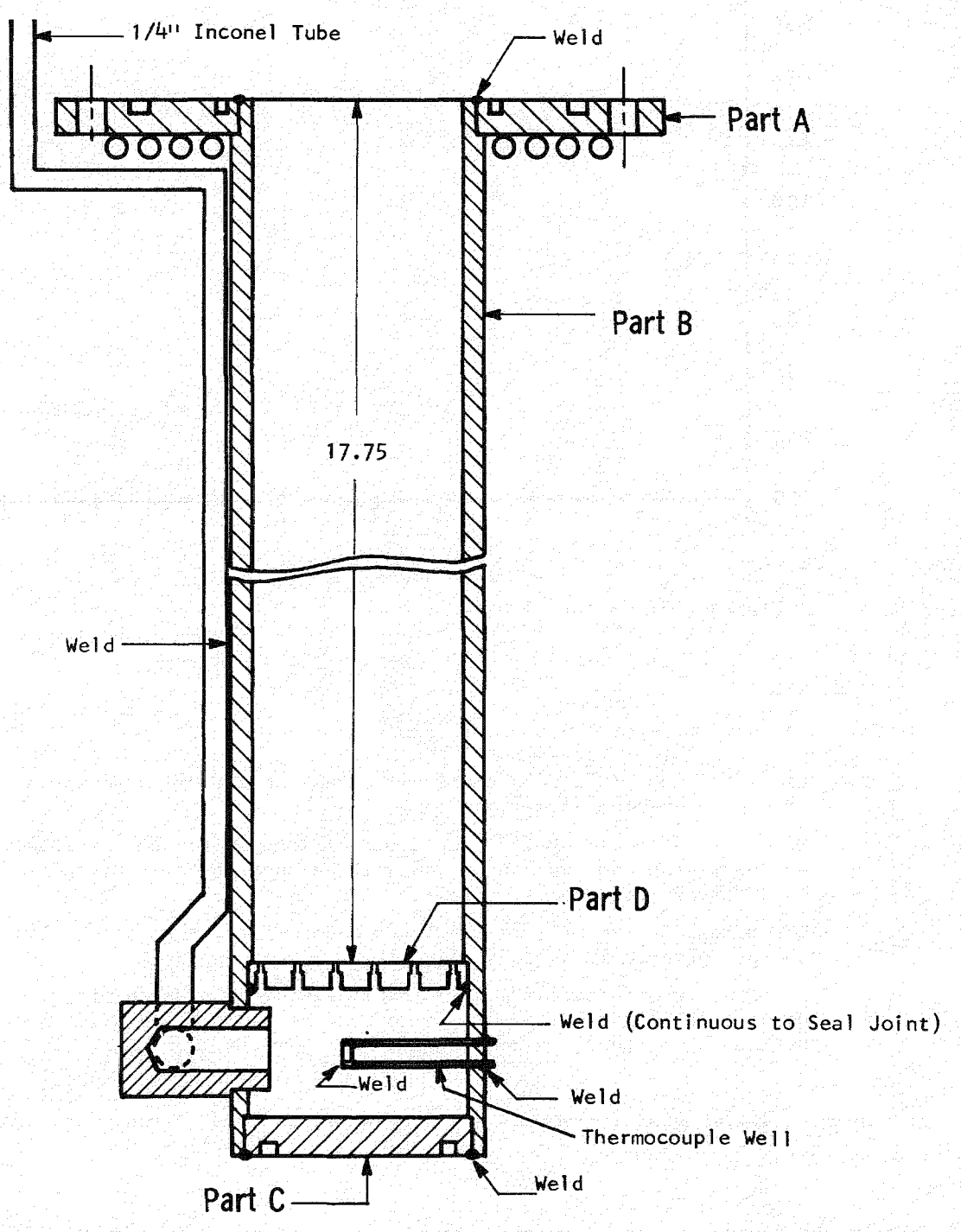

Figure 2-7. Reactor Assembly

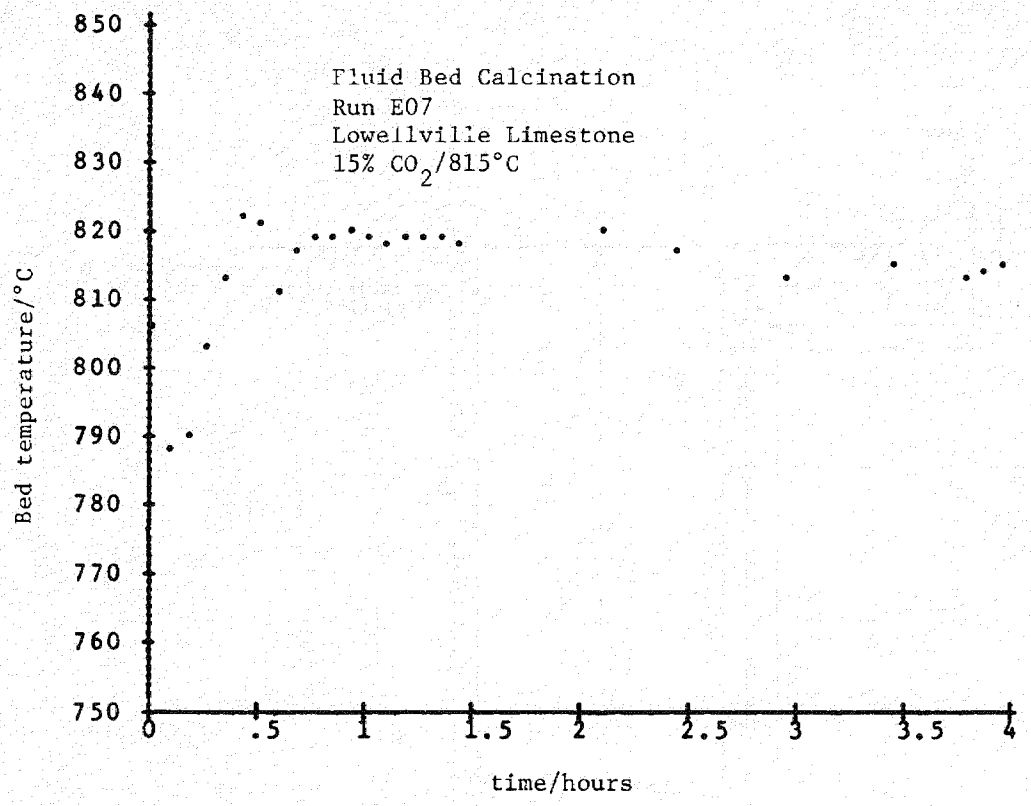

Figure 2-8. Sample Temperature During Fluid Bed Calcination

2.2.2 Materials

The following sorbents were chosen for this study:

Limestone 1359 (Virginia) - (Provides a standard of performance from previous fbc investigations)

Greer Limestone (W. Va.) - (an impure limestone tested previously by Pope, Evans and Robbins which will be used in the ERDA sponsored Rivesville afbc facility)

Dolomite 1337 (Ohio) - (a fairly pure dolomite for which previous fbc performance is available)

Lowellville Limestone (Ohio) - (typical of stones which might be used at the Alliance, Ohio location of the Babcock and Wilcox/ EPRI 6' x 6' fluid bed combustor).

The chemical analysis of the sorbents are shown in Table 2-2 along with grain size estimates.

Calcium and magnesium were determined by EDTA titrations. Sorbents were dissolved in 2M HCl and then neutralized with NaOH. Patton and Reeder's indicator was used

Table 2-2

CHEMICAL ANALYSIS OF SORBENTS

% weight

Stone	Grain Size, μm	Ca	Mg	Na	K	Si	Al	Fe	Acid Insol.	Loss on Calcination
Dolomite 1337	27	21.5	12.9	0.016	0.024	0.20	0.07	0.075	1.2	46.75
Limestone 1359	6	38.5	0.6	0.0022	0.046	0.27	0.12	0.19	1.4	43.84
Lowellville Limestone	40	37.3	0.45	0.012	0.076	0.86	0.37	2.51	3.5	41.83
Greer Limestone										
Batch #1	6	22.4 .	0.9						16.7	36.41
Batch #2		27.2	1.2	0.199	0.842	7.42	2.38	1.45		

to determine calcium at a pH between 12 and 14 where magnesium quantitatively precipitates as hydroxide. Titration using Eriochrome Black T as the indicator gave total calcium and magnesium. The magnesium concentration was then found by subtraction. NBS standard reference material 88a was used to check analytical accuracy. Sodium and potassium were determined by standard atomic absorption analyses of soluble and insoluble fractions. The soluble fraction was defined as that which is soluble in dilute HCl with heating. The insoluble residue was dissolved in hydrofluoric and perchloric acid. Silicon was determined gravimetrically by dehydration with perchloric acid and volatilization with hydrofluoric acid. Aluminum was analyzed by EDTA titration. In sorbents with less than 0.2% iron, a colorimetric determination was made. The other sorbents were assayed for iron by titration with dichromate after reduction to ferrous iron.

Planar grain size estimates were made from optical micrographs taken under polarized light, as shown in Figures 2-9 and 2-10.

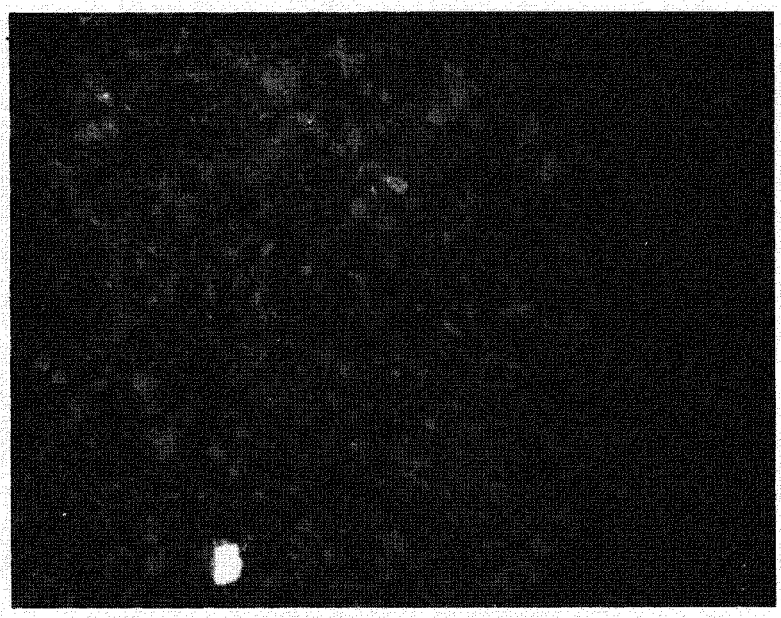

Limestone 1359 (X100)

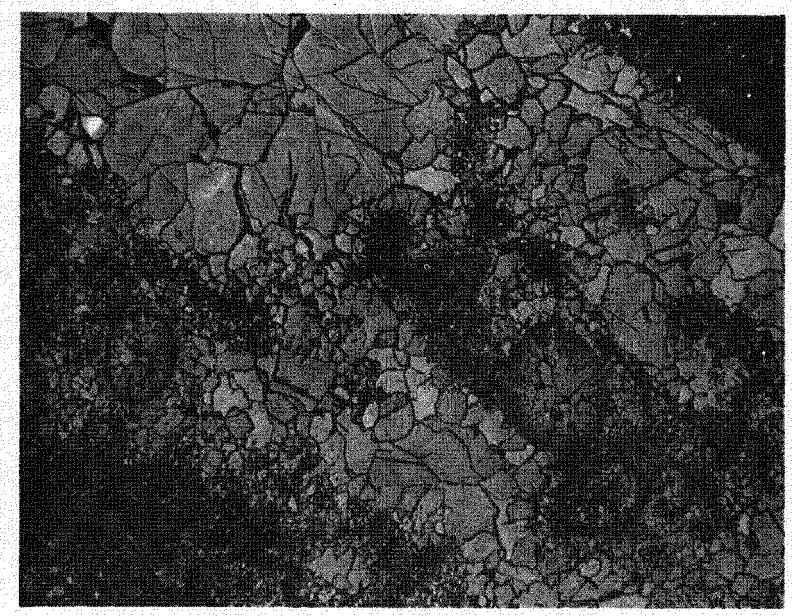

Lowellville Limestone (X100)

Figure 2-9. Optical Micrographs of Sorbents

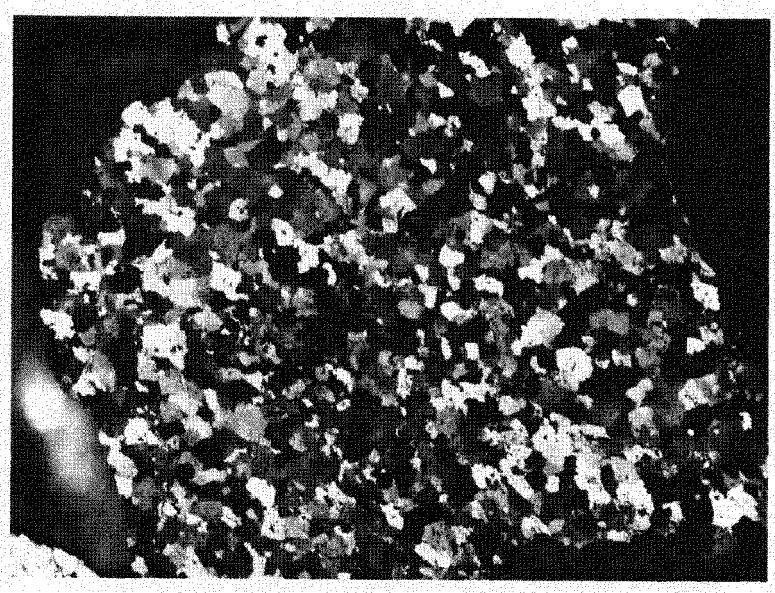

Dolomite 1337 (X50)

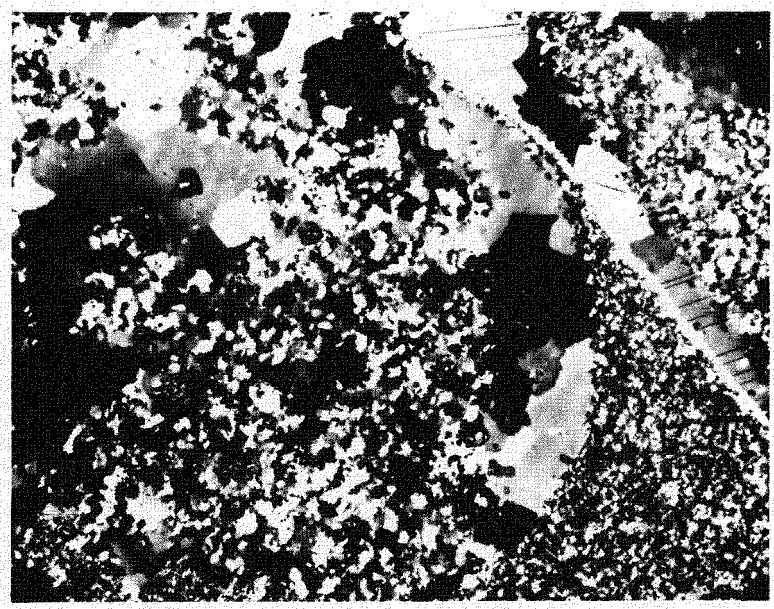

Greer Limestone (X100)

Figure 2-10. Optical Micrographs of Sorbents

Section 3

EXPERIMENTAL RESULTS

3.1 TG CALCINATION EXPERIMENTS

3.1.1 Scope of the Calcination Experiments

The kinetics of limestone calcination were studied in an attempt to simulate the rates of calcination occurring in fluidized beds under various operating conditions. Samples were heated to the temperature of calcination at 10°C/min. Continuous monitoring of temperature, weight, and time occurred as each sample was calcined in various atmospheres of nitrogen and carbon dioxide. The atmosphere of a fluidized bed combustor was simulated: carbon dioxide levels were representative of those released from fuel combustion and from calcination. Unlike sorbents in the fluid bed, samples in the TGA were not exposed to shock heating because of the limited heating rates available with this type of apparatus. Sorbents could be calcined isothermally or nonisothermally (at a constant heating rate) depending on the atmosphere in which it was heated to temperature. In isothermal calcinations, the sorbent was preheated to temperature in a partial pressure of CO_2 greater than the equilibrium pressure. Once the desired temperature was attained the CO_2 concentration was decreased to that of the calcination study.

The nonisothermal calcinations were used to deduce kinetic parameters for the reaction, and, to some extent, simulate the sorbent's exposure to temperature change when heated in a fluid bed.

3.1.2 Nonisothermal Calcinations in Nitrogen

In nonisothermal calcinations weight loss measurements were taken as the sample was heated at a constant rate. The data were plotted using the method of Coats and Redfern[13] in the form of $F(\alpha)$ vs $1/T$, where

$$F(\alpha) = - \ln \frac{1-(1-\alpha)^{1-n}}{(1-n)\ T^2}$$

α = Fraction of sorbent calcined

T = Temperature, K

n = "order" of reaction, 2/3

The slope yields the activation energy (slope = $-E_a/R$) and the intercept may be used to deduce an average value of the pre-exponential factor, A

$$\text{intercept} = \ln \frac{A\,R}{BE_a} \left\{ 1 - \frac{2\,RT}{E_a} \right\}$$

R = gas constant

B = heating rate (K/min)

Some authors prefer to designate A and E_a as temperature coefficients of reaction, rather than identifying them as the activation energy and pre-exponential factor, respectively.

Previous data on the nonisothermal calcination of Limestone 1359 gave A and E_a values of $(5.01 \pm 1.96) \times 10^5$ sec^{-1} and (40212 ± 1000) cal $mole^{-1}$ at a mean particle size of 498 microns. If the decomposition is simply a function of surface area, then increasing the particle size to 16/18 mesh (1095 μm) should only affect the A factor. The results of nonisothermal tests on 16/18 mesh Limestone 1359 confirm this with measured values of E_a = (39603 ± 502) cal/mole and $A = (2.89 \pm 0.72) \times 10^5$ sec^{-1} where the predicted value of A would be 2.28×10^5 sec^{-1}. Both measurements are within their average deviations.

Nonisothermal parameters for the four sorbents are shown below:

Stone	E_a (cal/mole)	A(sec^{-1})
1359 (8 runs)	39,683 ± 502	$(2.89 \pm 0.72) \times 10^5$
Greer (4 runs)	41,470 ± 2049	$(9.39 \pm 5.24) \times 10^5$
1337 (2 runs)	46,812 ± 672	$(2.21 \pm 0.61) \times 10^7$
Lowellville (1 run)	41,688	1.38×10^6

The poor homogeneity of Greer limestone is reflected in the larger average deviations obtained for the stone. The high activation energy of the dolomite could be due to retardation of the reaction by CO_2 generated when the magnesium fraction calcines.

Sample plots for each sorbent according to the Coats and Redfern analysis are shown in Figures 3-1 through 3-4.

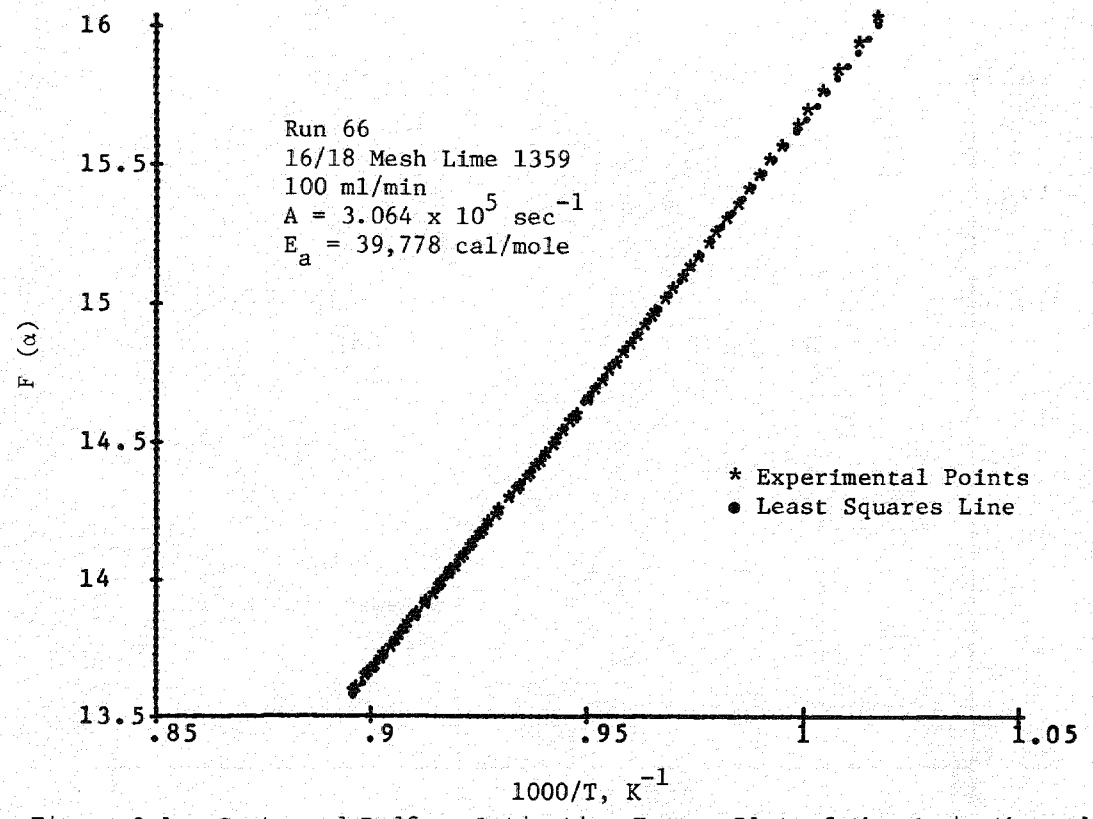

Figure 3-1. Coats and Redfern Activation Energy Plot of the Nonisothermal Calcination of Limestone 1359 in N_2

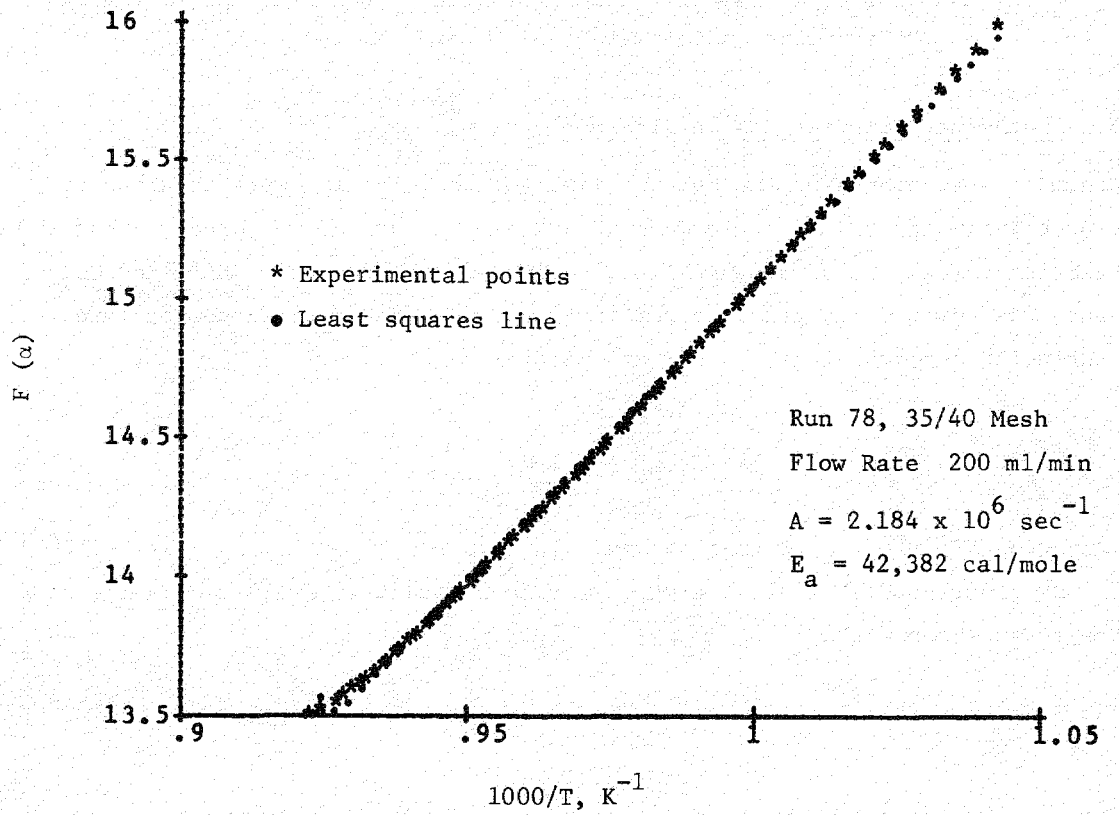

Figure 3-2. Coats and Redfern Activation Energy Plot for the Nonisothermal Calcination of Greer Limestone in N_2

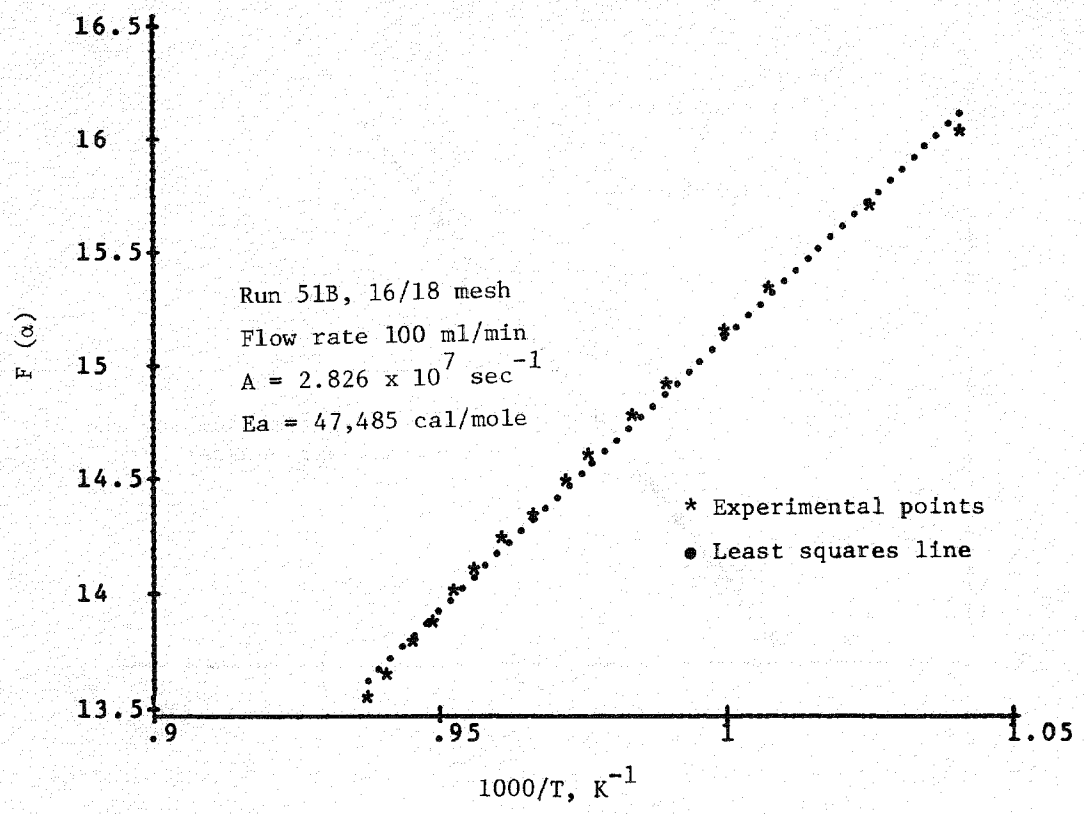

Figure 3-3. Coats and Redfern Activation Energy Plot of the Nonisothermal Calcination of Dolomite 1337 in N_2

3.1.3 Isothermal Calcinations in Nitrogen

Isothermal measurements of the rate of limestone calcination were obtained by heating the sorbent to temperature in a partial pressure of CO_2 greater than the equilibrium value. This postponed calcination of the limestone until the CO_2 pressure was lowered and all calcination occurred at the desired temperature. The shrinking core model of a spherical particle

$$\left(\frac{d\alpha}{dt} = K(1-\alpha)^{2/3}\right)$$

was used to calculate the rate constant. Integration gives $G(\alpha) = 3[1-(1-\alpha)^{1/3}] = Kt$. By plotting $G(\alpha)$ against time, the rate constant is evaluated as the slope of the least squares line.

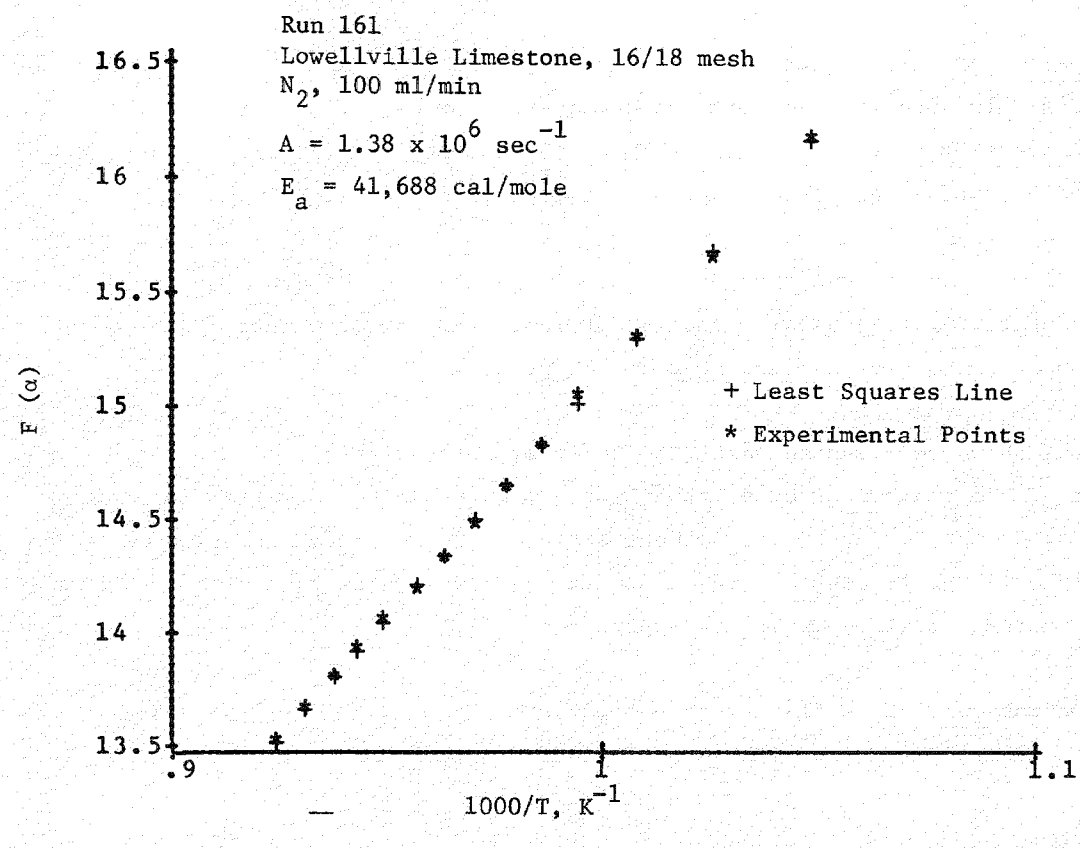

Figure 3-4. Coats and Redfern Activation Energy Plot of the Nonisothermal Calcination of Lowellville Limestone in N_2

The isothermal calcination of 16/18 mesh limestone 1359 in N_2 at 830 (see Figure 3-5) yielded a rate constant of 0.2593 min^{-1}. The predicted value from the reported nonisothermal parameters is 0.239 min^{-1}. Thus, the shrinking core model for calcination provides an adequate description of limestone calcination in nitrogen of 1,000 micron size particles.

3.1.4 Isothermal Calcination in Carbon Dioxide

The isothermal calcination in carbon dioxide/nitrogen mixtures was studied in order to test the extent to which the ambient partial pressure of carbon dioxide suppresses reaction. The literature contains several works in which it is assumed that the reaction rate is suppressed by the factor $(1 - P_{CO_2}/P_{eq})$.[15] (See Appendix 1.)

The experiments carried out are summarized in Tables 3-1 and 3-2. The derived rate constants were compared with those obtained by calculating the rate from the A and E_a parameters and adjusting them by the suppression factor. In general, the predicted rate was 3 times faster than the observed rate.

For the lower temperature runs, a definite accelerating phase was observed: such an accelerating rate phase is usually attributed to the growth of nuclei of decomposition over the external surfaces of the particles.

This could have been caused partly by the time interval required to sweep excess CO_2 out of the reactor or by an annealing effect reducing potential nucleation sites for decomposition on the sorbent surface. The delay in removing CO_2 was probably only partly contributing since it was not evident to the same extent in the isothermal experiments in nitrogen.

The repeatability of isothermal rate constants in CO_2 was poor. At 814°C in 10% CO_2, the following results were obtained for 16/18 mesh limestone 1359:

Run No.	K (min^{-1})
39	2.89×10^{-2}
57	2.79×10^{-2}
58	1.58×10^{-2}

In 17% CO_2 at 830°C, results were:

Run No.	K (min^{-1})
40	2.432×10^{-2}
59	8.080×10^{-3}

The poor reproducibility of the isothermal rate constants may be attributed to the fact that the entire reaction in CO_2 does not follow the shrinking core model, as illustrated by the lack of linearity for nonisothermal data taken in CO_2 (TG-60 see Figure 3-6). Due to this poor fit, isothermal rate constants were measured from the initial 20% of reaction only (see Figure 3-7).

Table 3-1

ISOTHERMAL CALCINATION OF LIMESTONE 1359

RUN NO.	FLOW RATE (ml/min)	% CO_2	TEMPERATURE °C	U.S. MESH STONE SIZE	K(MIN^{-1})	COMMENT
FBCAL TG8,3	600	15	817	16/18	4.455×10^{-2}	Stone used was previously nonisothermally calcined and recarbonated
FBCAL TG9,3	600	15	815	35/40	2.849×10^{-2}	
Run 24	600	5.61	816	16/18	1.376×10^{-2}	
Run 25*	600	5.61	828	16/18	2.571×10^{-2}	
Run 26*	600	15	827	16/18	1.419×10^{-2}	
Run 27*	600	15	850	16/18	2.163×10^{-2}	
Run 28*	600	22	850;872	16/18	1.436×10^{-3}	Points taken were at initial T of 850°C
Run 39	100	10	814	16/18	2.886×10^{-2}	
Run 40	100	17	830	16/18	2.432×10^{-2}	
Run 57	100	10	814	16/18	2.789×10^{-2}	
Run 58	100	10	812	16/18	1.583×10^{-2}	
Run 59	100	17	830	16/18	8.080×10^{-3}	
Run 60	100	10	830	16/18	1.635×10^{-2}	

*Reaction did not go to completion

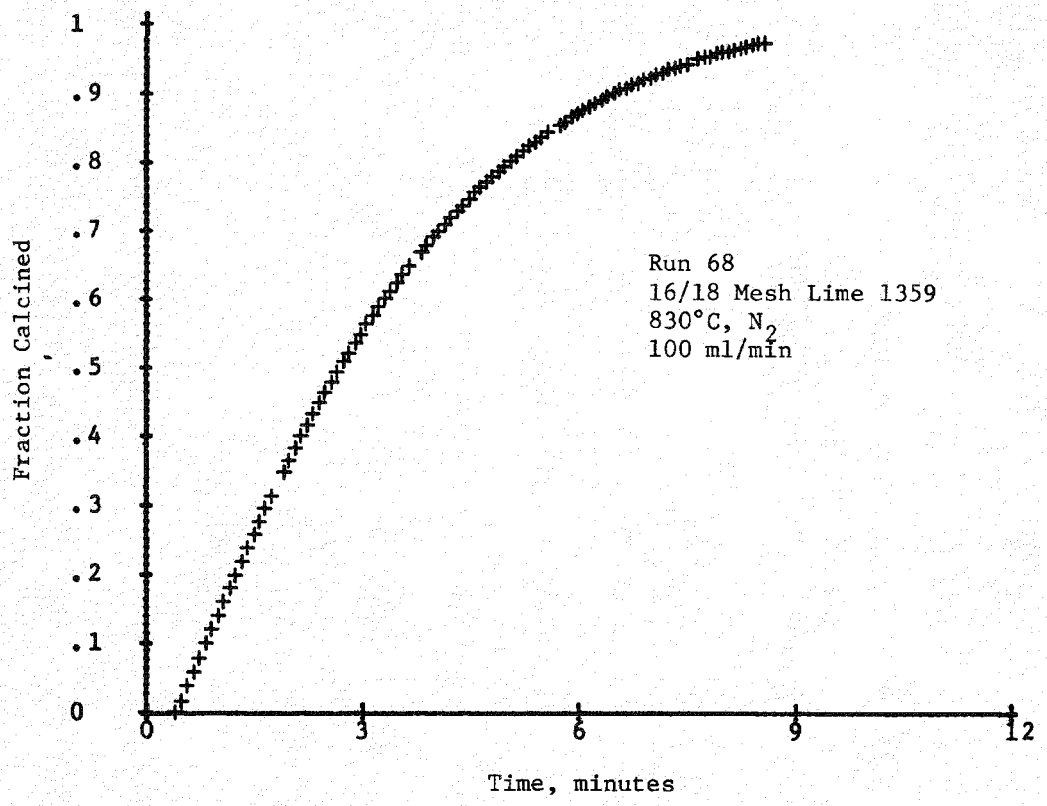

Figure 3-5. Isothermal Calcination of Limestone 1359 in N_2

Table 3-2

ISOTHERMAL CALCINATION OF LIMESTONE 1359 IN NITROGEN CONTAINING CARBON DIOXIDE

T	P_{eq}	P_{CO_2}	$1 - \frac{P_{CO_2}}{P_{eq}}$	K NON-ISO. PREDICTION	K MEASURED
814	0.2501	0.10	0.6002	0.1043	0.029
815	0.2543	0.15	0.4102	0.0725	0.028
816	0.2586	0.0561	0.7830	0.1407	0.0138
817	0.2629	0.15	0.4294	0.0784	0.045
827	0.3098	0.15	0.5158	0.1111	0.0142
828	0.3149	0.0561	0.8218	0.1799	0.025
830	0.3252	0.17	0.4773	0.1079	0.024
850	0.4468	0.22	0.5077	0.1579	0.0014
814	0.2501	0.10	0.6002	0.1043	0.028
812	0.24	0.10	0.5833	0.1014	0.016
830	0.3252	0.17	0.4772	0.1079	0.0081
830	0.3252	0.10	0.3075	0.0695	0.016

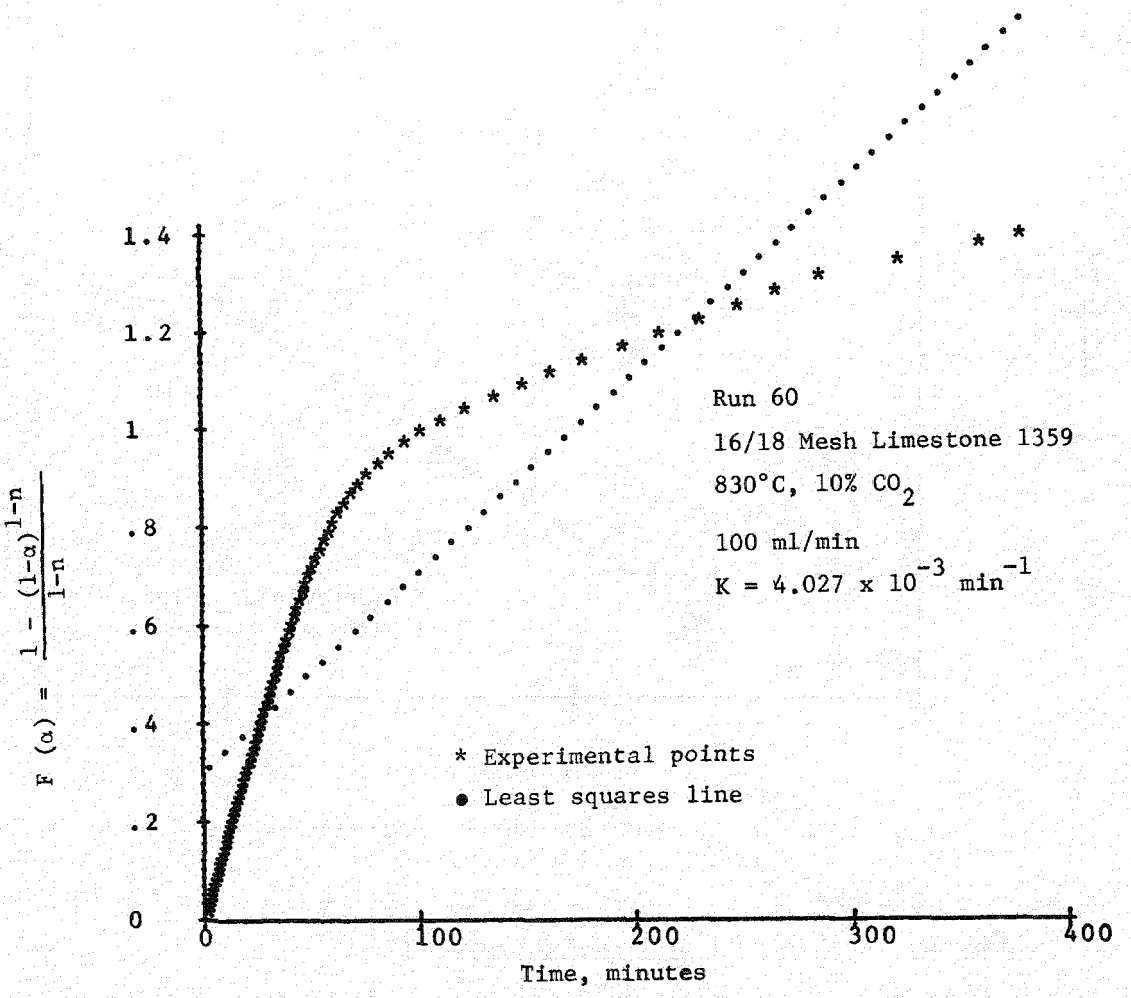

Figure 3-6. Isothermal Calcination of Limestone 1359 in CO_2, Entire Reaction

Whatever the reason for suppression by CO_2, it is clear that the reaction is slower than would be predicted, and these results are in agreement with fluidized bed results, as determined by CO_2 evolution curves. The TG isothermal data predict the following times for fluid bed calcination at 815°C in 15% CO_2:

Sorbent	Calcination Time
1359	160-400 minutes
Greer	95-230
1337	92 minutes
Lowellville	240 minutes

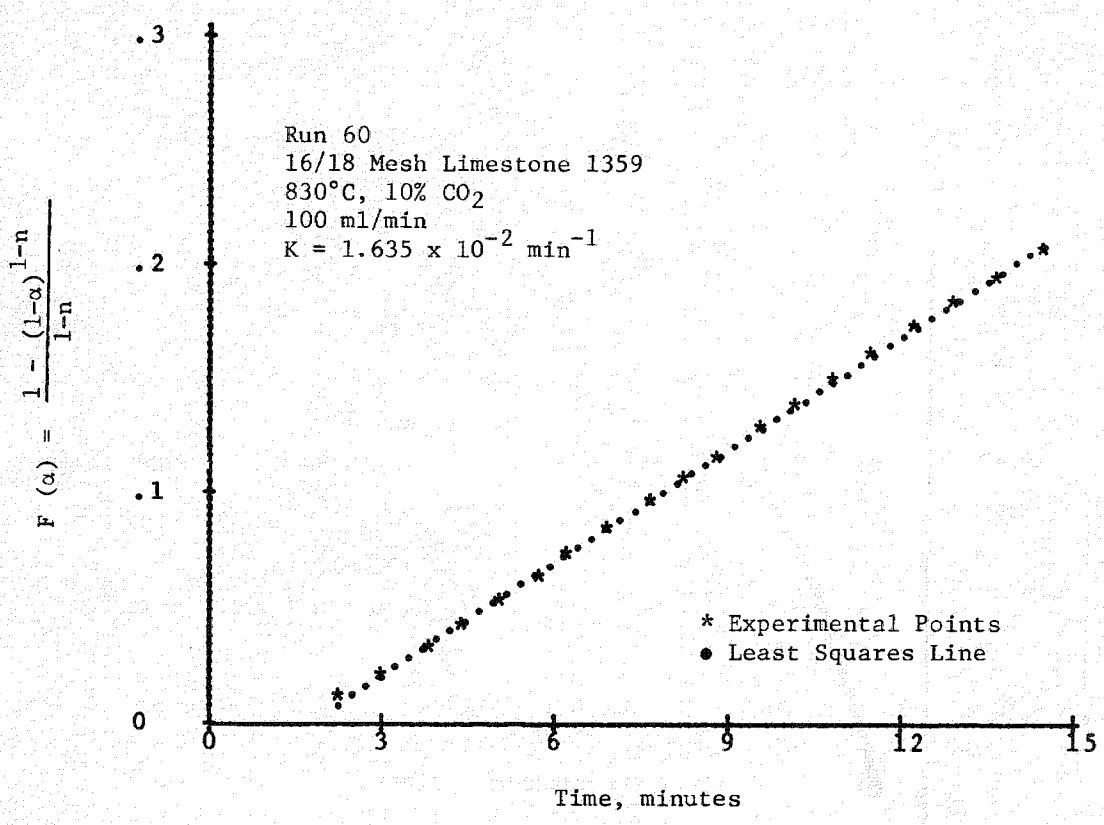

Figure 3-7. Isothermal Calcination of Limestone 1359 in CO_2, Initial 20% of Reaction

3.1.5 Nonisothermal Calcinations in Carbon Dioxide

Because the C&R plot[13] offers a rapid method of deriving parameters which describe the calcination over a wide range of temperature, we tested the possibility that running nonisothermal experiments in a fixed partial pressure of carbon dioxide would yield A and E_a values applicable to the derivation of calcination rates retarded by carbon dioxide.

The activation energy for limestone 1359 reflects retardation of calcination due to 10% CO_2 (E_a = 103,586 ± 6106 cal/mole). However, the C&R plot had a distinct curvature (see Figure 3-8). This is further evidence that the shrinking core model may not be valid in calcinations with CO_2.

Two runs on 1000 μm dolomite 1337 in 10% CO_2 gave E_a = (47611 ± 1964) cal/mole. The C&R plot was linear (see Figure 3.1.9), but the activation energy did not reflect the retardation of reaction in CO_2. Evidently, the CO_2 produced from the magnesium fraction calcining has about the same retardation effect in N_2

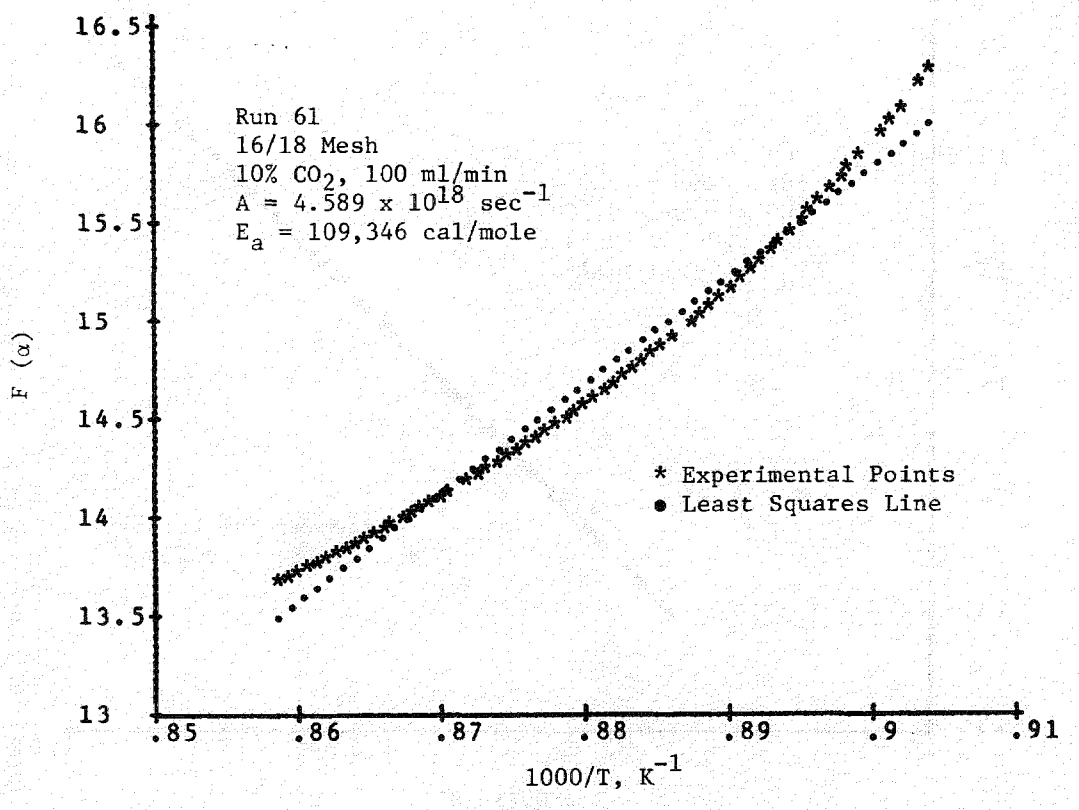

Figure 3-8. Coats and Redfern Activation Energy Plot of the Nonisothermal Calcination of Limestone 1359 in CO_2

or 10% CO_2. Furthermore, the linear C&R plot indicates the calcination is occurring as if unaffected by CO_2. This could be the case if the CO_2 produced by the magnesium fraction calcining postpones the calcium calcination until higher temperatures are reached. Here, 10% CO_2 is much less than the equilibrium pressure of CO_2, and the reaction more closely parallels one in nitrogen.

The kinetic parameters obtained for Greer limestone weren't repeatable. This could be due to the wide variation in chemical composition of the stone and the presence of much coal found in the first batch of Greer limestone.

The A and E_a values were relatively poor predictors of rate as measured in isothermal experiments, as shown below. This resulted partly from the fact that the rates measured isothermally in carbon dioxide were not very reproducible.

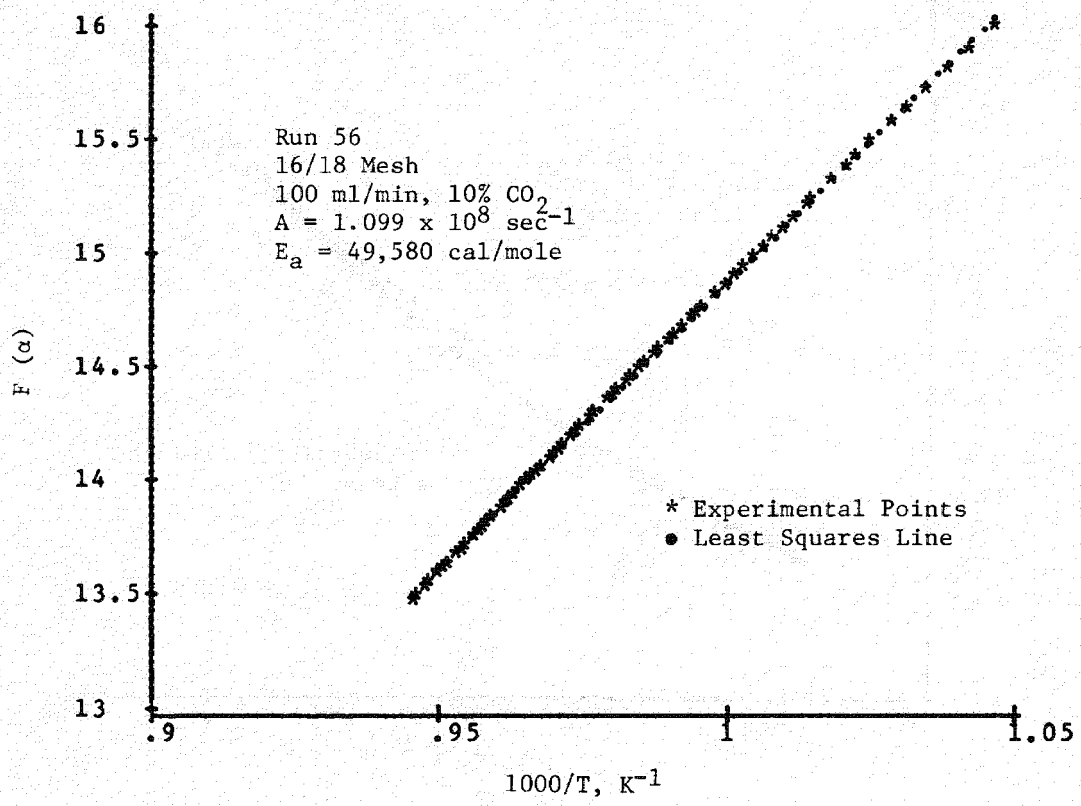

Figure 3-9. Coats and Redfern Activation Energy Plot of the Nonisothermal Calcination of Dolomite 1337 in CO_2

It was concluded that A and E_a values obtained by this method should not be used to project isothermal rates of reaction in carbon dioxide.

Nonisothermal Values Limestone 1359, 15% CO_2

A	E_a	k_{pred}	k_{obs}
3.21×10^{22}	130,649	0.073	0.022 (850°C)
		0.022	0.014 (827°C)
			0.026

Nonisothermal Values Limestone 1359, 10% CO_2

A	E_a	k_{pred}	k_{obs}
2.00×10^{18}	103,586	0.18	0.016
		0.36	0.024

3.1.6 Fluid Bed Calcination Experiments

Four calcination experiments were performed in the fluidized-bed unit in preparation for subsequent experiments in which calcined lime would be generated under different partial pressures of carbon dioxide.

These four experiments were carried out by heating a charge of 70 g of sized limestone to 815°C, and then fluidizing the bed at about 2.5X minimum fluidizing velocity (as determined by visual observation at room temperature and then temperature corrected).

The equilibrium partial pressure of carbon dioxide at 815°C is 0.254 atm.[15] In the lower gas flow rates (required to fluidize the two finer-sized batches of limestone) the rate of reaction was sufficiently fast to generate the equilibrium CO_2 composition in the outlet gas: the weight loss in these experiments corresponded to increasing the carbon dioxide pressure to 0.247 and 0.256 atm. throughout the thirty minutes of the experiment.

The calcination studied in the first experiment was clearly not limited by equilibrium production of carbon dioxide, and so an attempt was made to calculate the rate of decomposition of the limestone from the observed weight loss. The average rate of decomposition (probably almost constant over the first 50% of the stoichiometric reaction) was corrected for the prevailing carbon dioxide atmosphere to yield the isothermal rate of reaction. This rate is shown in Figure 3.1.10 and compared with the projected rate from TG experiments and with the literature data on the isothermal rate of reaction. The spread in the value for the fluidized-bed experiment is caused by uncertainty in the time period; since the sample self-cooled initially, the period of time the reaction proceeded at 815°C may have been only twenty minutes.

The conditions for the first six trials are summarized in Table 3-3. The non-homogeneous product obtained at 53 cm/sec from E-0-1 (noted by extreme color variation of different particles, and the uncalcined state of some particles, as determined by TG analysis) indicated that the velocity was too low for good solid mixing. The Greer stone was therefore calcined at superficial velocities ranging from 57 to 130 cm/sec. The extent of calcination noted, as determined by weight loss (elutriation was negligible) appeared to increase with superficial velocity. This led to the conclusion that calcination was suppressed to a greater extent in the fluidized bed than in the TG experiments. However, later

Table 3-3

Fluid Bed Calcination of Sorbents (14/18 Mesh)

STONE	T°C	GAS CO_2/N_2	TIME MIN.	% WT. LOSS	VEL cm/sec	COMMENT	EXPT. NO.
1359	815	15/85	120	22.92	53	Non-homogeneous product Probably not fluidized	E-0-1
1359	815	0/100	120	43.86	53	Non-homogeneous product Probably not fluidized	E-0-2
Greer	815	15/85	120	32.20	57	Non-homogeneous product Probably not fluidized	E-0-3
Greer	815	15/85	120	29.35	81		E-0-4
Greer	815	15/85	120	30.58	100		E-0-5
Greer	815	15/85	124	36.01	130		E-0-6
Lowellville	815	15/85	240	40.95	81		E-0-7
Glasshouse (1337)	815	15/85	240	47.59	81		E-0-8
1359	815	15/85	240	33.54	81	Incomplete calcination	E-0-9
Greer	815	15/85	240	31.10	81		E-0-10
Lowellville	900	60/40	90	30.11	81		E-0-11
1337	900	60/40	82	45.68	81		E-0-12
Greer	815	0/100	240	39.04	81		E-0-14
1337	900	15/85	82	67.12	81		E-0-15
Greer	900	15/85	50	38.36	81	Heated at 900 for additional 70 min in air	E-0-16
1359	900	14.4/85.6	120	38.54	81		E-0-17
Greer	900	14.4/85.6	120	38.26	81	See CO_2 Evolution Curve	E-0-18
Greer	900	60/40	120	27.58	81	Incomplete calcination	E-0-20
1359	900	60/40	120	--	81	Incomplete calcination	E-0-21

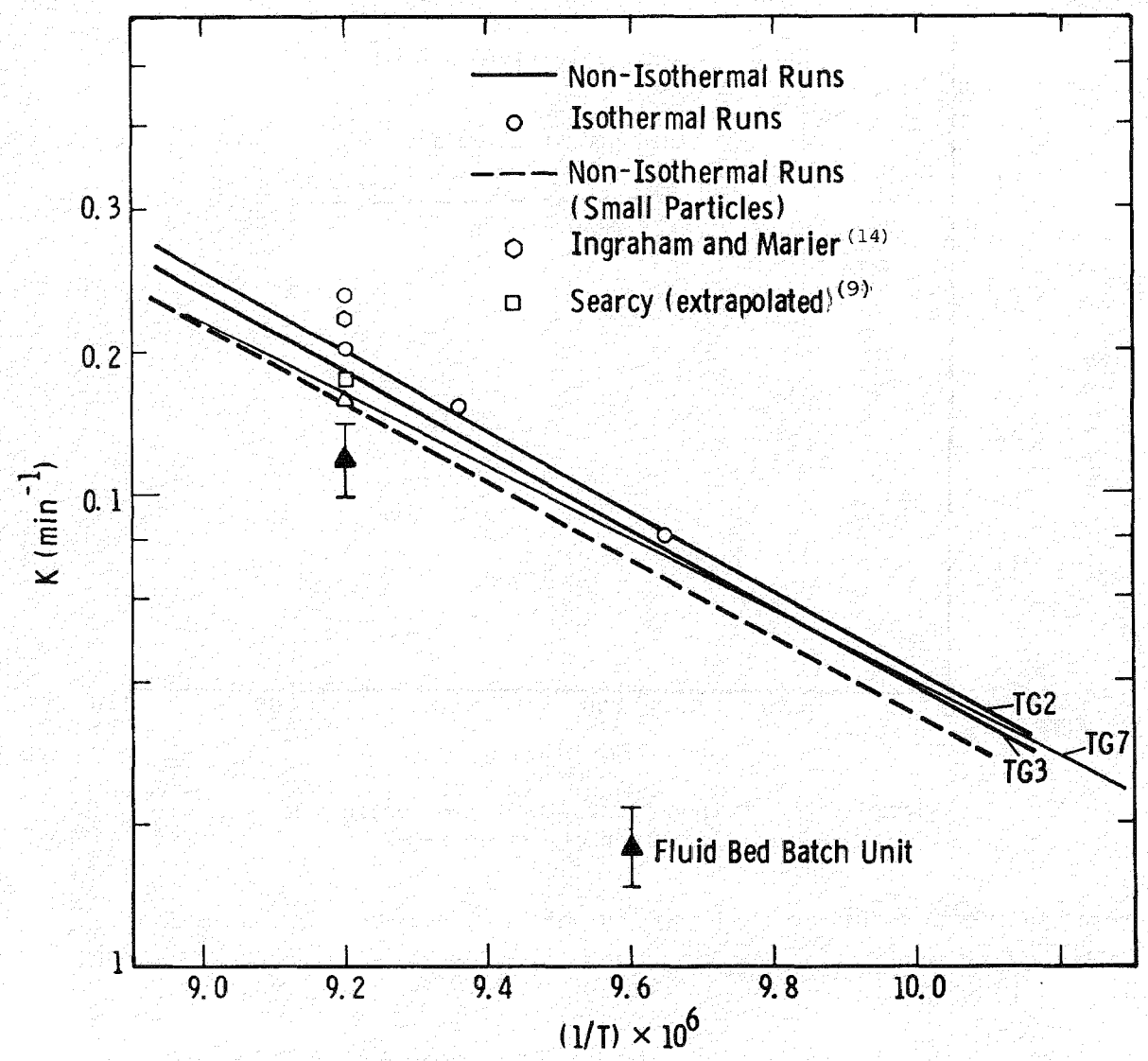

Figure 3-10. The Calcination of Limestone - Estimates of Reaction Rate for 1187 Micron Diameter Particles[14,9]

results from TG calcinations showed that the average weight loss from this sample of Greer limestone in calcination was 35.84 ± 3.12%, so there is no significance in the variation of weight loss observed over the superficial velocity range of 0.57-1.30 m/sec (1.87-4.27 ft/sec).

Samples of the effluent gas were taken at regular intervals during the calcination of E-0-7 and E-0-18. Figure 3-11 shows the CO_2 evolution during the calcination of the Lowellville stone. The two odd values, have been ignored in drawing the trend line, since the mass balance for the system refutes their validity. The

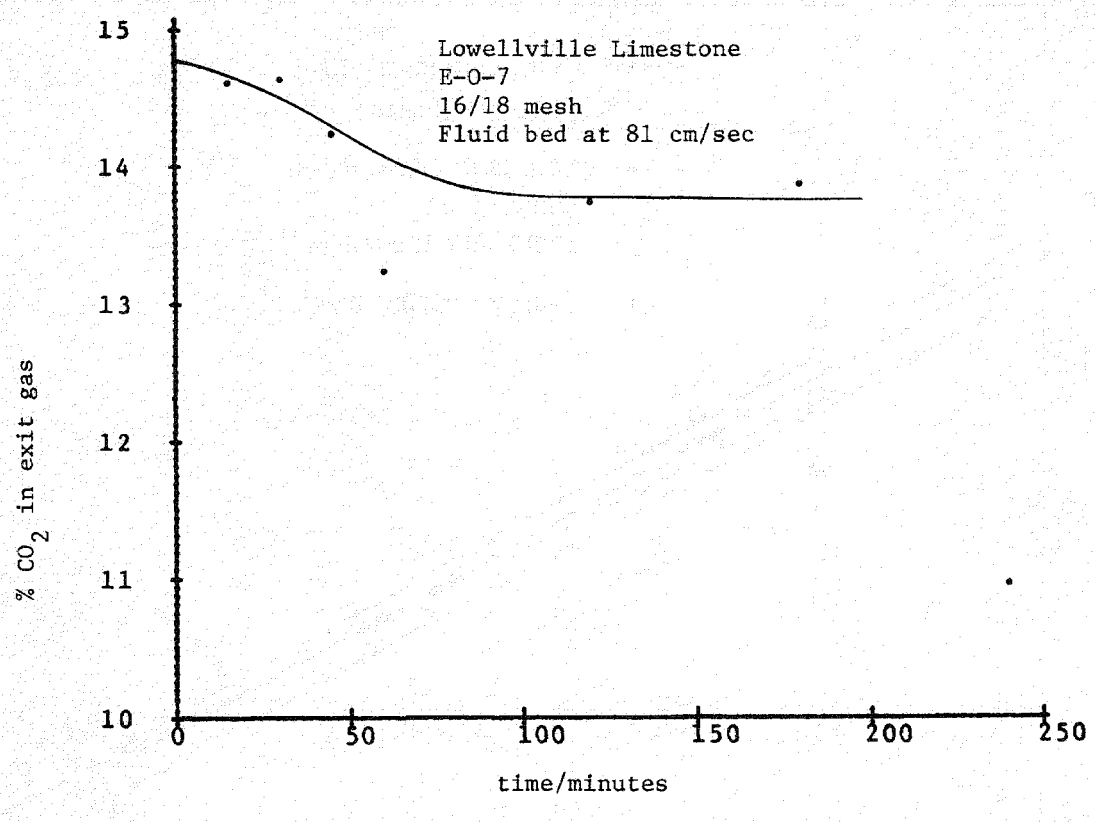

Figure 3-11. Carbon Dioxide Evolution during the Calcination of Sample E-0-7

evolution curve is similar to the values obtained for E-0-4 with Greer stone which showed that reaction had been completed after about 70 minutes, in accord with the TG results.

The scatter apparent in the gas chromatographic determinations suggest that they may only be useful as rough guides to the course of reaction. However, it seems that in the first 20 minutes, calcination is fairly rapid. The later stages of calcination are apparently very slow, and it may be that the influence of diffusion of CO_2 from the inner core through the oxide product is becoming rate controlling, because of the slow "sintering" of the product oxide layer.

The CO_2 evolution curve produced from the calcination of Greer limestone, run E-0-18 in the fluidized bed unit, shows that the reaction was ∿80% complete in the first ten minutes, (Figure 3-12). This correlates well with the TG calcination run No. 93, in which 90% of the weight loss occurred in the first ten minutes of calcination.

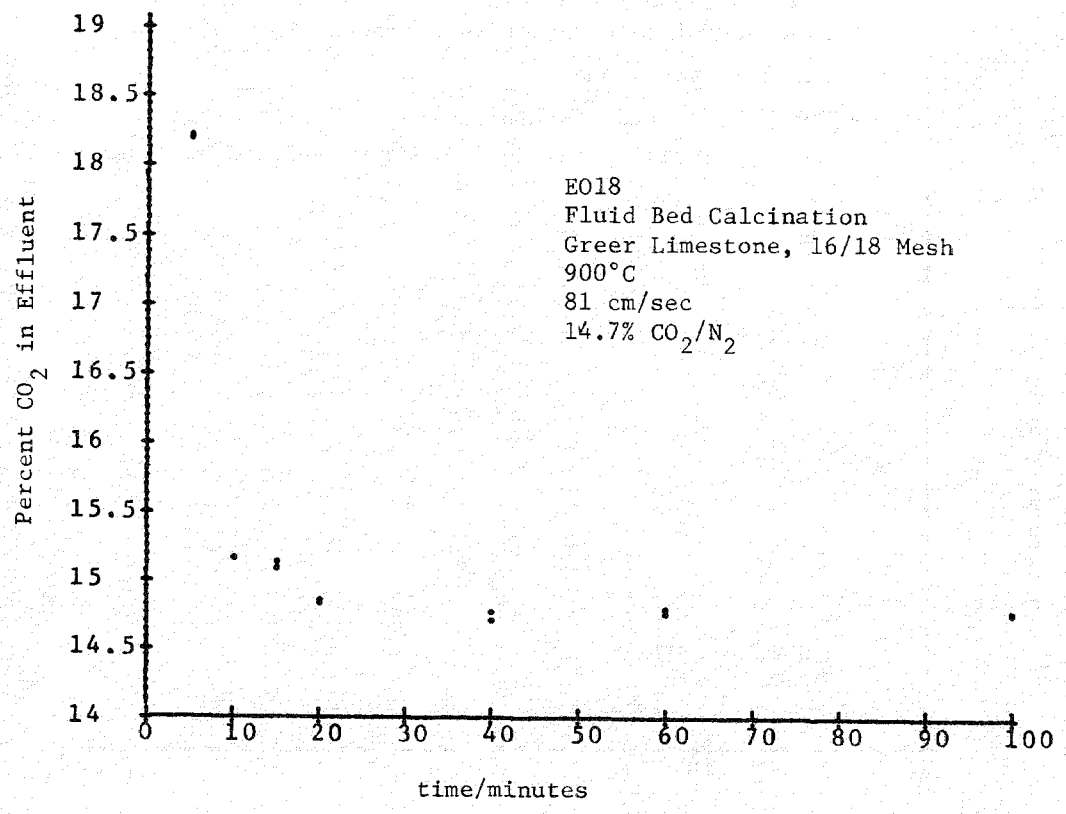

Figure 3-12. The Evolution of CO_2 in the Calcination of Greer Limestone at 900°C

Additional fluid bed calcines were prepared for comparison with the sulfation properties of calcines prepared in the TGA. A list of these calcines is shown in Table 3-3. A comparison of weight loss measurements indicate that samples E-0-9, E-0-20, and E-0-21 may have suffered incomplete calcinations. Calcinations in the TGA of the residual carbonate were studied to determine if these sorbents were incompletely calcined or if recarbonation of the stone had occurred while cooling in the fluid bed.

The nonisothermal calcination of recarbonated limestone 1359, fluid bed calcine E-0-1, and the raw sorbent are compared in Figure 3-13. The calcination of the fluid bed stone is distinctly slower than that of the raw stone and the recarbonated stone. Since the decomposition is a function of surface area only, and recarbonation proceeds from the outer surface inward, the recarbonated particle behaves similar to the raw stone until the CaO core is reached. Had incomplete calcination occurred in the fluid bed, a particle would act as a

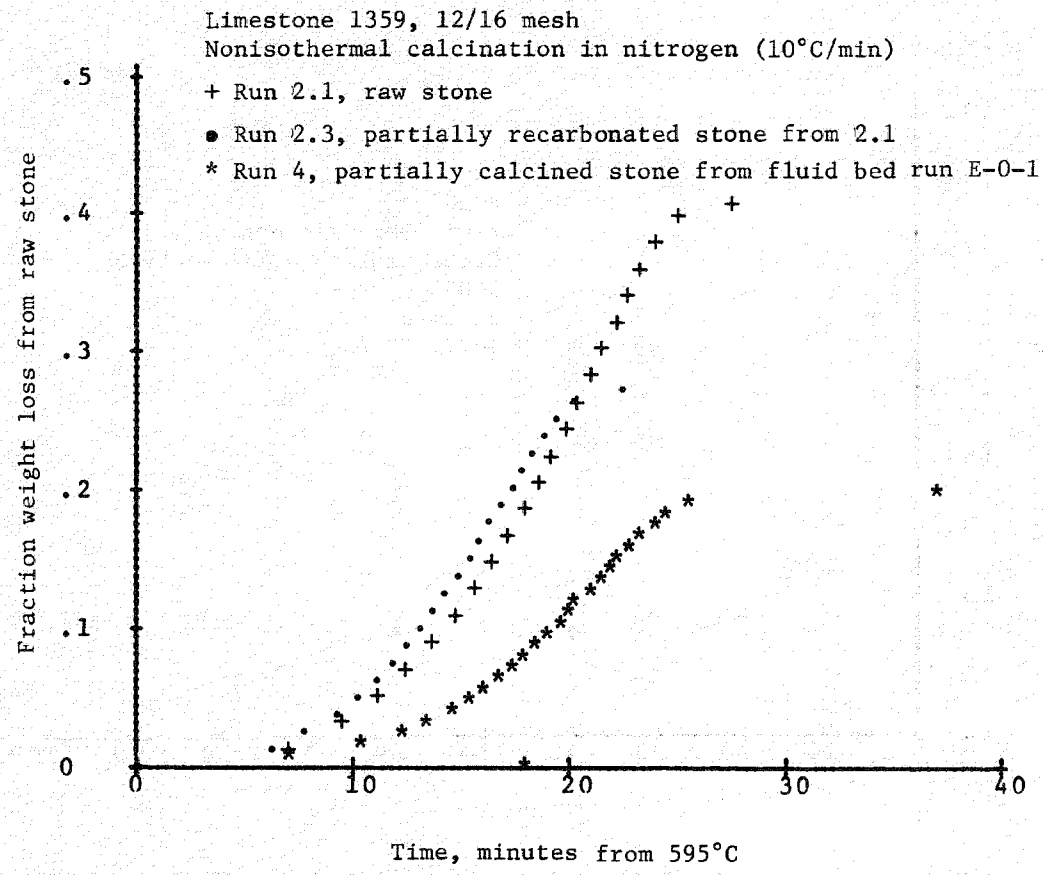

Figure 3-13. Nonisothermal Calcinations of Raw, Recarbonated, and Partly Calcined Limestone 1359

calcining particle with a smaller radius. The activation energies and the pre-exponential factors derived from Coats and Redfern plots of these three calcinations reflect this relationship:

TG Run	E_a (cal/mole)	A(sec^{-1})
2.1 (raw stone)	38030	1.4×10^5
2.3 (recarbonated stone)	38455	1.8×10^5
4 (fluid bed calcine)	39388	4.1×10^5

All three runs gave activation energies close to the average reported for limestone 1359 (39683 ± 502 cal/mole). The A values are similar for the raw and recarbonated stones; however, the fluid bed calcine shows a larger A, close to that expected for a smaller radius stone. Therfore, given a fluid bed calcine with incomplete weight loss, a distinction between an incompletely calcined stone and a stone which was calcined, but picked up some CO_2 while cooling, can be made.

Calcination of the residual carbonate of fluid bed samples E-0-9 and E-0-21 indicated that the stones were incompletely calcined in the fluid bed (See Figure 3-14). However, calcination of fluid bed calcined Greer limestone (E-0-20) was inconclusive (See Figure 3-15) in that the calcination is initially faster than that of the raw sorbent, and then gradually falls behind. It may be that the stone was both incompletely calcined and partially recarbonated, or the impurities in the Greer stone may account for the difference in initial weight loss. Since this Greer stone (E-0-20) was calcined under the same conditions as E-0-21, a limestone 1359 sample which did not completely calcine, this sorbent may have also been incompletely calcined in the fluid bed.

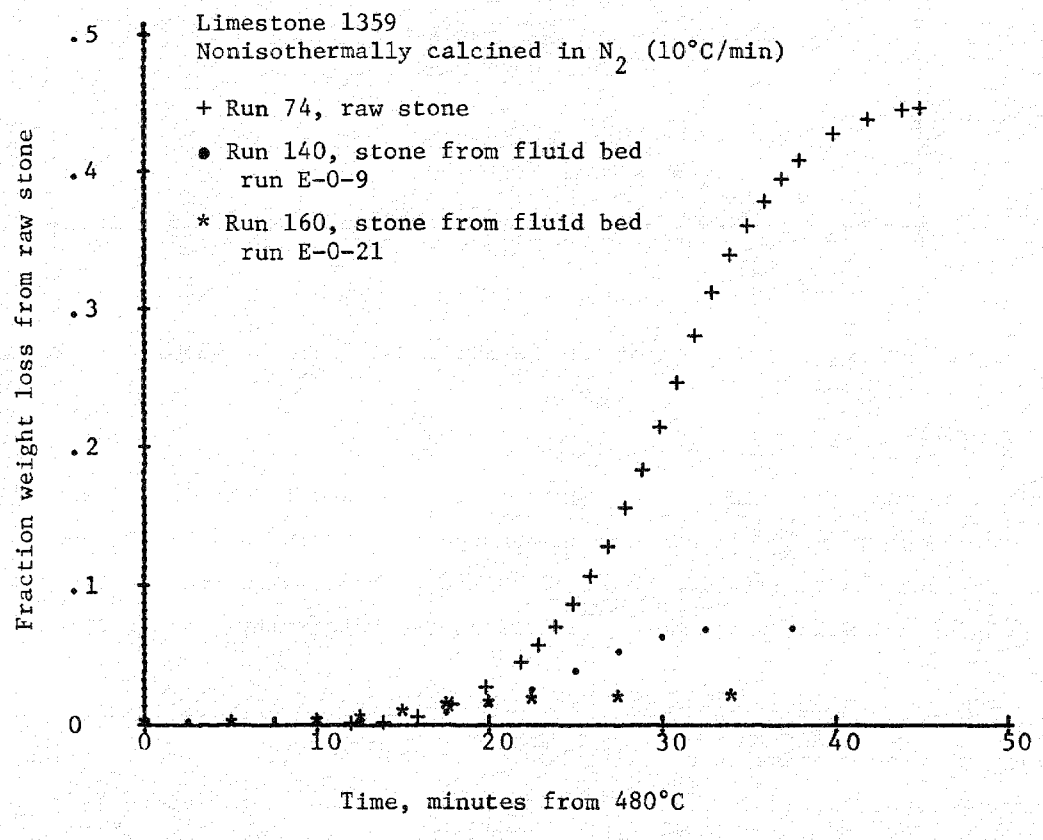

Figure 3-14. Calcination of the Residual Carbonate of Samples E-0-9 and E-0-21

3.2 SULFATION EXPERIMENTS

Thermogravimetric sulfations were carried out on calcines prepared in the fluid bed unit and in the TGA to determine the effect of limestone calcination conditions on the subsequent sulfation of the calcines. The data for the sulfation experiments and a list of the sulfation experiments carried out are shown in Appendix 3.

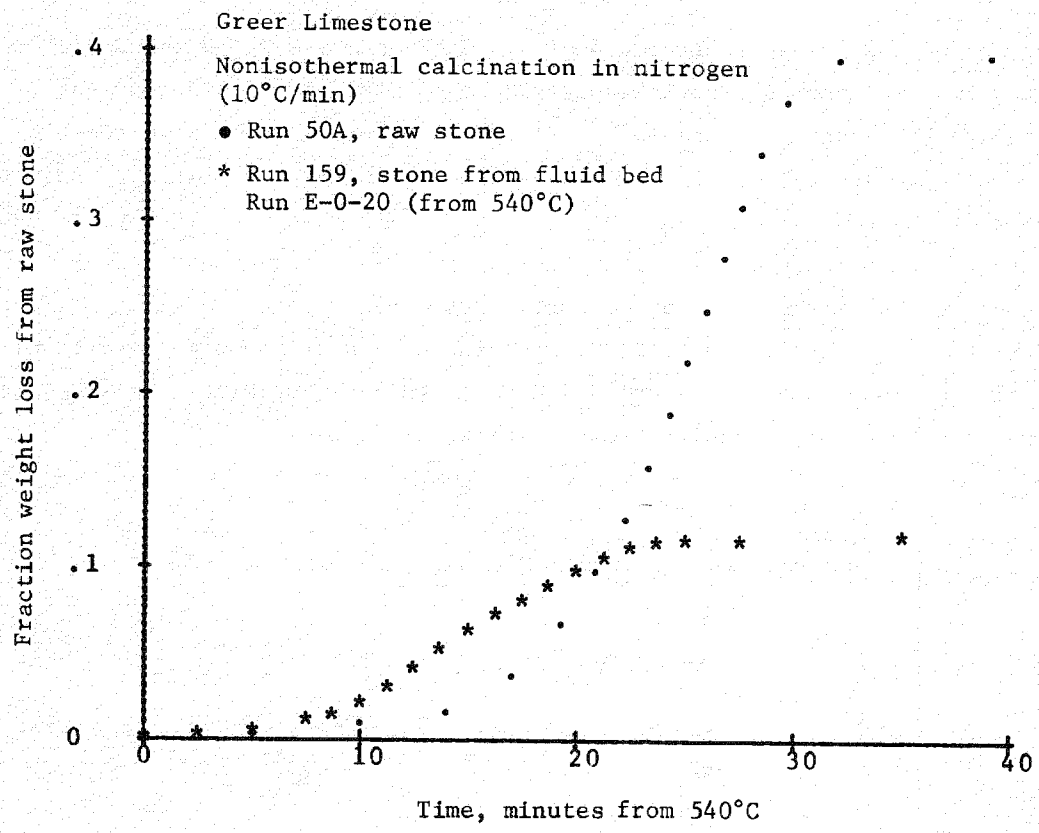

Figure 3-15. Calcination of the Residual Carbonate of Sample E-0-20

3.2.1 Sulfations at 815°C

Sulfations of numerous calcines, prepared on the TGA and in the fluid bed unit, were carried out at 815°C in a nitrogen atmosphere containing 0.5% SO_2 and 4% O_2. The extent of sulfation obtained by the sorbents when the rate fell below 0.1% Ca sulfating per minute was used as the reactivity index for the calcines.

The sorbent effectiveness on a weight basis was dolomite 1337 > Lowellville limestone > limestone 1359. Greer limestone was more easily affected by calcination conditions, so its ranking varied. A summary of the sulfur sorption obtained for the sorbents calcined under different conditions follows:

Sorbent	SO_3 Pickup (mg/mg Raw Stone)				
	TG, N_2 at 815°C	TG, 15% CO_2 at 815°C	Fluid Bed 15% CO_2 at 815°C	TG, 60% CO_2 at 900°C	Fluid Bed 60% CO_2 at 900°C
1337	0.22	0.34	0.42	0.36	0.43
Lowellville	0.13	0.18	0.22	0.29	0.32
1359	0.08	0.09	0.09	0.28	0.20
Greer	0.09	0.16	0.31	0.31	0.26

Repeatability of Sulfation Results. The repeatability of the sulfation results was excellent. Table 3-4 shows the extent of sulfation achieved for like runs, based on the reactivity index (the rate necessary to maintain 80% sulfur removal in a fluid bed).

Comparison of Sulfation Data for Fluid-Bed and TG Calcines. Comparisons of the extent of sulfation of fluid-bed calcines with similar TG calcines were good except for Greer limestone. The results are summarized below.

Sorbent	Calcination Atmosphere		% Sulfation Fluid-Bed Calcines	% Sulfation TG[a] Calcines
1359	N_2, 815°C		6	11
1359	15% CO_2/N_2, 815°C		12	12
Lowellville	15% CO_2/N_2, 815°C		30	25
Lowellville	60% CO_2/N_2, 900°C		38	33
1337	15% CO_2/N_2, 815°C		98	80
1337	60% CO_2/N_2, 900°C		100	85[f]
Greer	15% CO_2/N_2, 815°C	1;	43[b]	28[d]
		2;	40[b]	18[e]
		3;	55[c]	
Greer	15% CO_2/N_2, 900°C		57	62
Greer	60% CO_2/N_2, 900°C		49	55

(a) TG calcines were nonisothermally calcined up to temperature
(b) residence time of 2 hours
(c) residence time of 4 hours
(d) residence time of 100 minutes
(e) isothermally calcined, residence time of 27 minutes
(f) isothermally calcined

Table 3-4

REPEATABILITY OF SULFATION RESULTS

1 - Limestone 1359, 16/18 mesh, TG nonisothermally calcined at 10°C/min up to 815°C in N_2

Run No.	% Sulfation*
74	10.2
84	11.3
89	11.4

2 - Greer limestone, 16/18 mesh, fluid-bed calcined at 815°C in 15% CO_2 at a flow rate of 57 cm/sec for 2 hours

Run No.	% Sulfation*
92 (E-0-3)	44
111 (E-0-3)	42

3 - Greer limestone, 16/18 mesh, fluid-bed calcined at 815°C in 15% CO_2 at a flow rate of 130 cm/sec for 2 hours

Run No.	% Sulfation*
82 (E-0-6)	42
83 (E-0-6)	38

4 - Greer limestone, 16/18 mesh, fluid-bed calcined at 815°C in 15% CO_2 at a flow rate of 81 cm/sec for 4 hours

Run No.	% Sulfation*
133 (E-0-10)	56
136 (E-0-10)	55

5 - Limestone 1359, 16/18 mesh, fluid-bed calcined at 900°C in 15% CO_2 at a flow of 81 cm/sec for 2 hours

Run No.	% Sulfation*
154 (E-0-17)	30
155 (E-0-17)	29

*Extent of sulfation at which the rate of reaction fell below 0.1% Ca sulfating per minute at 815°C in 0.5% SO_2 and 4% O_2, balance N_2

Since the batch of Greer limestone used for experimentation was not homogeneous in calcium content, the variation in sulfation extent of the sorbent might have resulted from an inaccurate calcium basis used in the sulfation calculations. Samples 1-3 were analyzed for calcium. However, the results showed no correlation between calcium content and the extent of sulfation.

No.	% Ca	% Sulfation
1	45.04	43
2	41.47	40
3	40.92	55

The sulfation behavior of the Greer stone was highly dependent on stone residence time after calcination. In the fluid bed runs, the sorbent had to be held at calcination conditions long enough to ensure complete loss of CO_2. This time was difficult to predict since calcination kinetics in CO_2 were not adequately modeled. For this reason, fluid bed calcines were sometimes exposed to calcination conditions longer than necessary. The sulfation extent of Greer limestone became greater as the residence time of the calcine at 815°C was increased. This resulted in a poor correlation between fluid-bed and TG calcined Greer limestone sulfations.

It was concluded that the TG calcines are adequate simulations of fluid-bed calcines if the residence time of the sorbents is controlled so that calcination is completed in the fluid bed; however prolonged exposure of the calcine to temperature should be avoided.

Calcination Temperature and CO_2 Pressure of Effects on Sulfation. A summary of the sulfation capacity for each sorbent, calcined under various environmental conditions, appears in Table 3-5. The following observations were made:

- Sulfation improved for all sorbents when the calcination was suppressed by a partial pressure of CO_2 equal to 60% of the equilibrium CO_2 pressure for calcination at that temperature. (See Figure 3-16)
- Sulfation improved for all sorbents when the calcination temperature was increased from 815°C to 900°C, maintaining a partial pressure of CO_2 equal to 60% of the equilibrium value.

The effect of calcination temperature at a CO_2 partial pressure equal to 60% of the equilibrium value was further investigated using Lowellville limestone. The extent of sulfation improved as the sorbent was calcined at higher temperatures (Figure 3-17).

Table 3-5

THE SULFATION OF LIMESTONE AND DOLOMITE AS A FUNCTION OF CALCINATION TEMPERATURE AND GAS ATMOSPHERE

TG Calcines (Calcination Conditions)

	N_2 (815°C)[a]		N_2 (900°C)		15% CO_2 (815°C)		60% CO_2 (900°C)	
(16/18 Mesh)	% Util.*	SO_3 Pickup mg/mg Stone	% Util.*	SO_3 Pickup mg/mg Stone	% Util.*	SO_3 Pickup mg/mg Stone	% Util.*	SO_3 Pickup mg/mg Stone
1359	10.2	0.089	9.1	0.07	12[a]	0.12	40[b]	0.30[b]
	11.3	0.11						
	11.4	0.11						
Greer	16	0.09			28[a]	0.15	55	0.27
					18	0.10		
Lowellville	17	0.17	15.5	0.12	24.8[a]	0.20	40	0.30
					23	0.19	33[a]	0.28
1337	51	0.23			80[a]	0.37	85	0.37

Fluid Bed Calcines (Calcination Conditions)

	N_2 (815°C)		15% CO_2 (815°C)		60% CO_2 (900°C)	
Stone	% Util.*	Res. Time/Hours	% Util.*	Res. Time/Hours	% Util.*	Res. Time/Hours
1359	6	2	12	4	26	2
Greer	29	4	40	2	47	2
			43	2		
			55	4		
Lowellville			30	4	38	1.5
1337			98	4	100	1.36

*Values given are % utilization when the rate falls below 0.1%/min.

a) Nonisothermal calcination (10°/min) up to temperature given.

b) Data taken from Reference 1.

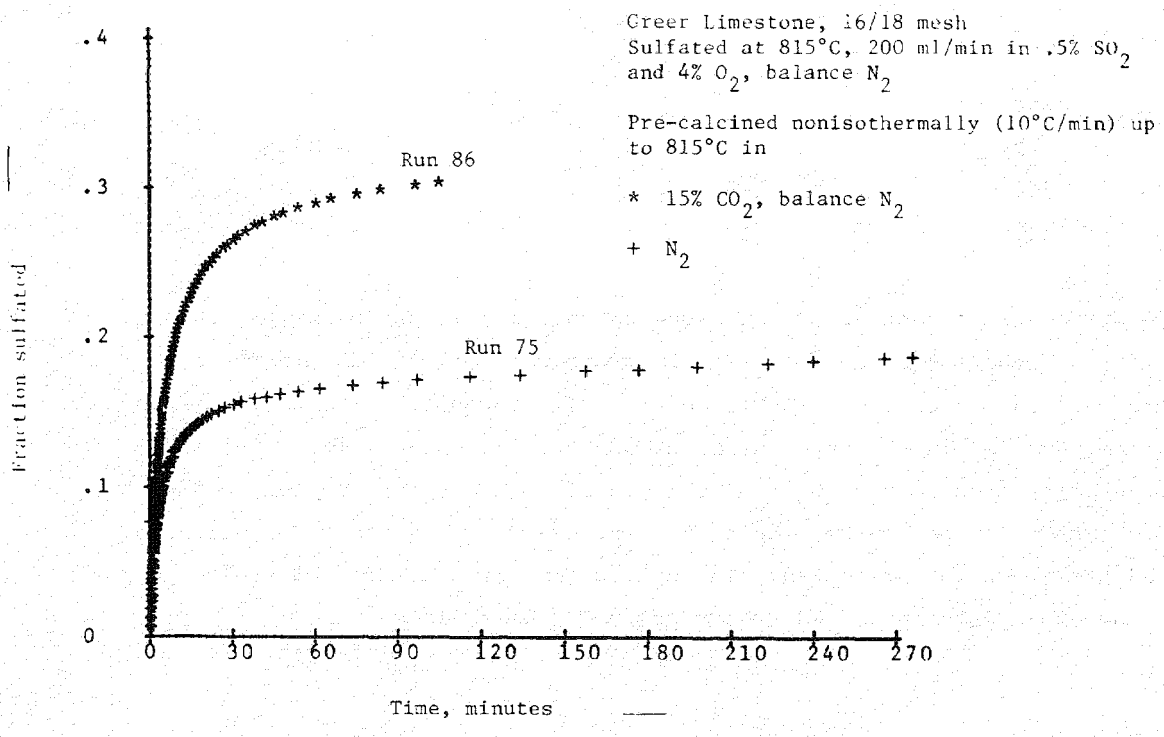

Figure 3-16. The Effect of Calcination Atmosphere on the Utilization of Greer Limestone in Sulfation

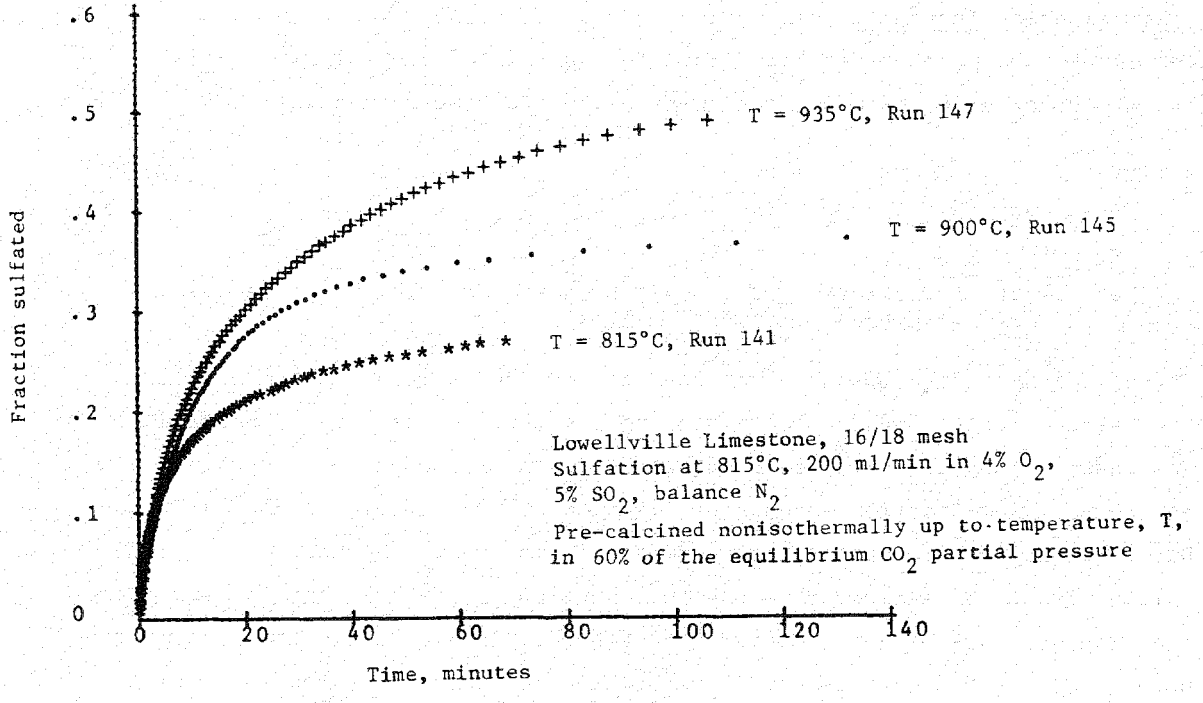

Figure 3-17. The Effect of Calcination Temperature on the Utilization of Lowellville Limestone in Sulfation

Calcination Temperature	% CO_2 = 0.6 P_{eq}	% Sulfation at 815°C
750	5	22
815	15	24.8
900	60	33
935	100	47

The systematic effect of CO_2 suppression during calcination on the subsequent sulfation behavior of Lowellville limestone was determined. The calcinations were carried out at 900°C in CO_2 and N_2. The sorbent's utilization improved as the percent CO_2 in the calcination atmosphere increased (Figure 3-18). Since the calcinations in 80% CO_2 required over five hours for completion, further calcinations in carbon dioxide partial pressures closer to the equilibrium, 0.94 atm, were not attempted. The utilization of limestone 1359 also improved as the 900°C calcination was retarded by CO_2 as follows:

% CO_2	% Utilization
0	9.1
60	37.3
80	47.0

Precalcination Treatment. In typical experiments, sorbents were heated to calcination temperature at 10°C/min. In a series of special experiments, the atmospheres in which sorbents were heated to temperature was varied as follows:

- Calcination atmosphere
- Pure CO_2
- Partial pressure of CO_2 just above the equilibrium concentration for calcination

If the calcination atmosphere was used to heat the sorbent to temperature, the calcium fraction began to calcine before the temperature for calcination was reached (nonisothermal calcination). In the latter two atmospheres, only the non-calcium fraction (magnesium fraction) of the sorbent could calcine before reaching temperature (isothermal calcination). In these cases, the calcium fraction calcined upon the introduction of the calcination atmosphere when the sorbent reached temperature. However, in some cases the sorbent was held in CO_2 at temperature until the noncalcium fraction of the sorbent completely calcined before introduction of the calcination atmosphere. All of

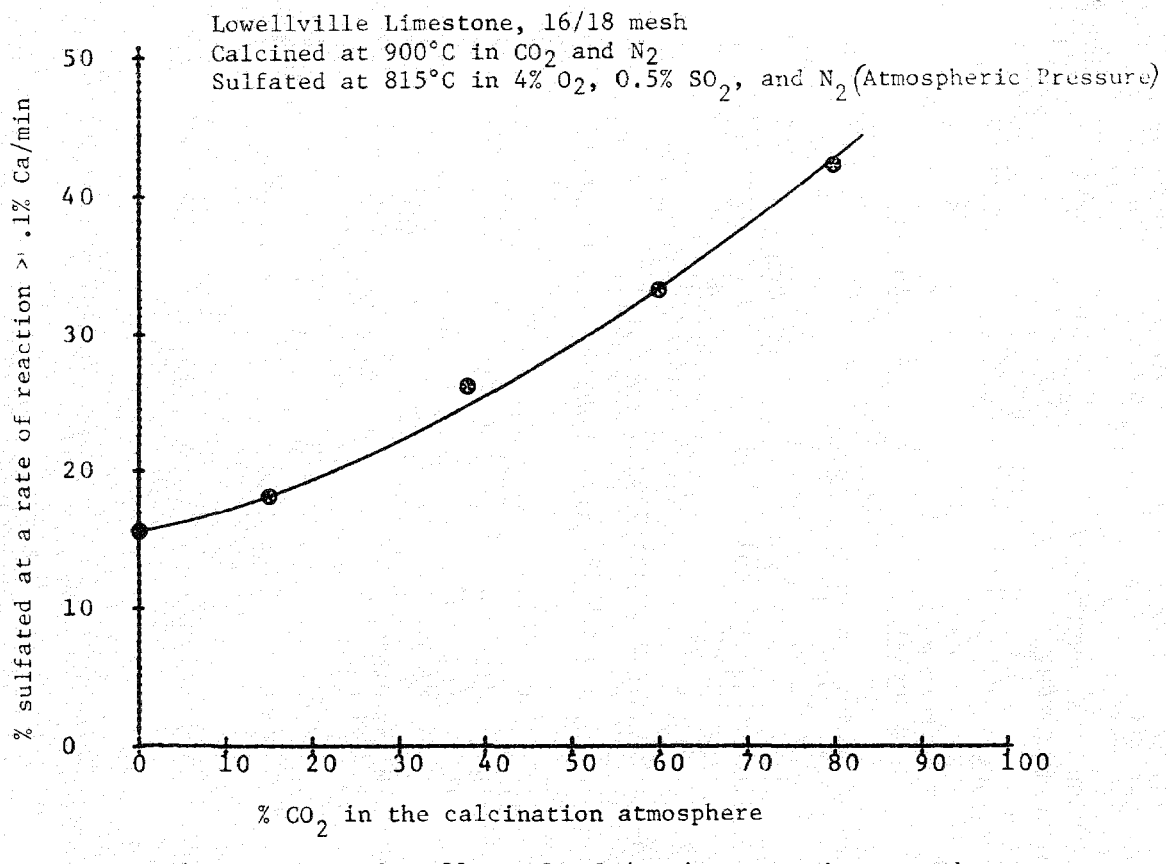

Figure 3-18. The Effect of Calcination Atmosphere on the Sulfation of Lowellville Limestone

these precalcination treatments affected the kinetics of limestone calcination. A summary of sulfation results obtained from such pretreatment appears in Table 3-6. The test results are insufficient to judge the exact effects of the precalcination treatments on the sulfation characteristics of the sorbent. However, the influence appears negligible, as can be seen in Table 3-6.

Effect of Sorbent Residence Time After Calcination, before Sulfation

Since Greer limestone calcines that were prepared in the fluid bed showed sensitivity to the time for which the sorbent was held under calcination conditions, the effect of residence time before sulfation in calcines was further investigated. At 815°C in 15% CO_2, Greer limestone calcined in the TGA in about 50 minutes. The Greer stone held under these conditions in the fluid bed for 2 hours was completely calcined, according to weight loss measurements. Thus, the Greer sorbents held at 815°C in 15% CO_2 in the fluid bed for 4 hours had at least 2 hours additional residence time after calcination. This

Table 3-6

THE SULFATION OF LIMESTONE AS A FUNCTION OF PRE-CALCINATION TREATMENT

Pretreatment

Run No.	Atmosphere	Time Held at T (minutes)	% Sulfation
	Greer Limestone, calcined at 900°C, 60% CO_2		
87	100% CO_2	28	55
110	100% CO_2	0	55
	Lowellville Limestone, calcined at 900°C, 60% CO_2		
116	100% CO_2	11	40
145	60% CO_2	0	33
	Lowellville Limestone, calcined at 815°C, 15% CO_2		
141	15% CO_2	0	25
144	30% CO_2	0	23
184	38% CO_2	120	20.2
186	100% CO_2	0	26
	Limestone 1359, calcined at 815°C, 15% CO_2		
143	100% CO_2	0	10.7
85	15% CO_2	0	12
	Limestone 1359, calcined in N_2 at 815°C		
163	100% CO_2	0	9
165	100% CO_2	60	7.7
166	38% CO_2	0	10
168	38% CO_2	60	8
74, 84, 89	0% CO_2	0	10.2, 11.3, 11.4

additional exposure to fluid bed conditions increased the utilization of the sorbent from 40 to 55%. The improved utilization obtained by Greer limestone calcines with longer exposure to temperature was also studied with the TGA. Greer limestone which was nonisothermally calcined up to 815°C in nitrogen obtained 16% sulfation. When this calcine was heated to 900°C for 130 minutes in flowing nitrogen before sulfation, the utilization in sulfation improved to 40%. This is illustrated in Figure 3-19. It should also be noted that the sorbent utilization obtained when the calcine was heated to 900°C after calcination was not as great as the 55% obtained when the calcine was actually prepared at 900°C in an atmosphere of 60% CO_2 and nitrogen.

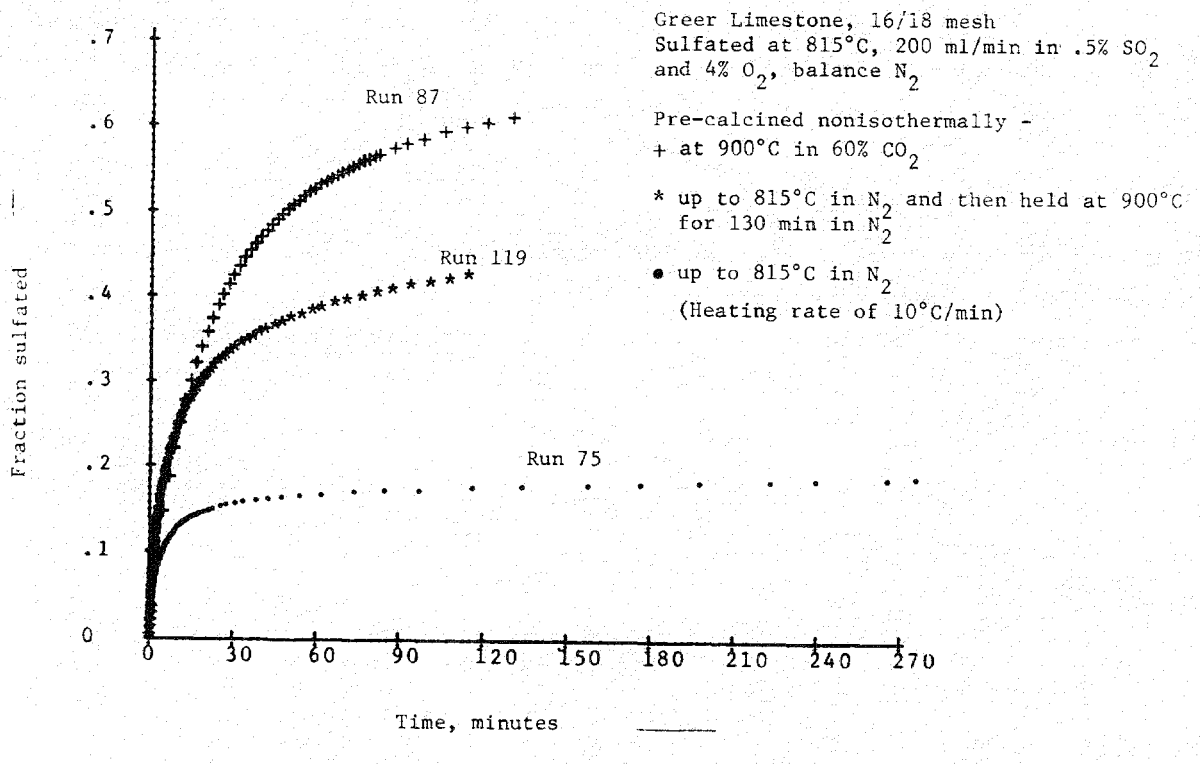

Figure 3-19. The Effect of Calcine Residence Time on the Utilization in Sulfation of Greer Limestone

To determine if a similar improvement in sorbent utilization could be obtained with other sorbents, fluid bed calcines of limestone 1359 and Lowellville limestone were prepared. A small fraction of the calcines were used to

determine the sulfation characteristics of these sorbents. The remaining calcines were again exposed to fluid bed conditions. The utilization in sulfation of the reheated sorbents showed the following:

Sample	% Util. of Original Calcine	Reheating Conditions Temp. (°C)	Time	% Util. of Reheated Calcine
E-0-2 (1359)	6	900	1 hour	10
E-0-11 (Lowellville)	38	900	2.5 hours	25

The different responses of the calcines exemplify the complexity of the residence time effect on the calcine. Evidently a certain amount of high temperature exposure improves the utilization of the sorbent. Extended exposure, as in the case of Lowellville (E-0-11) limestone which was initially calcined at 900°C, may have produced a sintered stone.

Sulfations in the Presence of 12% CO_2

Since carbon dioxide will be present in the fluidized bed combustion atmosphere, a few sulfation experiments were carried out in 12% CO_2 to determine if any differences would occur in sulfation kinetics. The CO_2 does not hinder the sorbent utilization obtained in sulfation as shown below.

Calcine	% Utilization	
	12% CO_2, 0.5% SO_2, 4% O_2/N_2	0.5% SO_2, 4% O_2/N_2
E-0-3	50	42, 44
E-0-10	56	55,56

3.2.2 High Temperature Sulfations

To be certain that the effect of calcination conditions on sorbent utilization in sulfation was not specific to 815°C sulfations, the sulfation of selected calcines was studied at 855°C and 895°C. The sulfation atmosphere remained at 0.5% SO_2 and 4% O_2 in N_2. The sorbent utilizations obtained at the different sulfation temperatures are listed:

	Utilization in Sulfation at T		
	T = 815°C	T = 855°C	T = 900°C
Greer (E-0-14)	29	25	22
Greer (E-0-18)	57	62	>67
1359 (Nonisothermally calcined up to 900°C in N_2)	9.1		7.45

As the sulfation temperature was increased, the utilization of E-0-18, prepared at 900°C in 15% CO_2 became increasingly larger than that of E-0-14, an 815°C calcination in N_2. This latter sample showed a decline in activity at temperatures above 815°C in line with previous fluid bed combustor investigations.

3.2.3 Conclusions

- Retarding calcination with CO_2 increases the calcines utilization in sulfation for all sorbents tested.
- Higher temperature calcinations (at least up to 900-935°C) produce more reactive sorbents.
- The residence time of a sorbent at high temperatures after calcination and before sulfation affects sorbent utilization, but this varies with sorbent type
- The treatment of a sorbent before calcination (the time a sorbent is held at high temperatures before calcination and the percent CO_2 in this atmosphere) has an insignificant effect on sorbent utilization in sulfation.
- The presence of CO_2 below the equilibrium pressure in the sulfating atmosphere does not decrease sorbent utilization.
- Differences in sorbent utilization resulting from the calcination remain at sulfation temperatures greater than 815°C.

3.3 SORBENT RESIDENCE TIME

The dependence of sulfation behavior on sorbent residence time was studied by simulating long sorbent residence times using low sulfur dioxide concentrations in the TGA. In burning coal that contains 4% S, the SO_2 resulting is in the range of 0.09-0.34%, depending on the quantity of excess air. The sulfation of calcium carbonate has been reported to be first order in SO_2.[7,16,17] Using 0.5% SO_2 provides sulfations that occur in less than 2 hours and, therefore, are convenient to study in the laboratory. However, sorbent residence times in fludized beds may be 6 to 25 hours. This extended exposure of a sorbent to temperature under a sulfating atmosphere may cause sintering of the stone and result in decreased utilization.

As noted earlier, to maintain 90% sulfur retention in a 4 ft fluidized bed at 8 ft/sec, k should have a value of 40 sec^{-1}. The required rates of limestone sulfation are (based on a first order reaction):

% SO_2 in Sulfating Gas Mixture	Rate of Reaction (% Ca Sulfating Per Minute)
0.5	1.0
0.3	0.6
0.1	0.2
0.05	0.1

The above rates were used as lower limits for determining the extent of sulfation.

Preliminary runs were made on 16/18 mesh limestone 1359. The sorbent was calcined by heating at a rate of 10°C/min up to 815°C in flowing nitrogen. The calcine was then sulfated at 815°C in 4% O_2, 0.05 - 0.5% SO_2, and nitrogen. Sulfur removal would be maintained at 90% at the following sorbent utilizations:

% SO_2	Ca Utilization, %	Time (minutes)
0.5	5.2	2.3
0.3	6	4.2
0.1	4.2	7
0.05	4.3	17

The sorbent utilizations varied from 4-6% with no correlation to the residence times. However, the low sulfation extents obtained by this limestone 1359 calcine made thermogravimetric measurements less accurate.

A more reactive limestone 1359 calcine, E-0-17, was used for further tests.

Pre-mixed and analyzed gases of 0.45% SO_2 in N_2 and 0.096% SO_2 in N_2 were used, diluting with 4% O_2. The rate curve for 0.096% SO_2 is shown along with the rate predicted for 0.45% SO_2 in Figure 3-20. The curves show the first order reaction being followed for the initial phase of the reaction. However, as the reaction proceeds the rate at low SO_2 concentration is much slower than predicted. This could result from sintering of the sorbent as the residence time increased. Tests were run to determine the effect of residence time on the sorbent. The calcine, E-0-17 was held at 815°C in N_2 for 200 minutes before sulfation in 0.5% SO_2 to investigate the effect of sintering on the

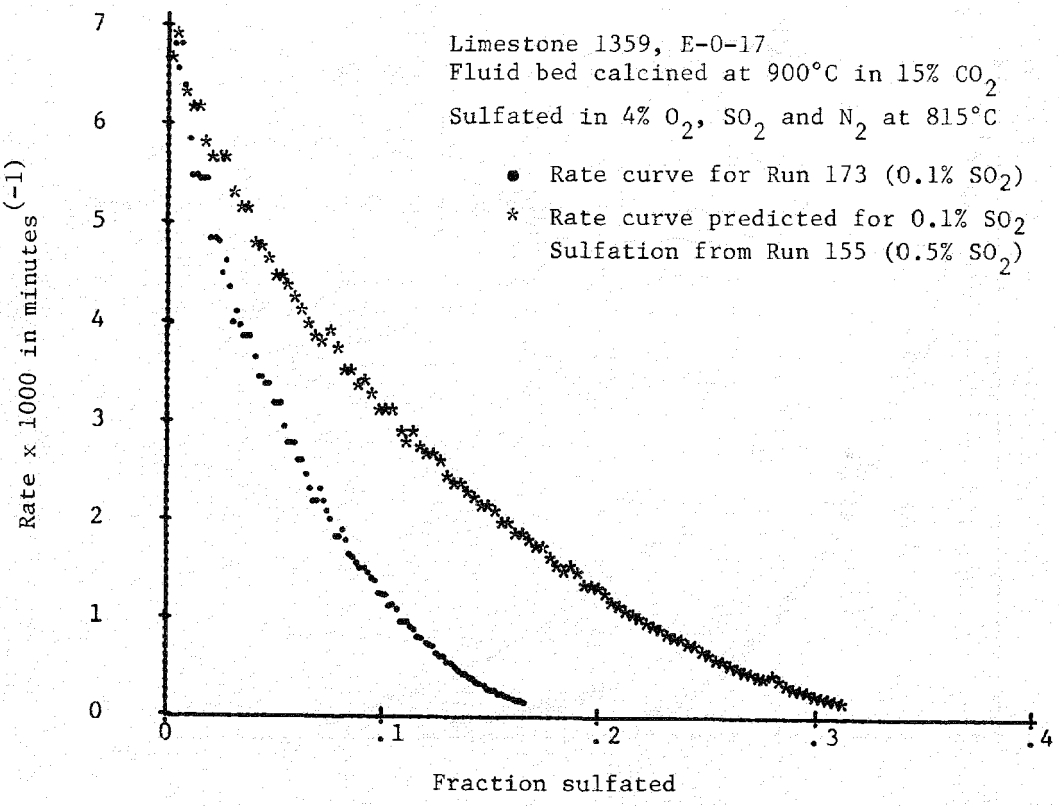

Figure 3-20. The Sulfation of Fluid Bed Calcine E-0-17 with Various SO_2 Concentrations

calcine. Figure 3-21 shows this decreased the rate of sulfation substantially. However, in the fluid bed, partially sulfated sorbent, not the pure calcine, is exposed to high temperatures for prolonged times. Thus, in Runs 192 and 193 the calcine was sulfated in 0.5% SO_2 for 9 minutes. The partially sulfated (14%) sorbent was held at 815°C for 130 minutes, the time it would take the sorbent to sulfate 14% in 0.1% SO_2. Sulfation was then continued in 0.5% SO_2. The effect of residence time on the 14% sulfated calcine is shown in Figure 3-22. Sintering does not solely account for the decrease in the rate of the low SO_2 reaction.

The evidence indicates that some sintering of $CaSO_4$ is occurring at prolonged sorbent residence times. It appears that the sulfation of limestone follows a first order reaction in SO_2 initially, but the apparent order with respect to SO_2 increases as the reaction progresses. Coutant (Battelle) reported that the apparent order of sulfation of limestone increased with sulfate loading.[18] It should also be noted that TVA[7] used the rate of sulfation after 1 minute

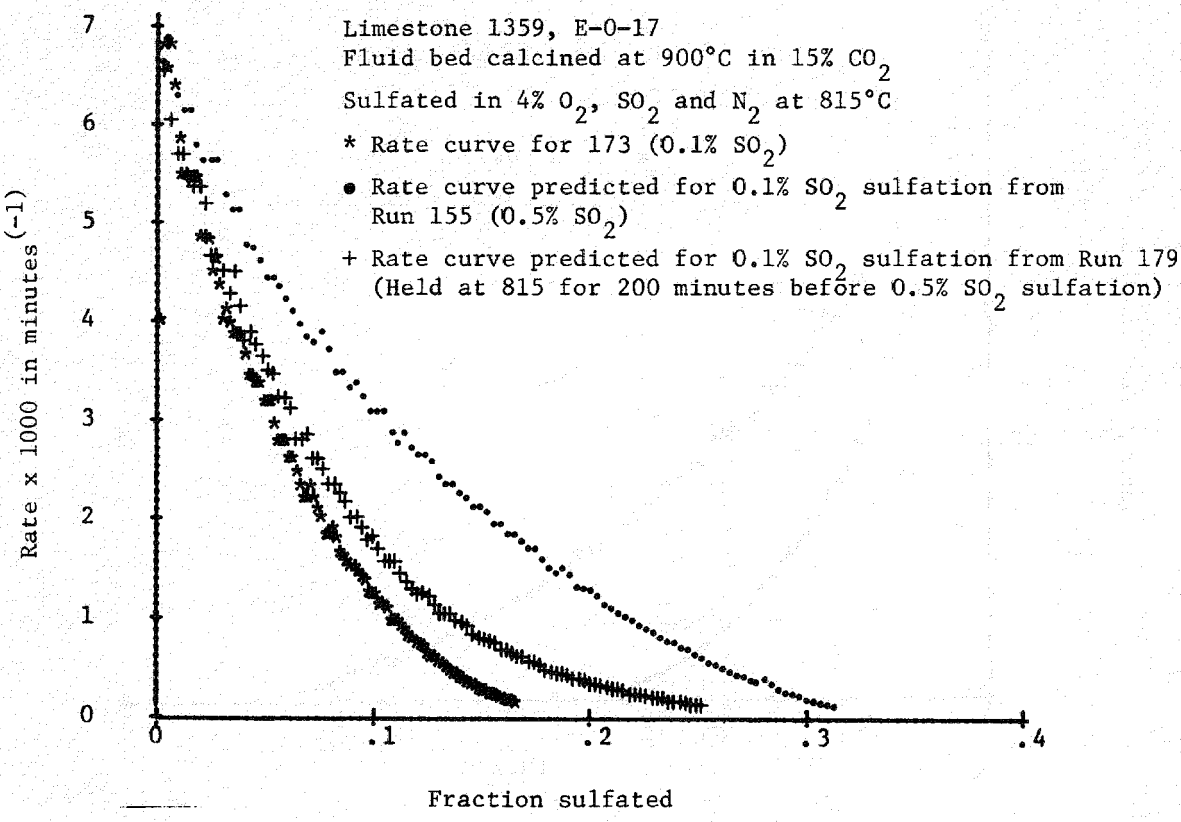

Figure 3-21. The Effect of Residence Time of the E-0-17 Calcine on its Sulfation Rate

of reaction to infer a first order reaction in SO_2. Borgwardt's[16] data were taken at 10.5% conversion of dolomite 1337 at 870°C. This, too, is early in the reaction since dolomite 1337 has been shown to sulfate 100% at 815°C.

Further work investigating the apparent order of sulfation as the reaction proceeds is needed. The observed effect of SO_2 pressure on the E-0-17 calcine could have resulted from sample inhomogeneity. Good repeatability of the E-0-17 sulfations is illustrated in Figure 3-23 where the effect of residence time on partly sulfated sorbent was investigated using two TGA's, the 900 and 990 consols. However, later TG experimentation has shown that impurities are present in the E-0-17 calcine. The repeatability shown in Figure 3-23 is not representative.

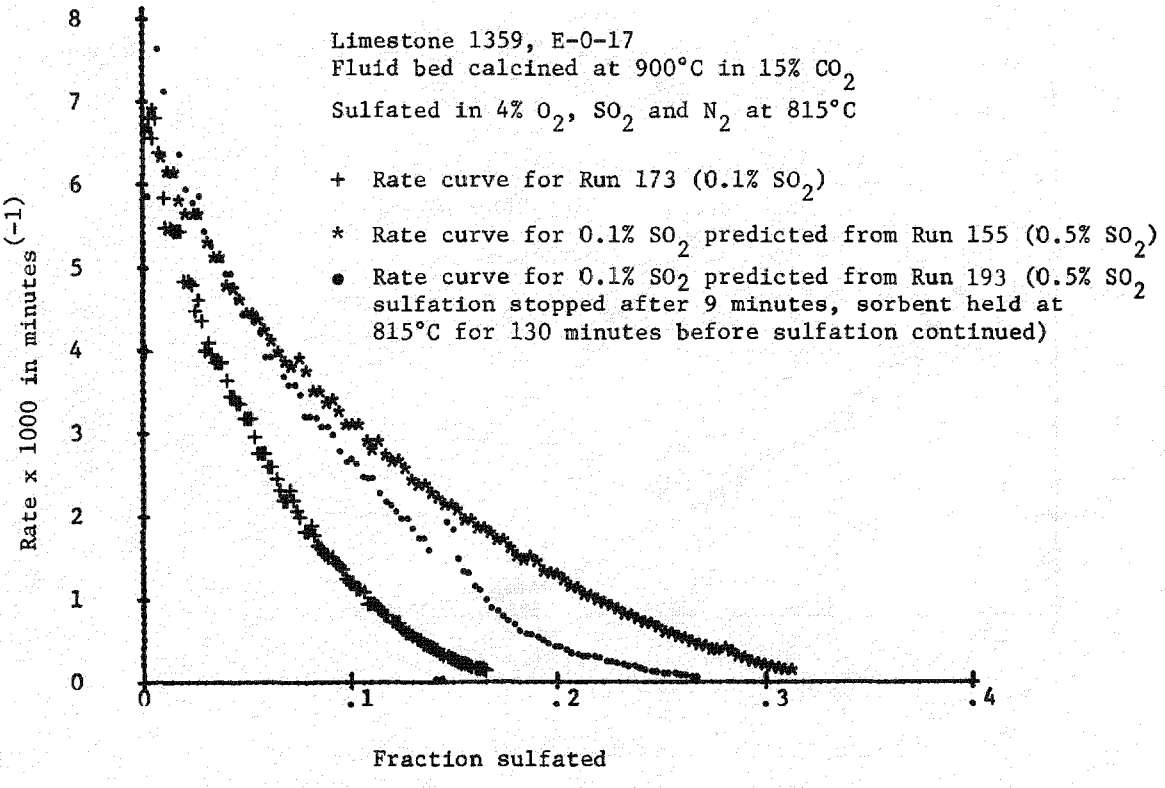

Figure 3-22. The Effect of Residence Time of Partially Sulfated E-0-17 on its Sulfation Rate

3.4 RECARBONATIONS

TG recarbonation experiments have indicated

(1) The recarbonation reactivity of a sorbent cannot be used as an index of sorbent efficiency in sulfur removal.

(2) When the sulfation rate of a sorbent is slow because of pore blockage with sulfate, the ability of the sorbent to react with CO_2 is also poor.

Little work has been reported on the recarbonation of calcium oxide. However, the reaction has some features which are of interest in promoting the activity of the oxide.

Recarbonation is typically rapid until 60-80% of the lime has formed calcium carbonate. The fast reaction is succeeded by an extremely slow reaction, in which diffusion of carbon dioxide through a layer of carbonate product on the

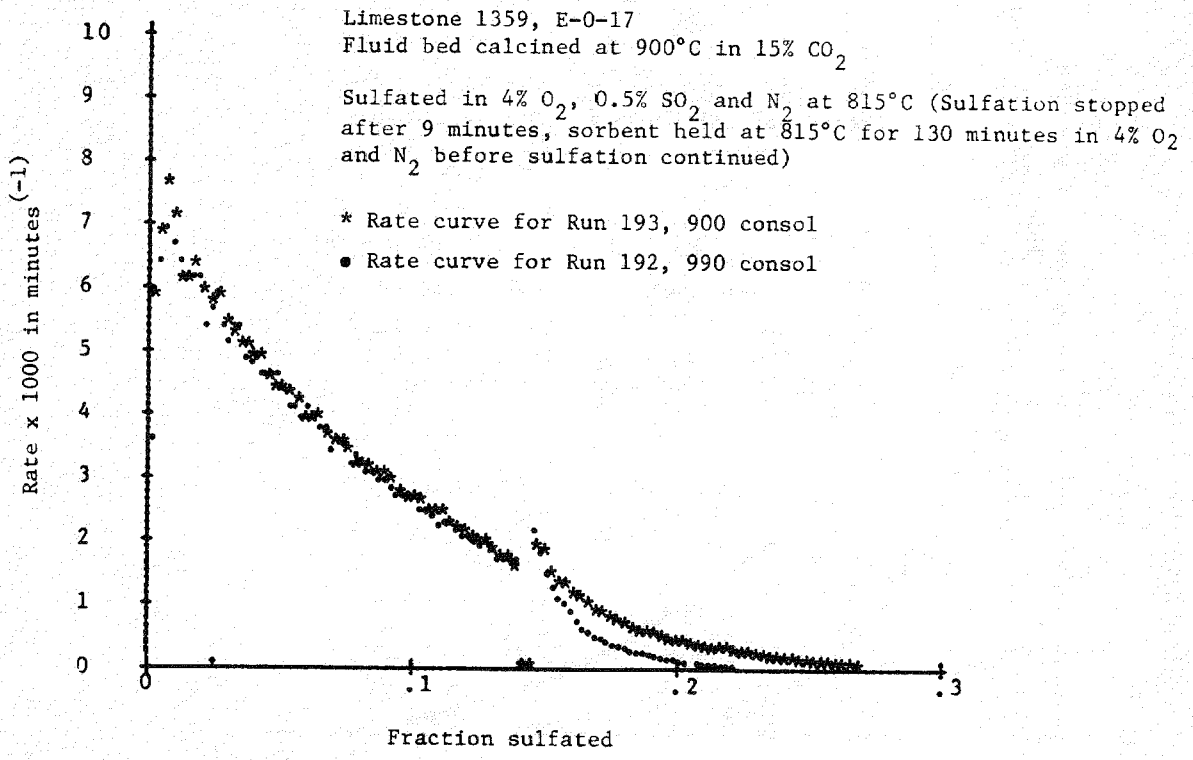

Figure 3-23. Repeatability of Sulfation Curves

individual grains of oxide is presumed to dominate the rate. If the solid is decomposed again and recarbonated, then a smaller fraction of the lime is readily recarbonated. Typically, after ten such cycles, only 30% of the lime readily recarbonates. However, if the inactive product is then allowed to "soak" in carbon dioxide, and is calcined and recarbonated, the activity revives to some extent. Barker[19] has suggested that there is a critical particle size (44 micron) below which diffusion will not hinder the rate of recarbonation, and lime particles below this size should react to 100% utilization with carbon dioxide. Clearly this is in accord with laboratory experiments on the sulfation of fine particles of lime, where utilization of 90% or more of the lime can be achieved.

For our purposes, recarbonations were studied to determine if the activity of sorbents to recarbonation could provide an index of sorbent sorption reactivity. Recarbonations of limestone 1359 were run at 750°C with 15% CO_2 in N_2. As the reaction proceeded, the rate of recarbonation showed the same pattern as rates of limestone:

- A phase of increasing rate for about 2 minutes as the CO_2 contacts the CaO

- A linear decrease in rate during the surface reaction of CO_2 with CaO
- The final phase as the rate decreases exponentially when diffusion of CO_2 through the $CaCO_3$ slows the reaction

The calcination conditions of limestone 1359 affected the recarbonation as follows:

- Limestone calcined at 830°C in N_2, recarbonated more slowly than limestone calcined at 815°C in N_2
- Of the stones calcined at 815°C, the one calcined in N_2 reached a higher rate of reaction, and recarbonated slightly faster than the stone calcined in CO_2

Thus, the recarbonation activity trend of limestone 1359 was opposite to that for sulfation activity.

Additional recarbonations at 815°C in 38% CO_2 were carried out on several fluid-bed calcines. The extent of recarbonation was not found to correlate with the extent of sulfation obtained by these calcines at 815°C. For limestone 1359 calcines, the extent of recarbonation obtained after 20 minutes was greater when the sorbent was calcined in N_2 rather than 15% CO_2. The Greer limestone, which was held at calcination conditions for a shorter residence time, recarbonated to a larger extent. Table 3-7 summarizes the recarbonation results.

The relative recarbonation reactivities on a weight basis of sorbents that were fluid-bed calcined at 815°C in 15% CO_2/N_2 were:

Dolomite 1337 > Lowellville Limestone > Limestone 1359 > Greer Limestone

This varies from the sulfation reactivity found for the calcines:

Dolomite 1337 > Greer Limestone > Lowellville Limestone > Limestone 1359

It was concluded that the reactivity of a sorbent in recarbonation is not a good index of its utilization in sulfation. The CO_2 pickup for limestone sorbents after 20 minutes in 38% CO_2 at 815°C correlates with the surface area of the calcines. This correlation does not appear between surface area and SO_3 pickup after 20 minutes at 815°C in 0.5% SO_2 and 4% O_2.

Table 3-7

COMPARISON OF RECARBONATION AND SULFATION
OF FLUID-BED CALCINES

Sample	Calcination Conditions			mg CO_2[a]/ mg Raw Stone	% Recarbonated[a]	% Sulfated[b]
	Temperature	% CO_2	Residence Time, min.			
E-0-2, Limestone 1359	815	0	120	0.26	62.07	6
E-0-9, Limestone 1359	815	15	240	0.19 0.18	44.71 43.22	12
E-0-6, Greer Limestone	815	15	124	0.19	61.94	40
E-0-10, Greer Limestone	815	15	240	0.10	31.41	55
E-0-7, Lowellville Limestone	815	15	240	0.19	46.05	30
E-0-8, Dolomite 1337	815	15	240	0.21	91.75	85

a) After 20 minutes
b) Fraction sulfated when the rate falls below 0.1% Ca sulfating per minute

Sample	mg CO_2/ mg Raw Stone	Surface Area m^2/g	mg SO_3/ mg Raw Stone
E-0-6	0.19	5.88	0.076
E-0-7	0.19	5.84	0.19
E-0-9	0.19	5.73	0.10
E-0-10	0.10	2.59	0.21
E-0-8	0.21	12.51	0.44

Since the carbonate ion is smaller than the sulfate ion, pore blockage by the product does not limit diffusion through pores formed in calcination, as it does in sulfation. Therefore sorbents with high surface areas and small pore diameters, those calcined quickly without CO_2 suppression, are reactive in recarbonation. Small pores are not as likely to be blocked by the $CaCO_3$ structure as they are by $CaSO_4$.

In the case of dolomite 1337, the surface area of 12.51 m^2/g is artificially high because of the magnesium fraction which is not able to pick up CO_2 or SO_3 at 815°C in the atmospheres used.

Recarbonation of Partly Sulfated Sorbents

Recarbonations of TG sulfated samples were carried out at 815°C in 38% CO_2 to determine if CO_2 could be adsorbed by partially sulfated sorbents. Samples from the TGA that had been sulfated to the point at which their rate fell below 0.1% Ca sulfating per minute were used. A dolomite sample which was 100% sulfated picked up no CO_2. Experiments with Greer limestone samples showed that sorbents with less sulfur were more susceptible to recarbonation. The more highly sulfated the sorbent, the less calcium is available to recarbonate. A summary of the recarbonation of sulfated sorbents after 20 minutes at 815°C in 38% CO_2 follows:

Sample	% Sulfated	mg CO_2/mg Raw Stone
78 (Greer)	27	0.13
93 (Greer)	62	0.036
138 (1337)	100	0
143 (1359)	11	0.19

The amount of CO_2 absorbed by low sulfur samples was high in comparison with the pure calcines (Table 3-7). The limestone 1359 which was 11% sulfated adsorbed

as much CO_2 in 20 minutes as the unsulfated calcine prepared under similar conditions (calcined at 815°C in 15% CO_2).

Run No.	% Sulfated	mg CO_2/mg Raw Stone
143	11	0.19
E-0-9	0	0.19

It is likely that the process of cooling the sulfated sorbents, and then later reheating them for recarbonation cracked the stones, exposing new surface area for recarbonation. Two sorbents were exposed to a recarbonation atmosphere immediately after their sulfation rate dropped. Thus, they were not exposed to the cooling/reheating treatment of previous sorbents. The CO_2 adsorbed by these samples was much less.

Sample	% Sulfated	mg CO_2/mg Raw Stone
187 (Lowellville)	20.2	0.004
188 (Greer)	15	0

Here the Lowellville limestone, which was 20.2% sulfated was much less reactive to recarbonation than the raw stone (calcined at 815°C in 15% CO_2).

Sample	% Sulfated	mg CO_2/mg Raw Stone
187 (Lowellville)	20.2	0.004
E-0-7	0	0.19

It was concluded that if sulfation is occurring under a recarbonation atmosphere in the fluid bed, we can expect CO_2 adsorption to interfere with sulfur removal. However, sorbents that are substantially sulfated are not likely to recarbonate. Further work on the relative rates of recarbonation and sulfation in a fluid bed atmosphere is needed to determine how recarbonation may influence sulfur removal.

3.5 PHYSICAL CHARACTERIZATION OF THE CALCINES

The pore volume/pore size distribution, density and surface area of calcines prepared in the fluid bed unit were determined. The results indicate that increased porosity in wide mouthed pores formed during calcination precede increased sorbent utilization in sulfation. The surface area, density, and total porosity of the calcines show no correlation with the sulfation utilization of the calcines.

Pore Volume Determinations

The porosity of samples calcined in the fluid bed unit was determined on a mercury penetration porosimeter. The repeatability of results for the E-0-7 calcine is shown in Figure 3-24; both determinations show that the pore volume is about 0.25 cc/gm and that most of the pores have diameters around 0.3 microns. For a second replicate set on E-0-11, the total pore volume was in less satisfactory agreement, but the pores lay in a similar pore diameter range, ~0.9 microns (Figure 3-25).

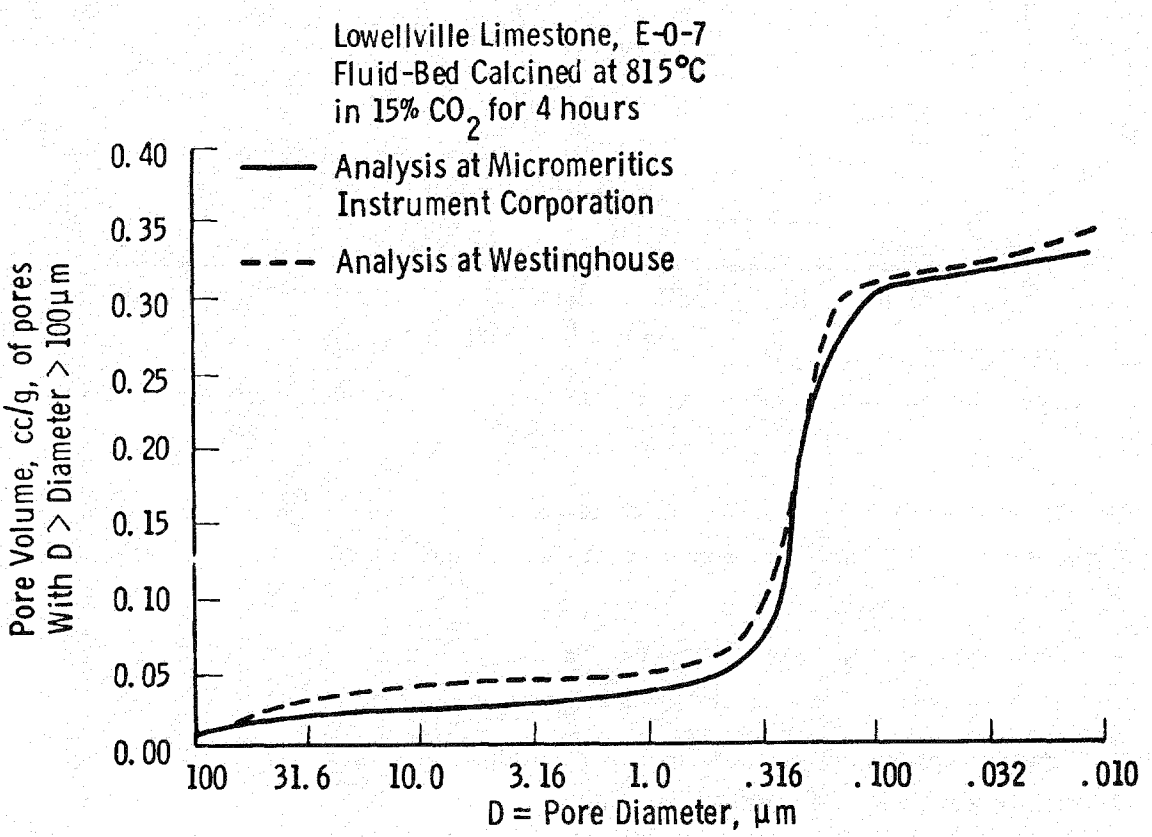

Figure 3-24. Repeatability of Pore Volume Distributions for the E-0-7 Calcine

In interpreting the pore-volume diagrams, it was assumed that most of the porosity in pores wider than about 1 micron arises from spaces between the loosely packed particles of calcine. The volume in pores <1 micron diameter was considered to be inside the particles.

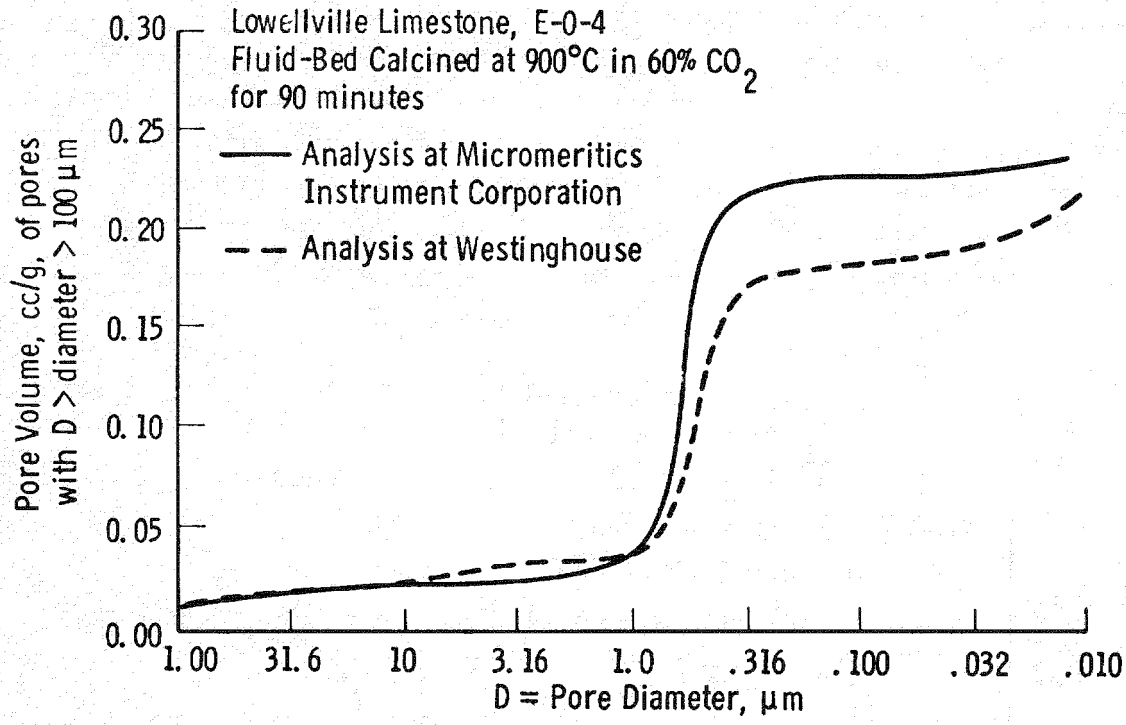

Figure 3-25. Repeatability of Pore Volume Distributions for the E-0-11 Calcine

For the calcined limestones tested, an increase in the pore volume composed of pores greater than (0.1-0.2) micron diameter was found when:

- CO_2 was used to suppress calcination
- The calcination temperature was raised from 815°C to 900°C
- The residence time of the calcine was varied

These shifts in pore-volume/pore-size distribution preceded increased sorbent utilization in sulfation at 815°C.

For dolomite 1337, the pore volume was concentrated in pores <0.2 microns in diameter, and did not vary much with pretreatment in the fluid-bed. For these samples, sulfation utilization varied from 85-100%.

CO_2 Suppression

The effects of CO_2 suppression during calcination on the pore volume/pore size distributions of limestone 1359 and Greer limestone are shown in Figures 3-26 to 3-30: more pores of >(0.1-0.2) µm were formed at the expense of pores

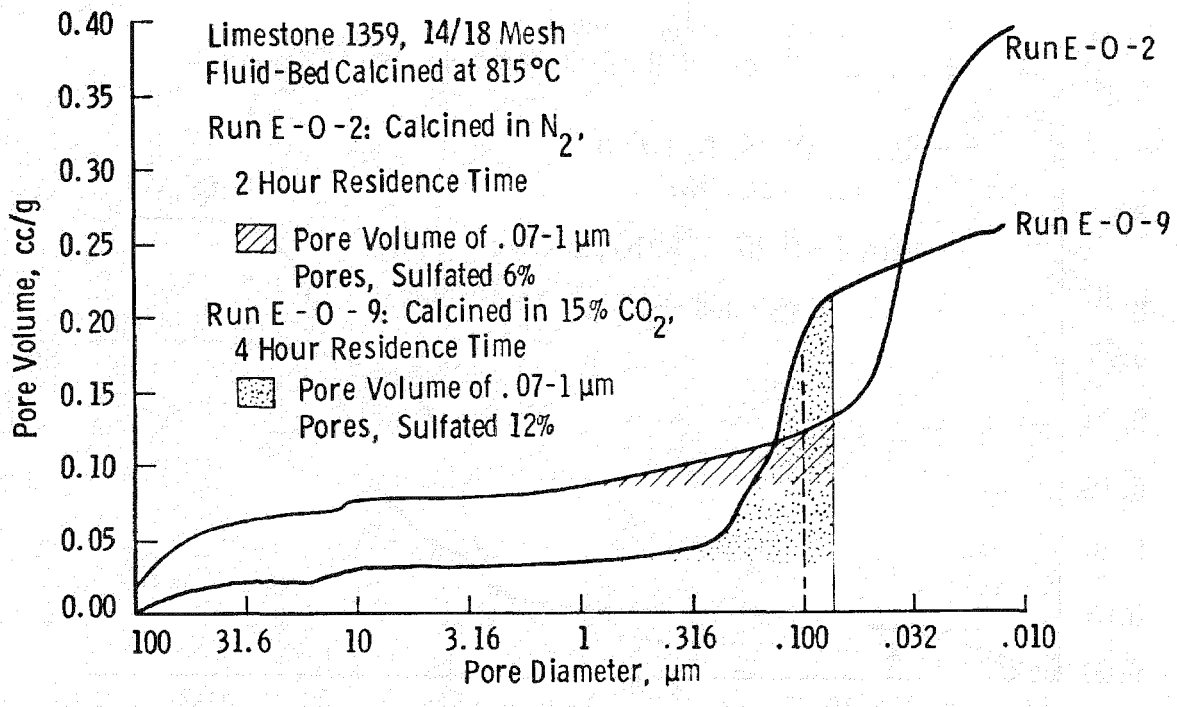

Figure 3-26. The Effect of Carbon Dioxide Suppression of Calcination on the Pore Volume Distribution of Limestone 1359 Calcines

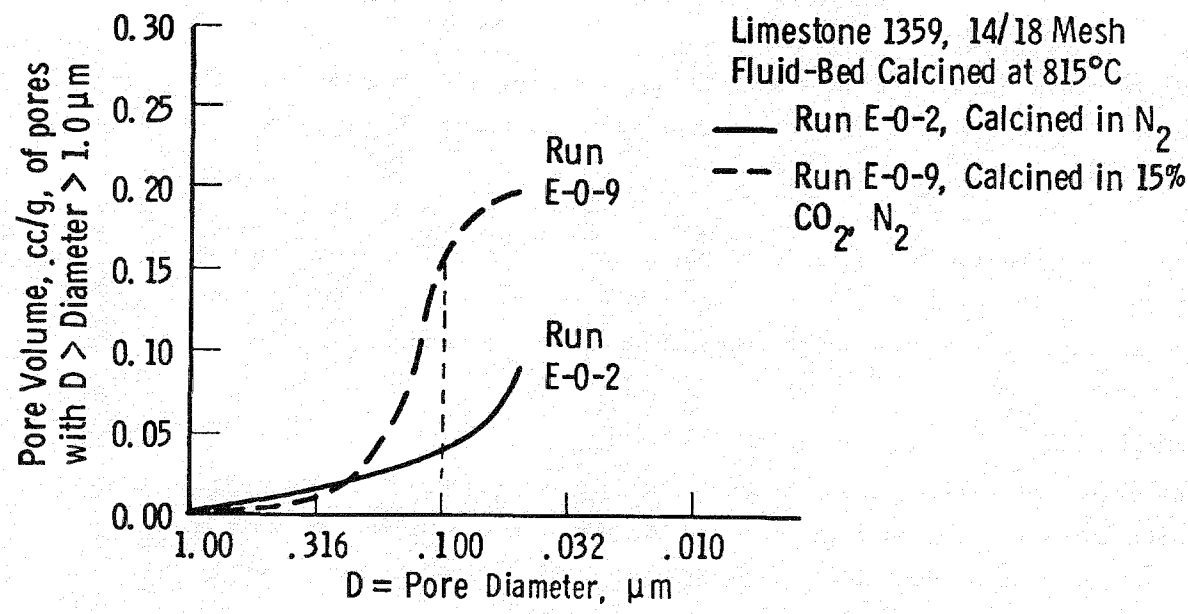

Figure 3-27. The Effect of Controlled Calcination in CO_2 on the Pore Volume Distribution of Limestone 1359 Calcines (Active Pores)

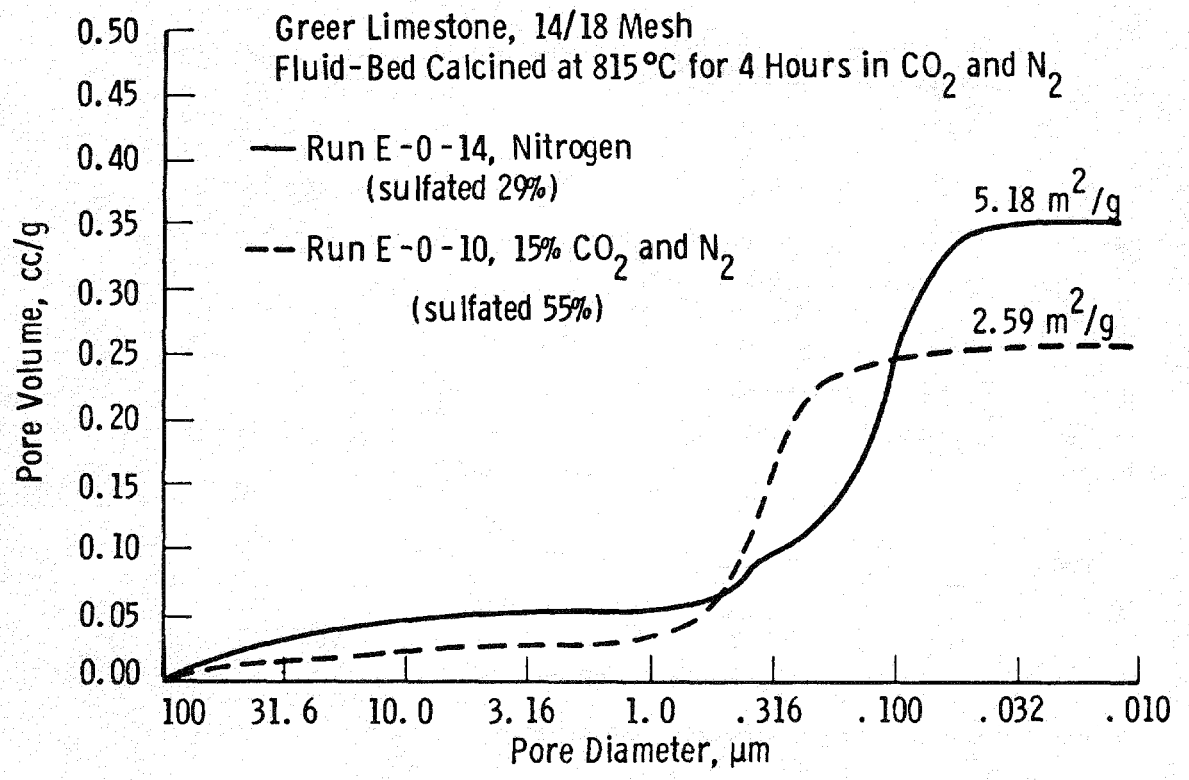

Figure 3-28. The Effect of Carbon Dioxide Suppression during Calcination on the Pore Volume Distribution of Greer Limestone Calcines

smaller than 0.1 μm. Figure 3-27 illustrates the effect by showing the cumulative pore volume of pores in the diameter range (1→0.1) microns for the 1359 calcines.

The interpretation of the results obtained in calcines prepared in 60% CO_2 at 900°C (Figures 3-29 and 3-30) was obscured by the fact that calcination was incomplete when the porosity measurements were made.

Temperature

The effect of raising calcination temperatures from 815°C to 900°C while maintaining the CO_2 partial pressure at 60% of the equilibrium value is shown for each sorbent in Figures 3-31 to 3-34.

For limestone 1359 (Figure 3-31), the temperature increase more than doubled the sulfation capacity of the calcine. This is reflected in the large shift in pore size from 0.1 μm to 1 μm diameter pores. The Greer stone (Figure 3-32 shows a shift from 0.2 μm to 2 μm pores and the sulfation extent improved from 40 to 47%.

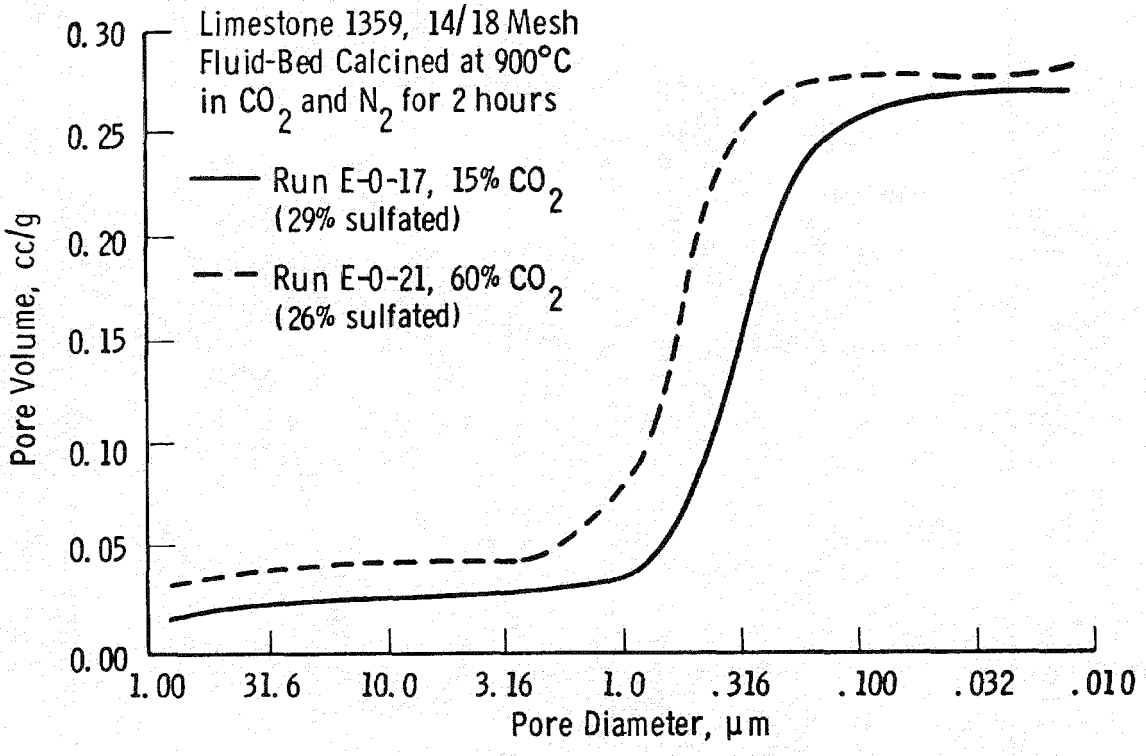

Figure 3-29. The Effect of CO_2 Pressure on the Pore Volume Distribution of Limestone 1359 Calcines

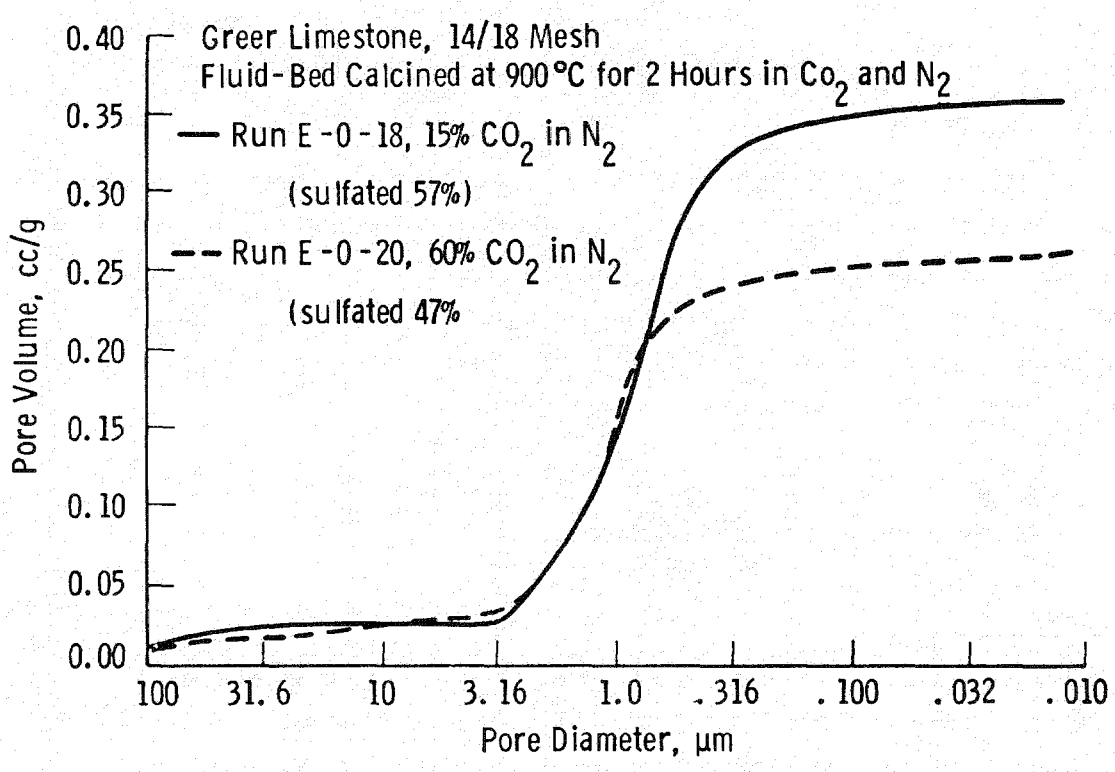

Figure 3-30. The Effect of Calcination Atmosphere on the Pore Volume Distribution of Greer Limestone Calcines

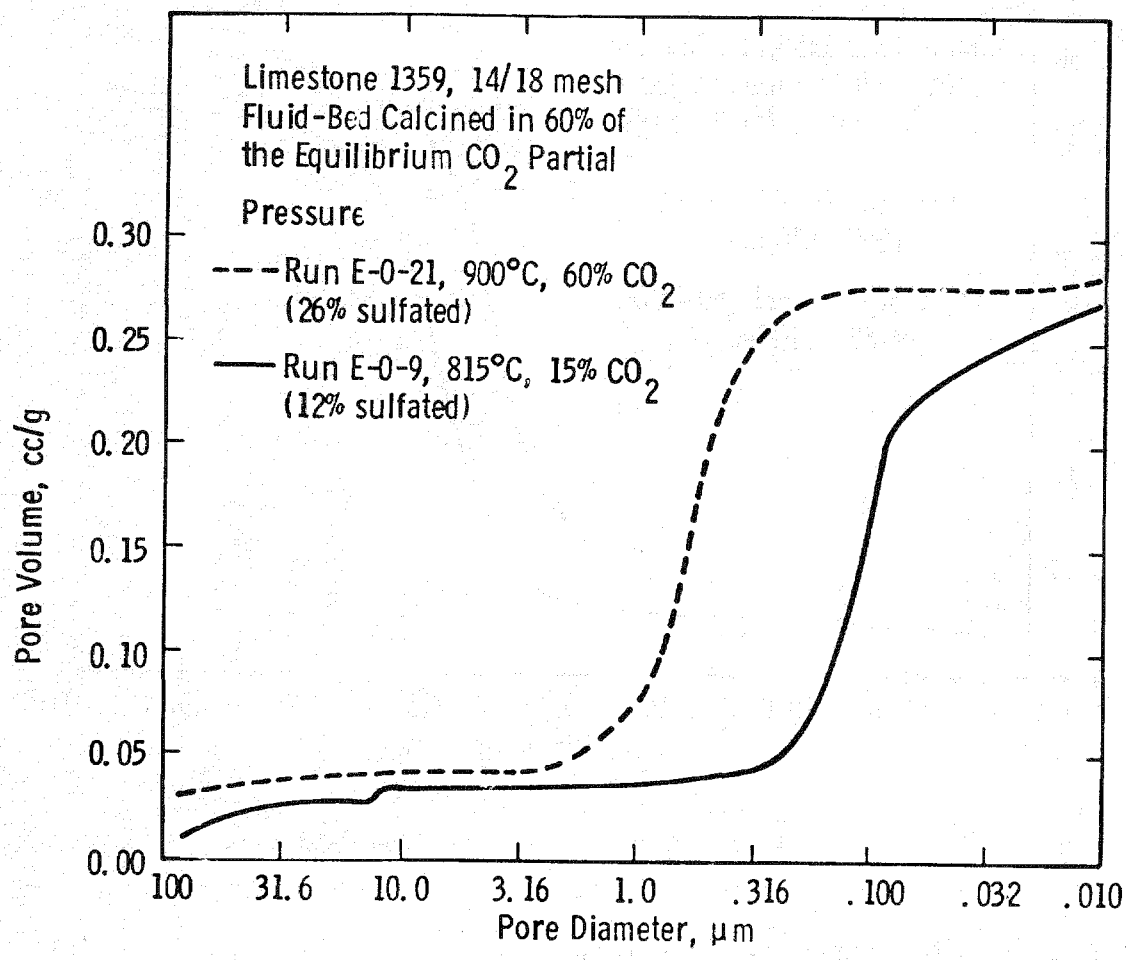

Figure 3-31. The Effect of Calcination Temperature on the Pore Volume Distribution of Limestone 1359 Calcines

The Lowellville stone (Figure 3-33) also shows a shift to larger pore sizes, but the total porosity decreases in the higher temperature calcine. Sulfur distributions obtained from this larger (∿40 μm) grained sorbent indicate a shift from intergranular to intragranular pores occurs with controlled calcination. This shift is needed for sulfur to penetrate the large grains and increase sorbent utilization.

Again, Dolomite 1337 (Figure 3-34) calcines have similar pore volume distributions which result in 98-100% sulfation.

Residence Time

The residence time of the calcines before sulfation has changed the pore volume distributions of the limestone calcines toward larger volumes made up of larger pores for those sorbents that also had improved sulfation extents.

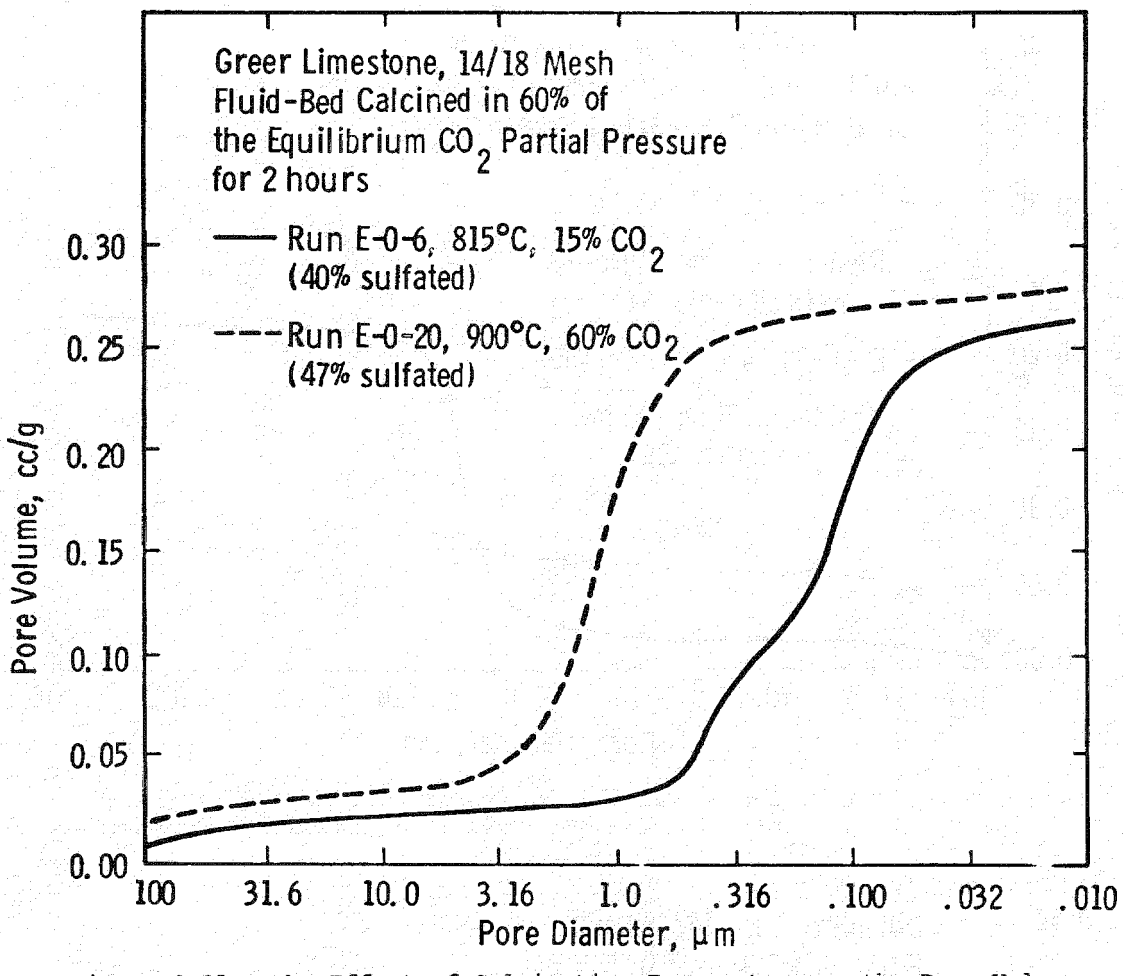

Figure 3-32. The Effect of Calcination Temperature on the Pore Volume Distribution of Greer Limestone Calcines

Limestone 1359 (Figure 3-35) at 815°C in N_2 showed more pores with diameters greater than 0.07 μm when it was reheated to 900°C for 1 hour. The shift in pore volume was followed by improved utilization (from 6 to 10%).

The two fluid bed calcines of Greer limestone analyzed were both prepared at 815°C in 15% CO_2, but the stone residence times differed. The sample calcined for 4 hours had a larger pore volume than the stone with a 2 hour residence time. The greatest concentration of pore volume occurred at 0.338 μm pores for the sample calcined for 4 hours. The sample with a 2 hour residence time had most of its pore volume in pores of 0.05 - 0.1 μm diameter (See Figure 3-36). The sample with the larger pore volume and with pores of greater pore diameter attained the greater sulfation extent, 55% compared to 40%. SEM photomicrographs of the calcines show the prolonged residence time of sample E-0-10 caused cracking of the sorbent (See Figure 3-37). This cracking evidently caused larger

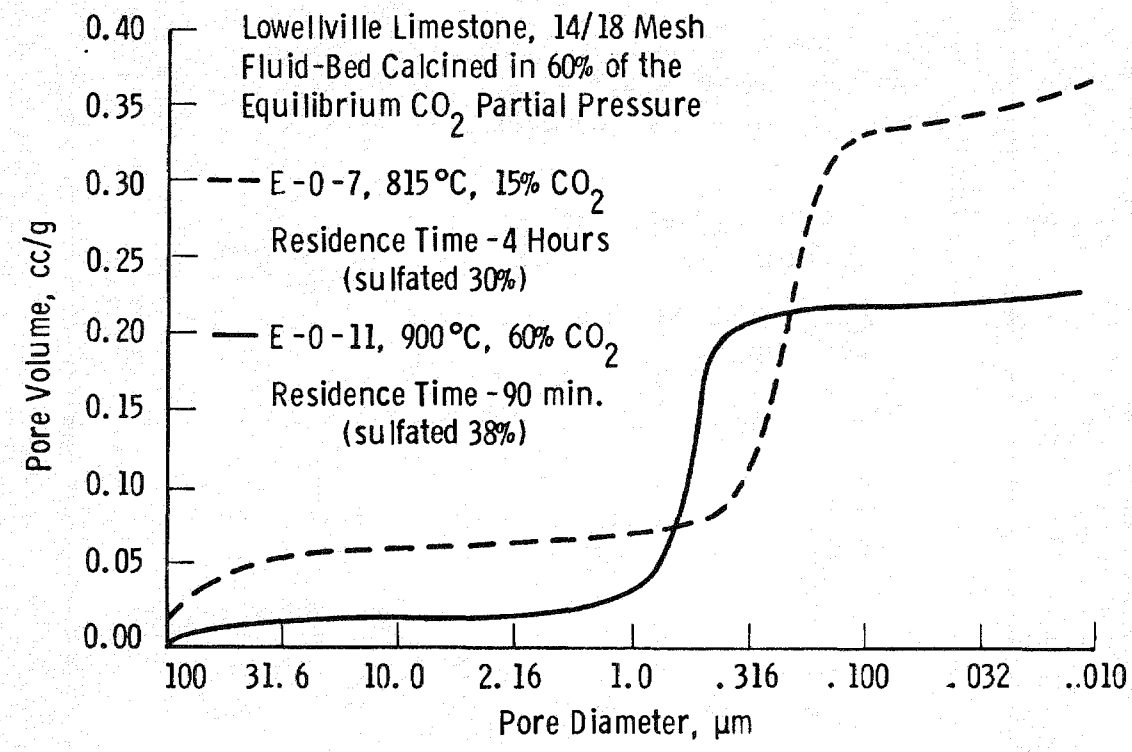

Figure 3-33. The Effect of Calcination Temperature on the Pore Volume Distribution of Lowellville Limestone Calcines

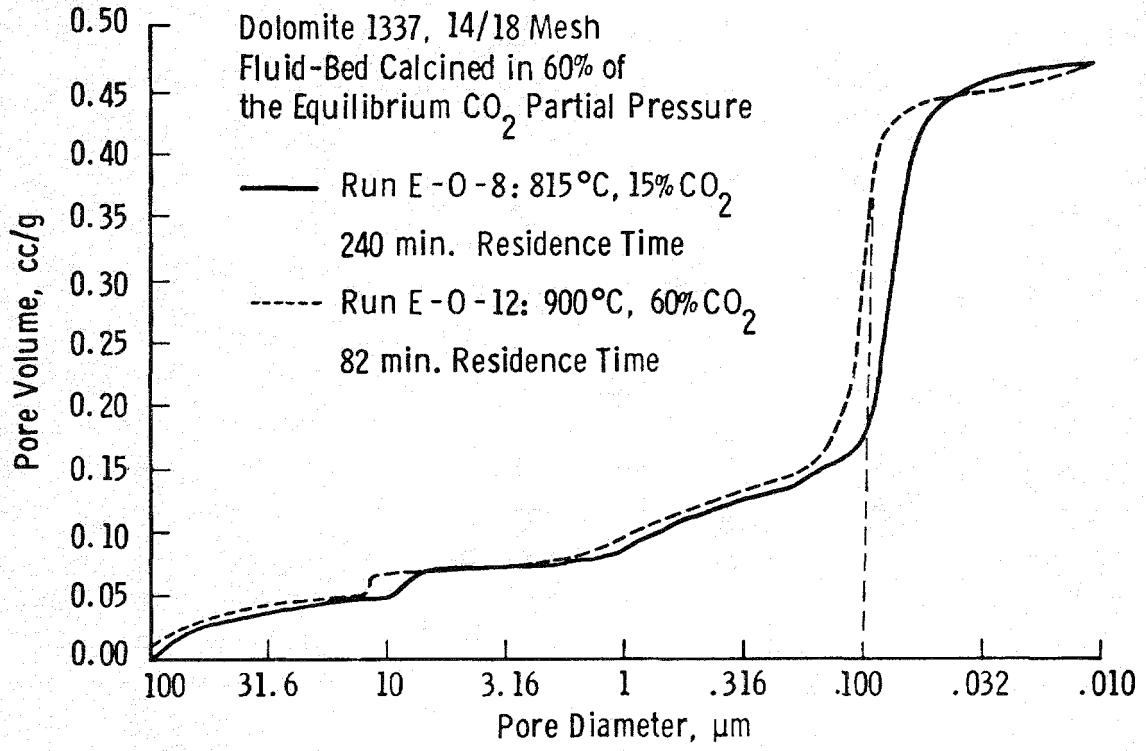

Figure 3-34. The Effect of Calcination Temperature on the Pore Volume Distribution of Dolomite 1337 Calcines

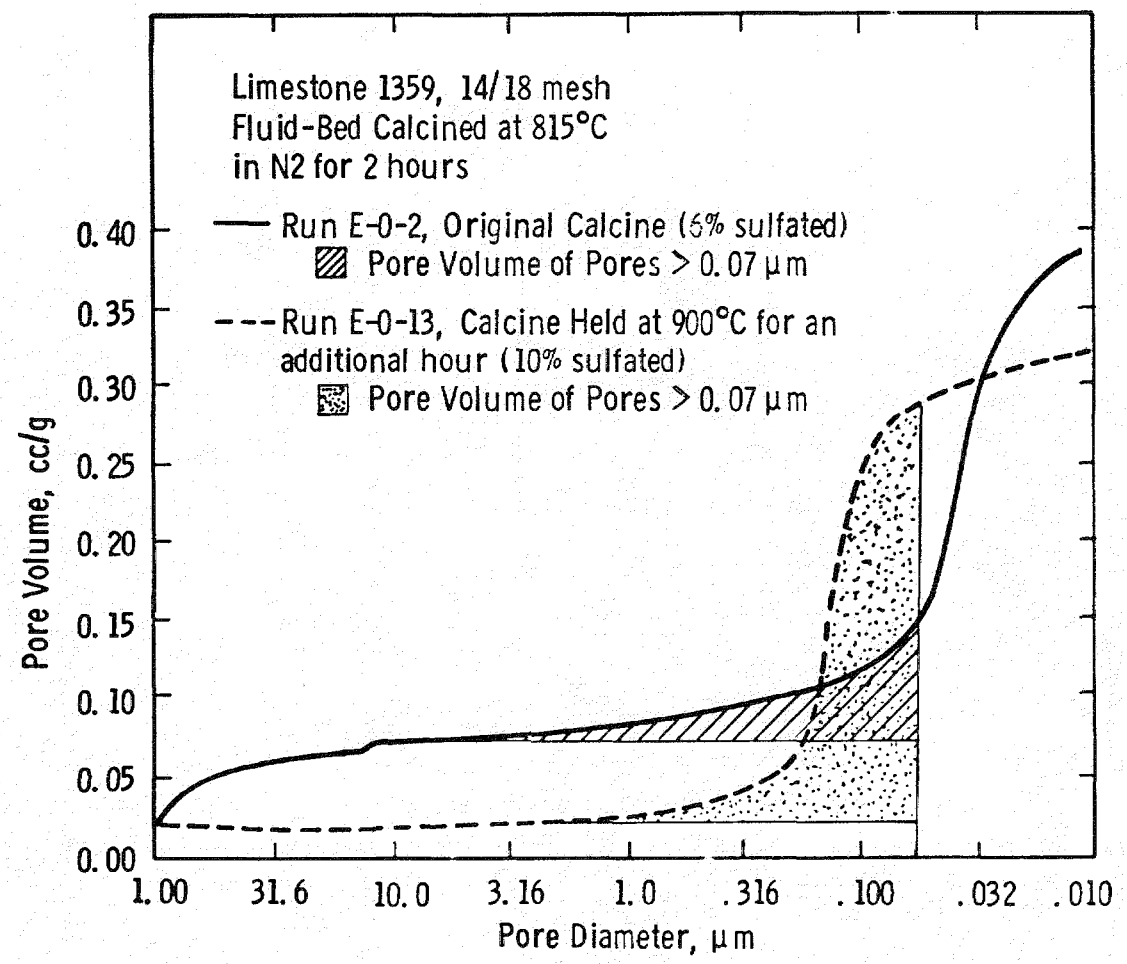

Figure 3-35. The Effect of Calcine Residence Time on the Pore Volume Distribution of Limestone 1359 Calcines

pores, but not greater surface area since the sorbent with the longer residence time has only half of the surface area of the shorter residence time calcine (See Table 3-8).

A sample of Lowellville limestone, calcined at 900°C in 60% CO_2, was reheated to 900°C for 150 minutes. The pore volume distribution of this calcine (Figure 3-38) did not shift and the reactivity of the sorbent decreased from 38 to 25% utilization.

Summary

The limestones showed a shift in pore volume distribution toward pores of larger diameter when the calcines were prepared in CO_2 or at high temperature (900°C). This shift led to greater sorbent utilization. The residence time

Table 3-8

PHYSICAL CHARACTERISTICS OF FLUID BED CALCINES

NO.	CALCINATION			PORE VOLUME		PORE DIAMETER OF MAXIMUM D(r)[1]	Density		TOTAL POROSITY, %	SURFACE AREA m^2/g	% Sulf.[2]
	TEMPERATURE	% CO_2 in N_2	RESIDENCE TIME (MINUTES)	0.1-1 μm pores	pores >0.07 μm		BULK (g/cc)	Hg (g/cc)			
Limestone 1359											
E-0-2	815	N_2	120	0.0380	0.0452	0.03					6
E-0-9	815	15	240	0.0967	0.1767	0.1				5.73	12
E-0-13 (E-0-2)	900	N_2	60	0.1685	0.2649	0.1	1.23	2.18	43.5		10
E-0-17	900	15	120	0.2109	0.2352	0.2	1.43	2.26	36.8	2.49	29
E-0-21	900	60	120	0.1943	0.2347	0.6	1.69	3.18	46.7		26
Greer Limestone											
E-0-6	815	15	120	0.1425	0.1880	0.09	1.14	1.67	31.5	5.88	40
E-0-10	815	15	240	0.2179	0.2209	0.3				2.59	55
E-0-14	815	N_2	240	0.1776	0.2535	0.1	0.81	1.32	38.4	5.18	29
E-0-18	900	15	120	0.2105	0.3258	0.5	1.01	1.57	35.8		57
E-0-20	900	60	120	0.0902	0.2326	0.2	1.19	1.77	32.6		47
Lowellville Limestone											
E-0-7	815	15	240	0.2622	0.2646	0.2	1.43	2.79	48.5	5.84	30
E-0-11	900	60	90	0.1414	0.1425	0.5	1.60	2.57	37.6		38
E-0-19 (E-0-11)	900	N_2	150	0.2453	0.3522	0.05	1.01	2.21	54.4		25
Dolomite 1337											
E-0-8	815	N_2	240	0.0880	0.2352	0.08				12.5	98
E-0-12	900	60	82	0.1963	0.3293	0.09				9.39	100
E-0-15	900	15	82	0.1974	0.3805	0.3	1.19	2.97	54.87		85

(1) Pore diameter at which the differential pore volume, dV/dr, is a maximum
(2) Sulfation extent obtained when rate fell below 0.1% Ca sulfating per minute

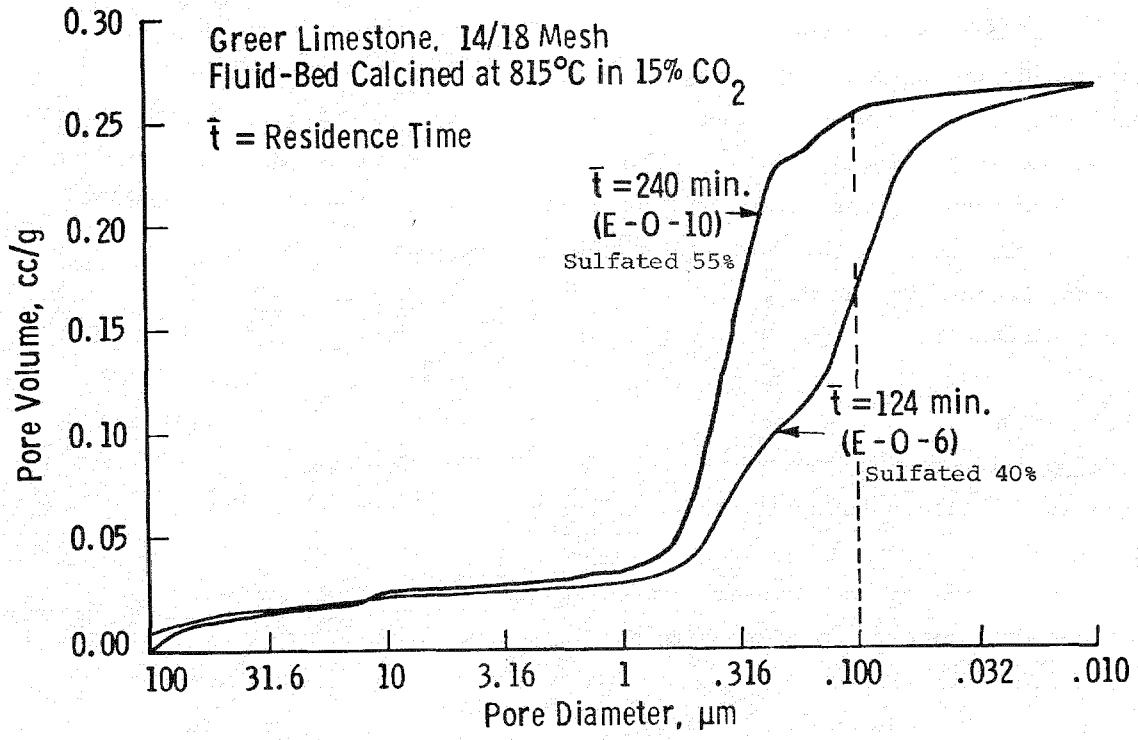

Figure 3-36. The Effect of Residence Time at Calcination Conditions on the Pore Volume Distribution of Greer Limestone Calcines

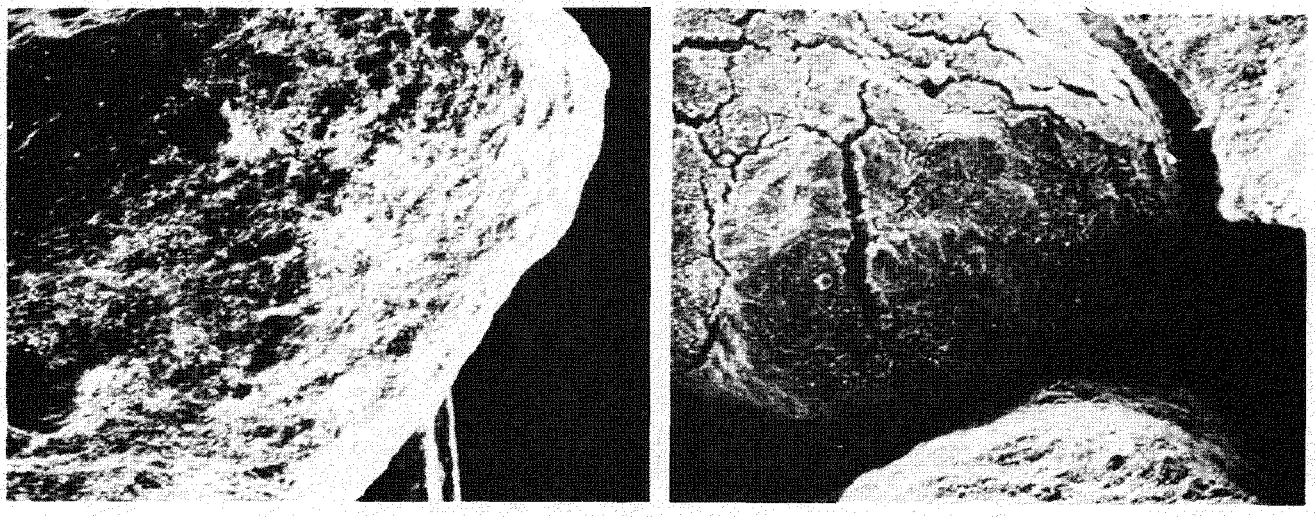

Figure 3-37. Electron Micrographs of Calcined Greer Limestone. Sample E-O-10 on the Right With the Large Fissures ~1-10 Micron, was more Heavily Sulfated (55%) than Sample E-O-6 on the Left (40%). (1,000 Micron Particles at 85X).

of a calcine (time held after calcination and before sulfation) exerts a specific effect on each sorbent. Limestone 1359 and Greer limestone are activated by increased calcine residence time. Lowellville limestone was deactivated with 150 minute added exposure to 900°C. Dolomite 1337 shows little pore volume in pores greater than 0.2 μm. The high utilization of the dolomite arises from a pore distribution which allows sulfur to penetrate into the grains as well as into the particle. The lower density of calcium in the dolomite (because of the magnesium fraction) permits higher calcium utilization without blockage of the pores by product sulfate

The sulfation capacity of the different sorbents is not solely characterized by the porosity of the calcine used. A combination of large pores (>0.2 μm) to transport sulfate intergranularly to the center of the particle and intragranular pores to allow complete sulfation of individual grains is needed. The particle size of the sorbent, and the grain structure of the parent limestone determine the optimum combination of transport and intragranular pores. Calcination controlled by CO_2 suppression alters the pore structure toward the desired distribution of pore sizes.

Density and Surface Area of the Calcines

The density and the surface area of the calcines (Table 3-8) showed no correlation with the sulfation extent obtained. Since the reactivity of a sorbent will depend on the distribution of pores throughout the sample, the over-all density (or surface area - See Figure 3-28), like the over-all porosity, will not measure potential sorbent utilization in sulfation.

3.6 SULFUR DISTRIBUTION IN THE REACTED SORBENTS

The sulfur distribution for samples of limestone was mapped by the electron microprobe. This technique examines the energy distribution of X-rays scattered from the sample surface by an electron beam, and shows where the element of interest is detected as the probe moves across the surface.

The samples examined showed a variety of sulfation patterns. The photographs of the sulfur scans are shown in Figures 3-39 to 3-68. The photographs for each sample were analyzed, (rather subjectively) with a view to answering the following questions.

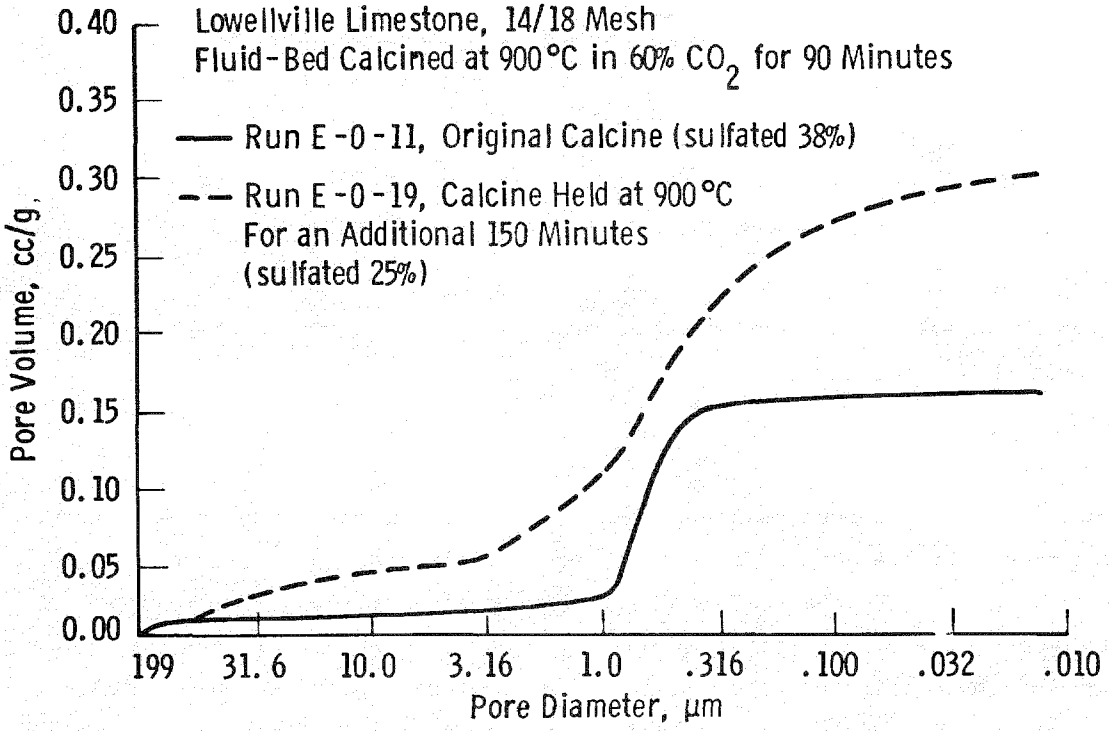

Figure 3-38. The Effect of Calcine Residence Time on The Pore Volume Distribution of Lowellville Limestone Calcines

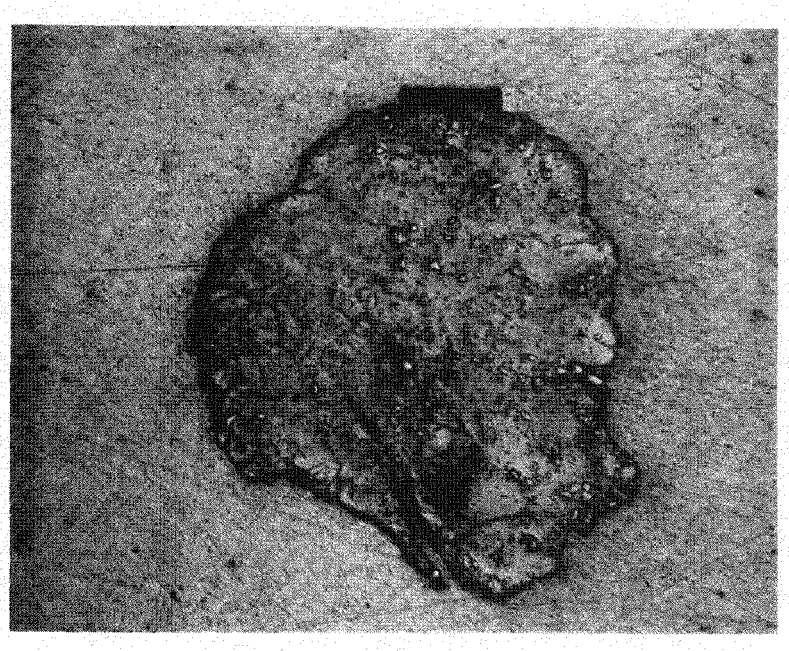

Figure 3-39. Sulfated Particle of Greer Limestone From Run 75 (X50)

Where is the sulfur?

Is there an obvious shell of calcium sulfate (and by shell is meant a sharp interface between $CaSO_4$ and CaO past which sulfur has not migrated)?

Did sulfur penetrate to the center of the stone?

Did the sulfur penetrate the individual grains of oxide within the particle?

Does the sulfur map correspond to expectations of sulfur content from the TG result?

The analysis of the photographs is shown in Table 3-9.

The conclusions have been outlined in Section 1.2.10. The photographs indicate that a model which accounts for both inter and intragranular diffusion is necessary to describe the sulfation rate mathematically. In order to apply such a model it would be extremely useful to have a more detailed examination of some of these sulfated particles to determine grain penetration by sulfur as a function of grain position along the particle radius. The examination of similar sorbent particles from a larger fbc facility would improve our understanding of the relationship between laboratory studies of sulfation, and "in-situ" sulfur removal in the fluidized bed combustor.

Table 3-9

CHARACTERISTICS OF THE SULFUR DISTRIBUTION
IN SULFATED SORBENTS

RUN NO.	SORBENT HISTORY	WHERE IS THE SULFUR	OBVIOUS SHELL?	SULFUR PENETRATION TO CENTER?	SULFUR PENETRATION OF INDIVIDUAL GRAINS	DOES SULFUR MAP CORRESPOND TO TG RECORD OF SULFATION
	GREER:					
75	16% $CaSO_4$	Edge	Yes	Yes - through large channels	?	Approx: <30%
87	55% $CaSO_4$	Varied	Yes	Yes	?	Approx: ∿78%
119	40% $CaSO_4$	Throughout	No	Yes	Yes	No ∿80%
	LOWELLVILLE:					
114	17% $CaSO_4$	Distributed - denser at edge	No	Yes	Some penetration near edge - original 40 micron grains not penetrated	Density distribution precludes simple estimation
116	40% $CaSO_4$	Thick shell varies in depth	Yes	?	Yes - at edge No - at center	Approx: 55%
141	25% $CaSO_4$	Near surface	Yes	No	To some extent at the surface	?
	DOLOMITE 1337:					
115	51% $CaSO_4$	Throughout	No	Yes	Yes - less penetration near center of particle	?
117	85% $CaSO_4$	Throughout except for small central portion	No	Almost	Yes	Obviously heavily sulfated

? indicates that the data shed no light on the question posed.

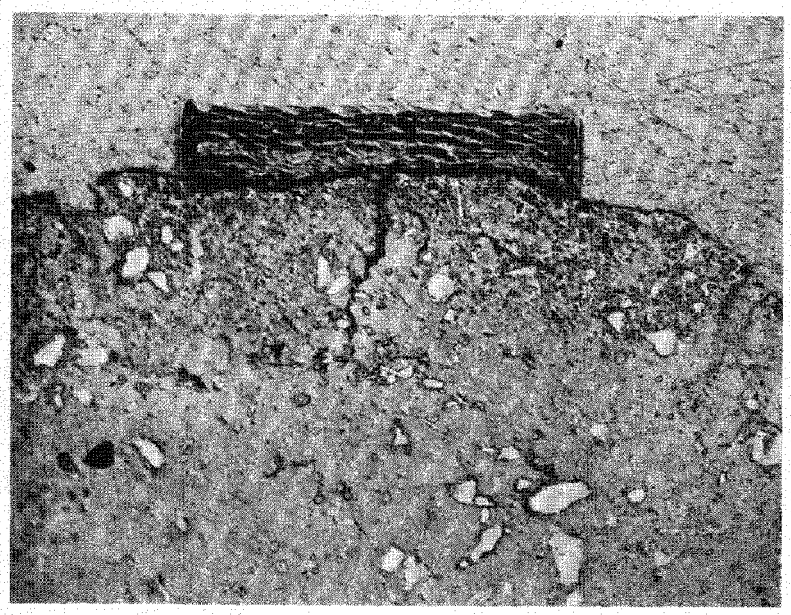

Edge
Section

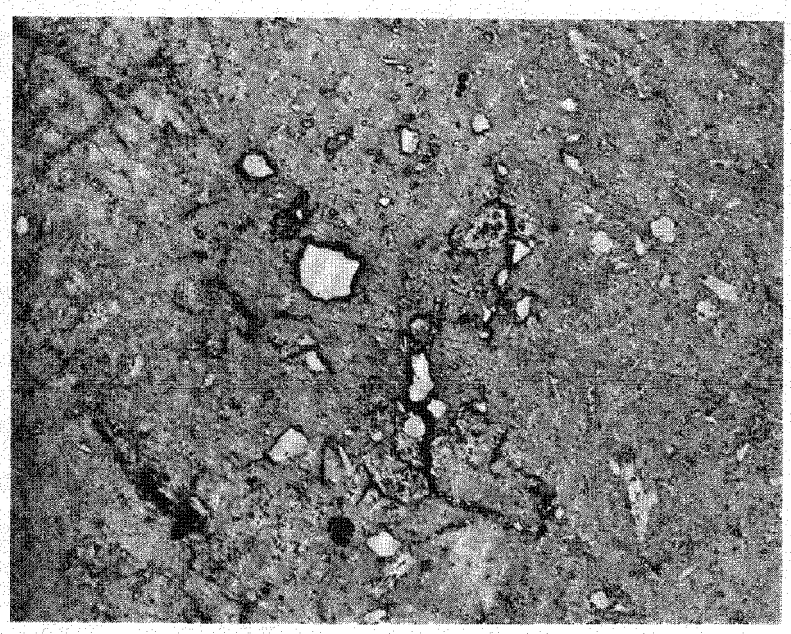

Center
Section

Figure 3-40. Sections of Particle From Run 75 Used For Electron Microprobe Scans (X200)

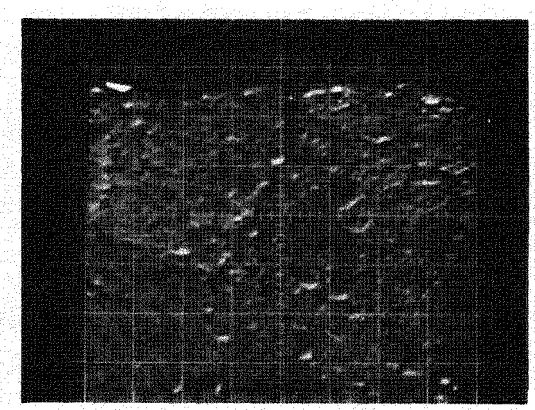

Photomicrograph of
Scanned Area

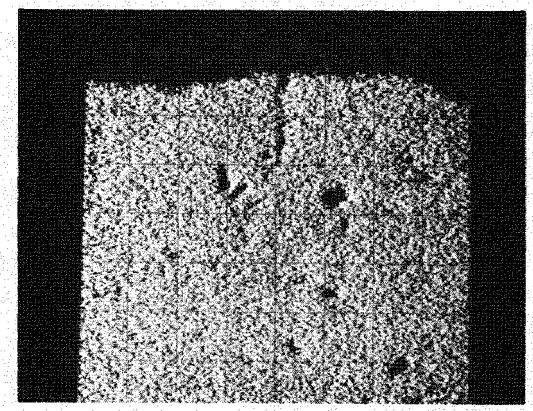

Calcium Scan

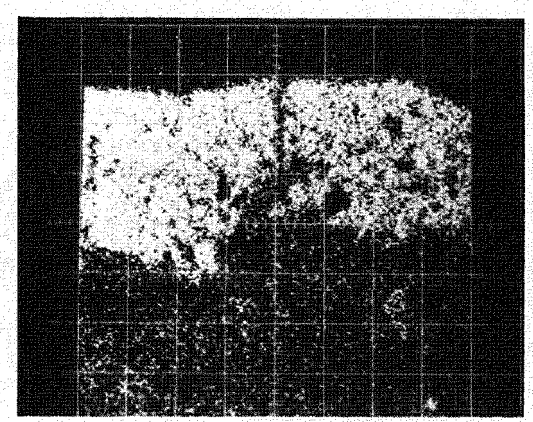

Sulfur Scan

Figure 3-41. Electron Microprobe Scans of Greer Limestone From Run 75, Edge Section (X225)

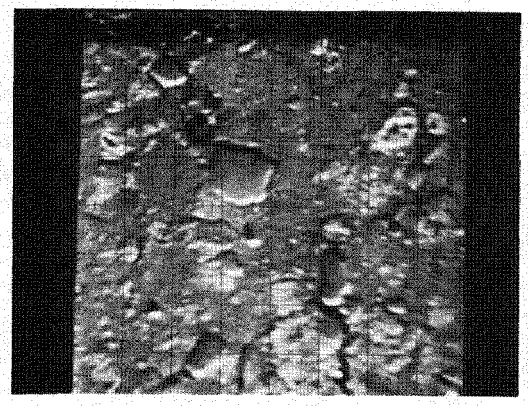

Photomicrograph of Scanned Area

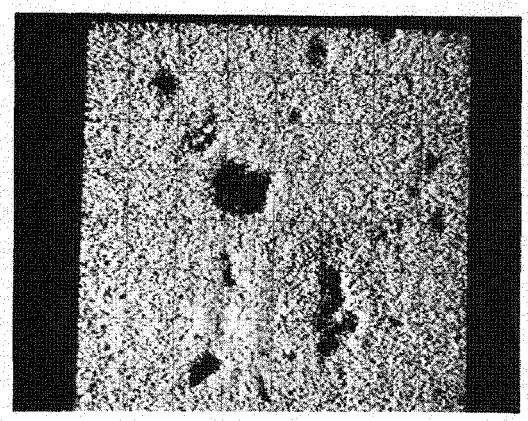

Calcium Scan

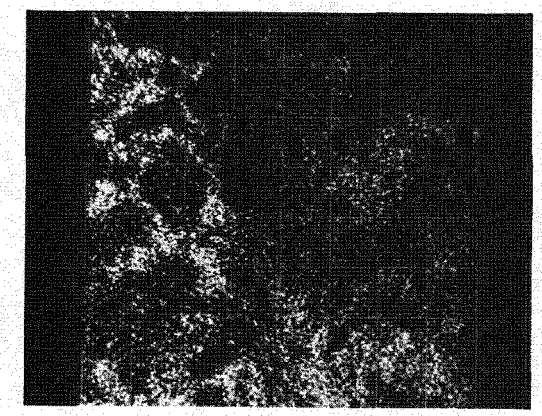

Sulfur Scan

Figure 3-42. Electron Microprobe Scans of Greer Limestone From Run 75, Center Section (X225)

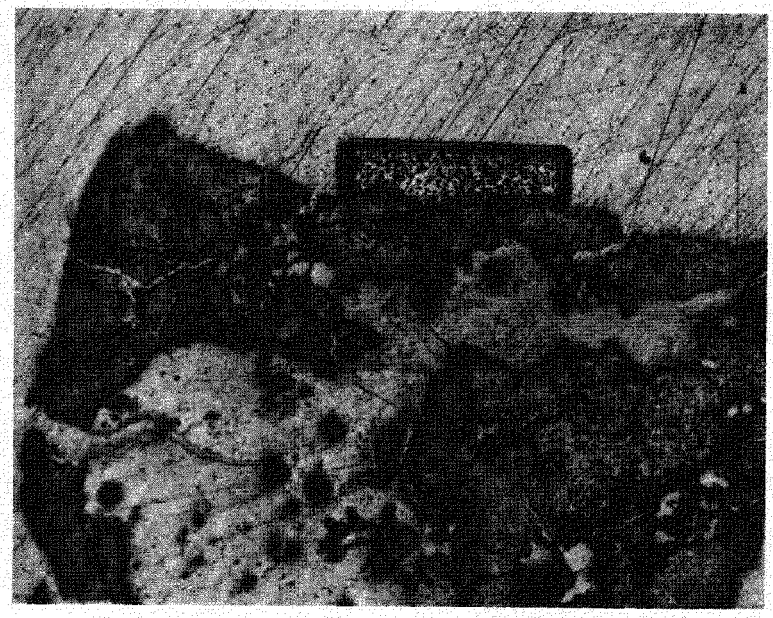

Figure 3-43. Sulfated Particle of Greer Limestone From Run 87 (X100)

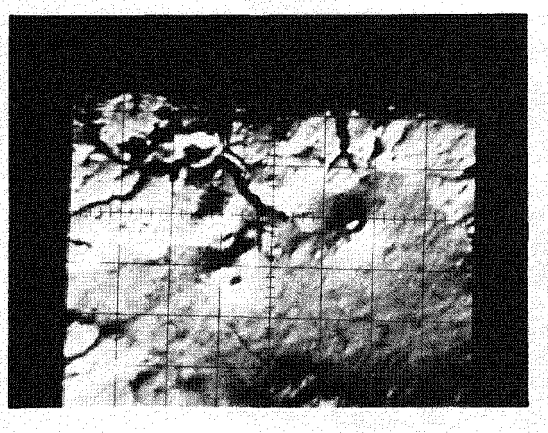

Photomicrograph of Scanned Area

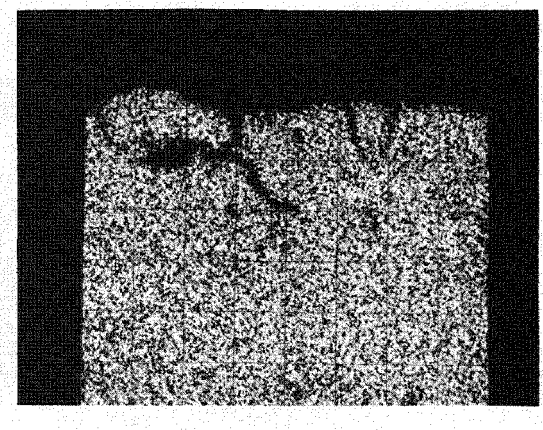

Calcium Scan

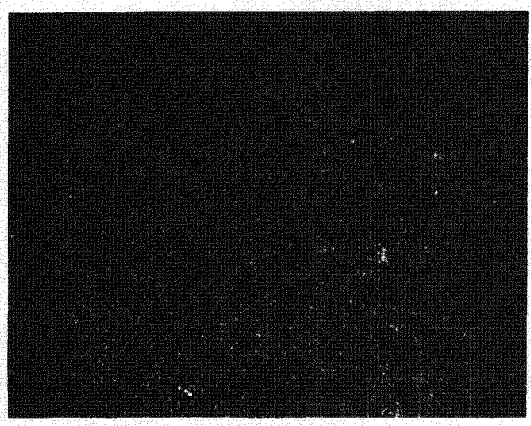

Magnesium Scan

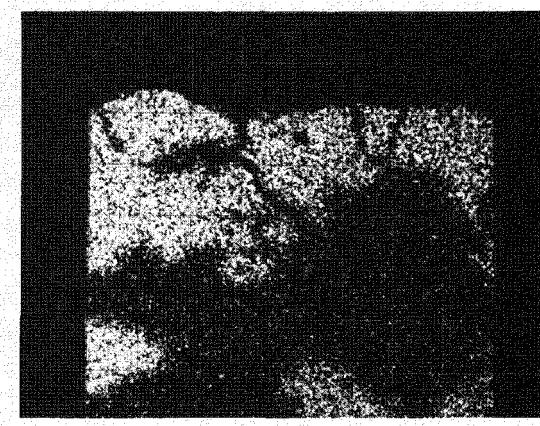

Sulfur Scan

Figure 3-44. Electron Microprobe Scans of Greer Limestone From Run 87 (X220)

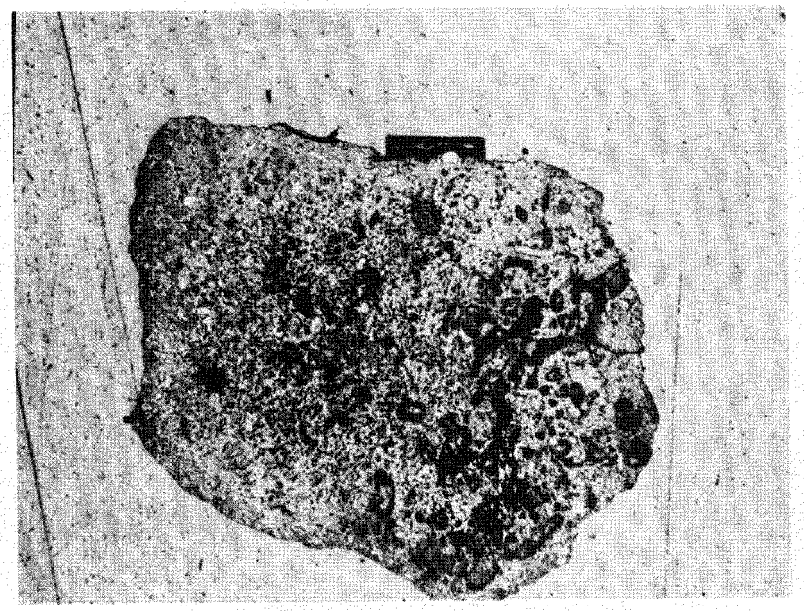

Figure 3-45. Sulfated Particle of Greer Limestone From Run 119 (X50)

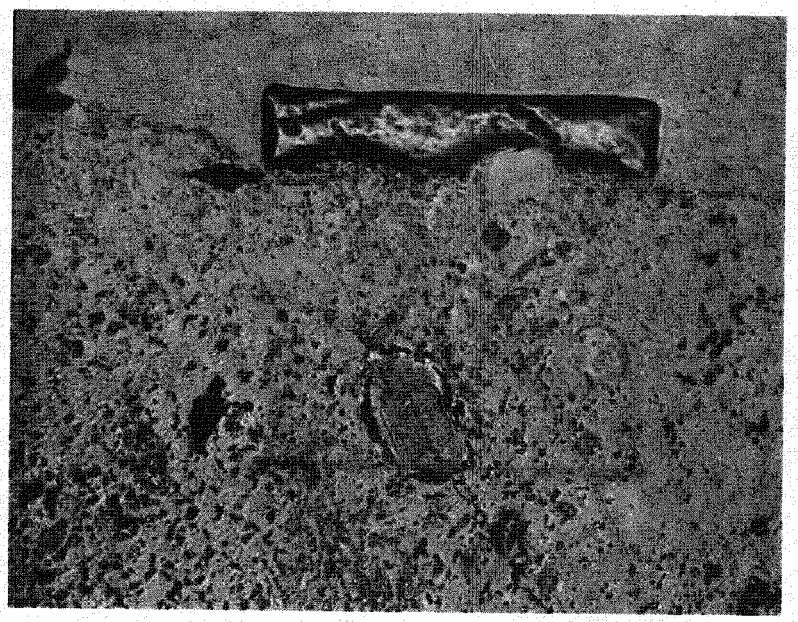

Edge
Section

Center
Section

Figure 3-46. Sections of Particle From Run 119 Used for Electron Microprobe Scans (X200)

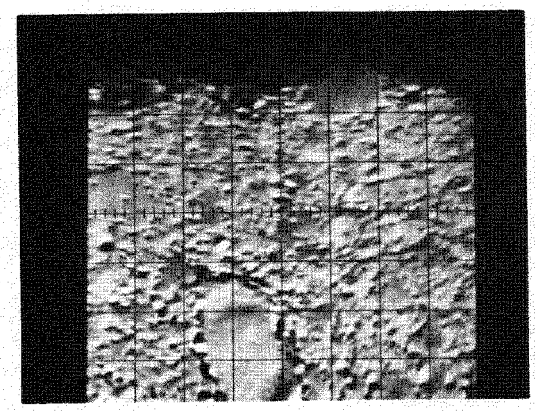

Photomicrograph of Scanned Area

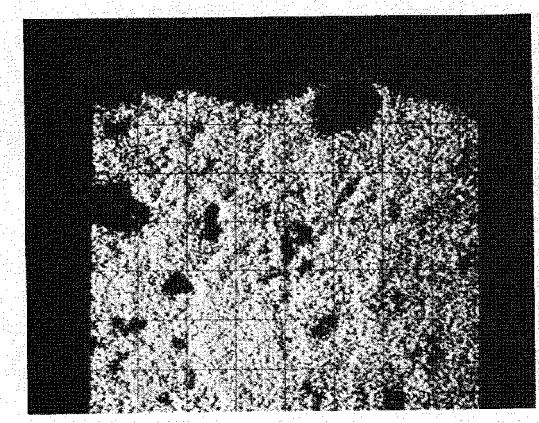

Calcium Scan

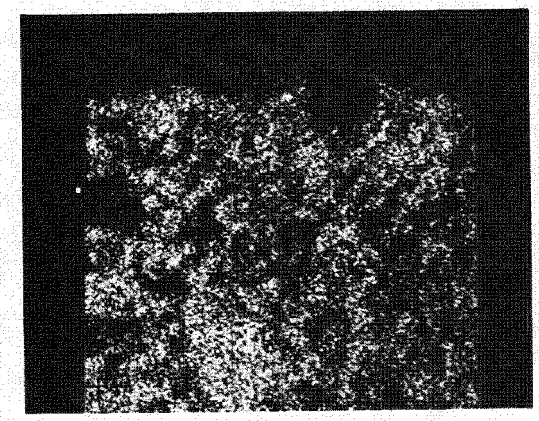

Sulfur Scan

Figure 3-47. Electron Microprobe Scans of Greer Limestone From Run 119, Edge Section (X225)

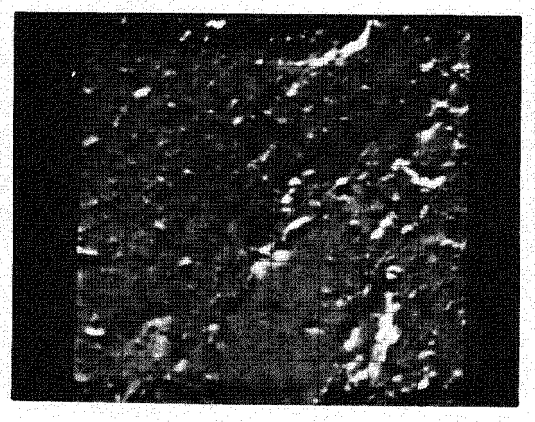

Photomicrograph of Scanned Area

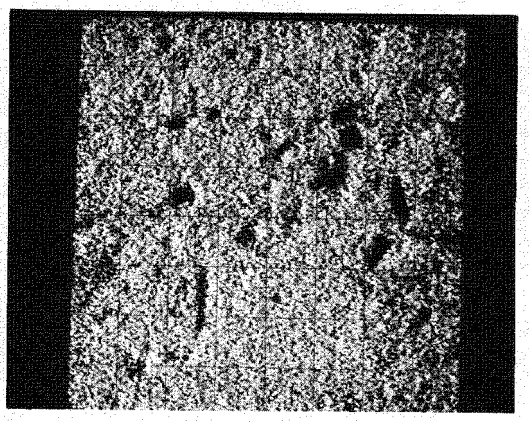

Calcium Scan

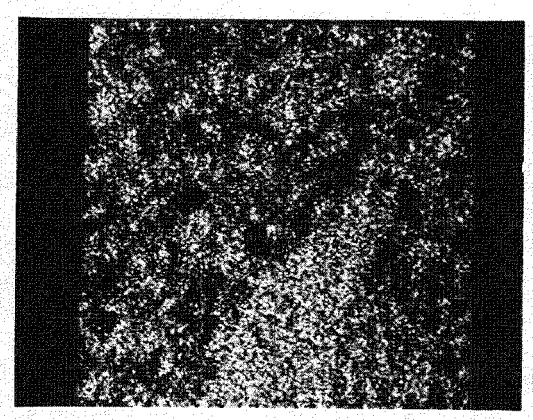

Sulfur Scan

Figure 3-48. Electron Microprobe Scans of Greer Limestone From Run 119, Center Section (X225)

Figure 3-49. Sulfated Particle of Lowellville Limestone From Run 114 (X50)

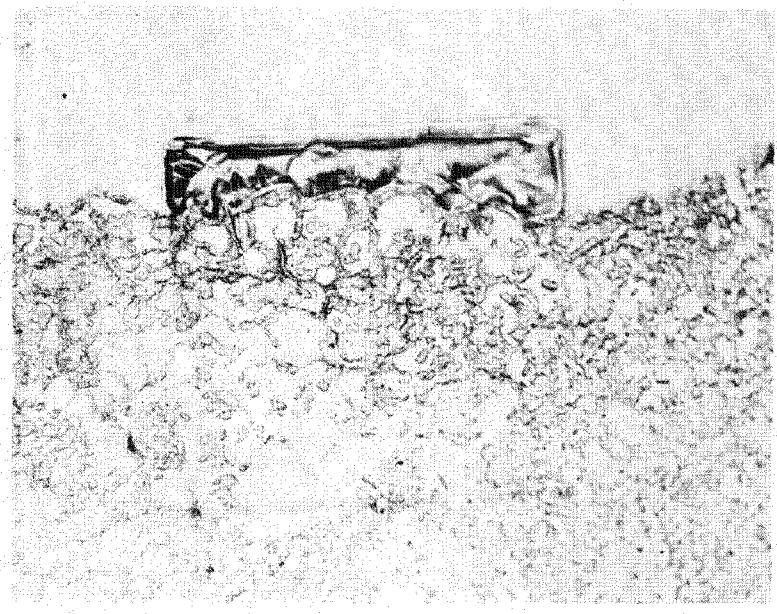

Edge Section

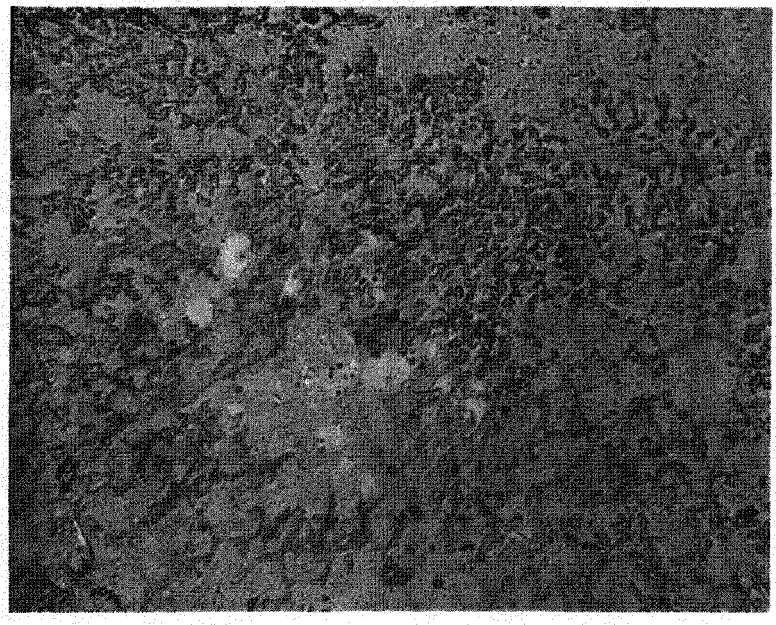

Center Section

Figure 3-50. Sections of Particles From Run 114 Used For Electron Microprobe Scans (X200)

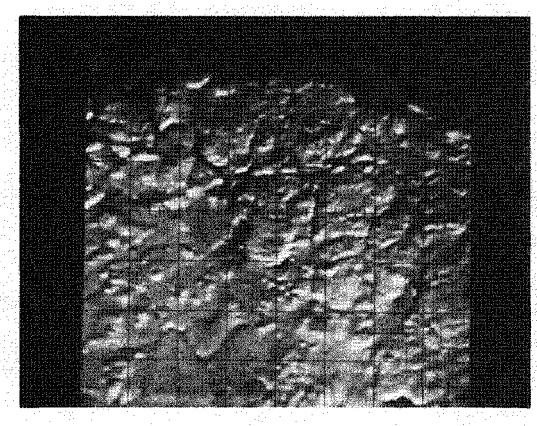

Photomicrograph of
Scanned Area

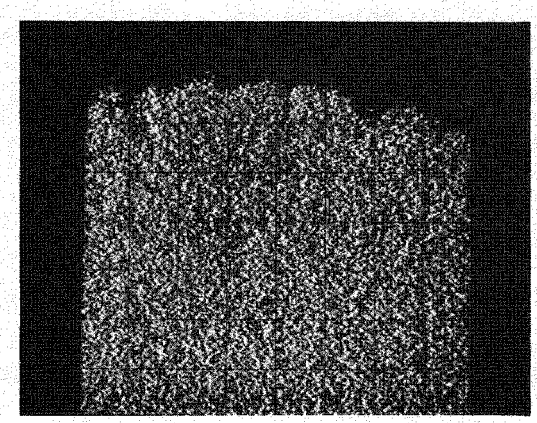

Calcium Scan

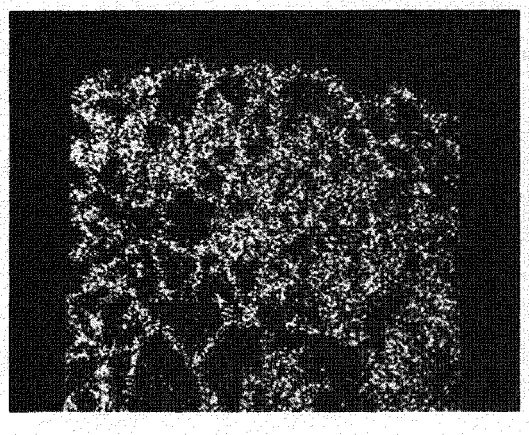

Sulfur Scan

Figure 3-51. Electron Microprobe Scans of Lowellville Limestone From Run 114, Edge Section (X250)

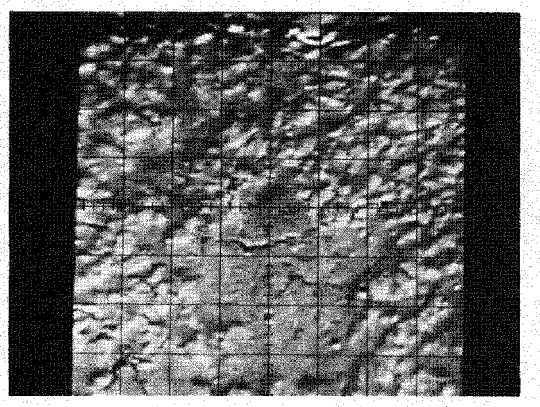

Photomicrograph of
Scanned Area

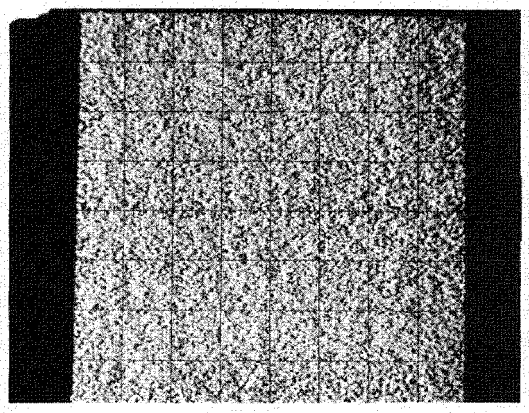

Calcium Scan

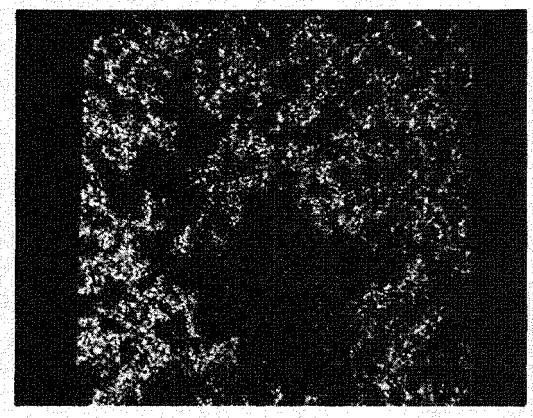

Sulfur Scan

Figure 3-52. Electron Microprobe Scans of Lowellville Limestone From Run 114, Center Section (X225)

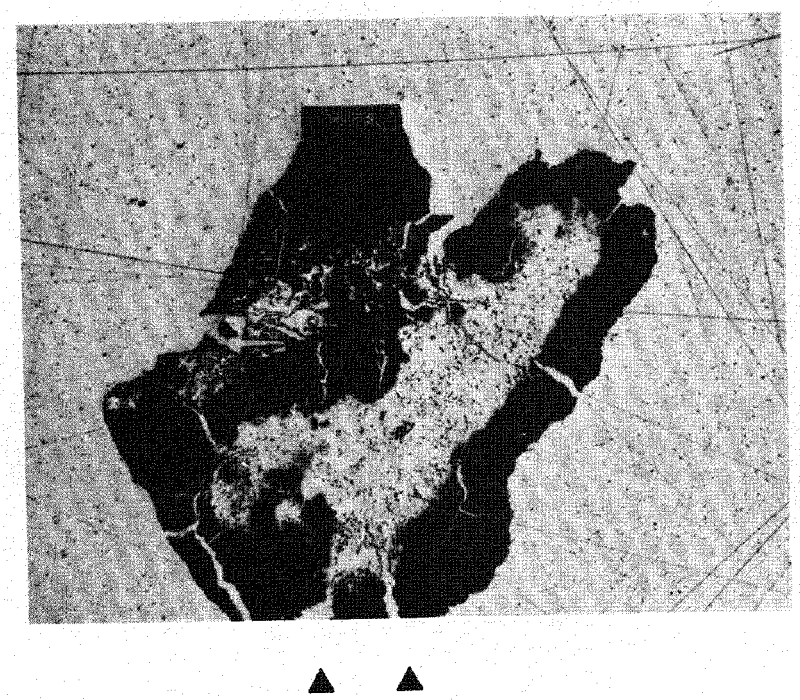

Figure 3-53. Sulfated Particle of Lowellville Limestone From Run 116 (X50)

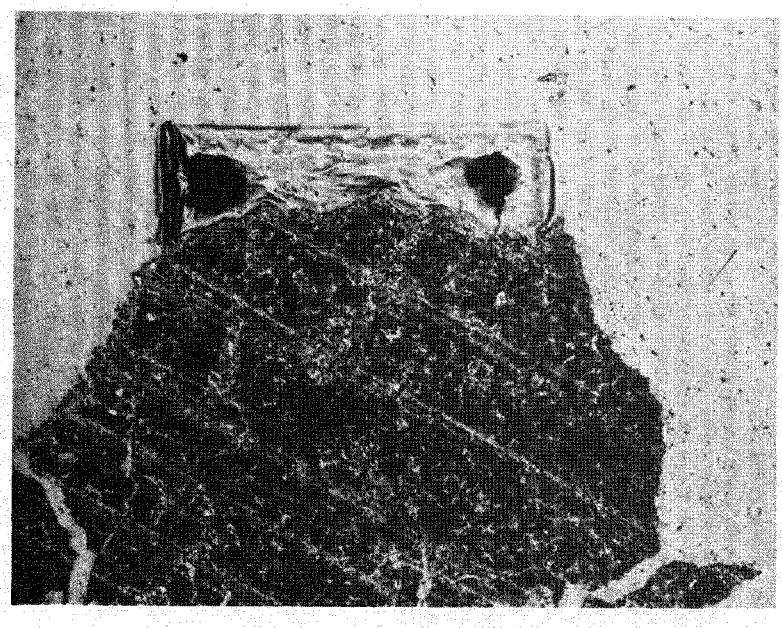

Edge Section

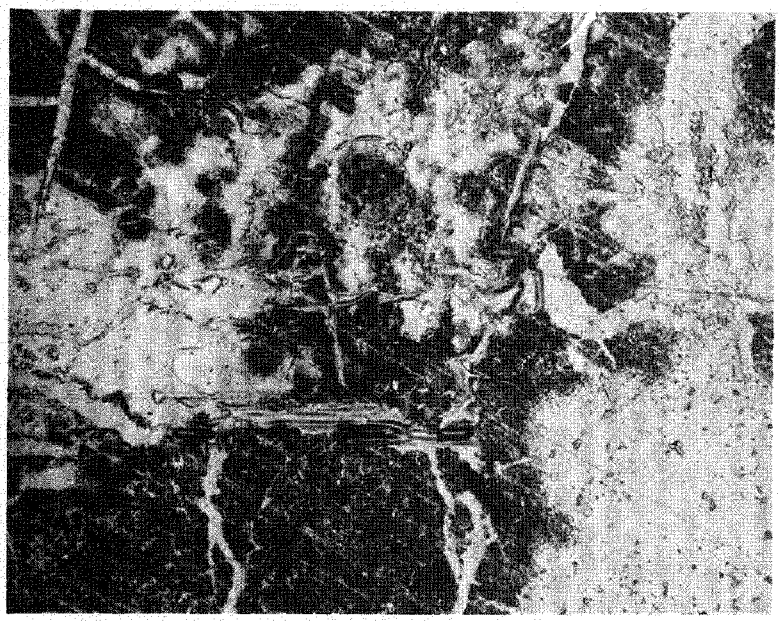

Center Section

Figure 3-54. Sections of Particle From Run 116 Used For Electron Microprobe Scans (X200)

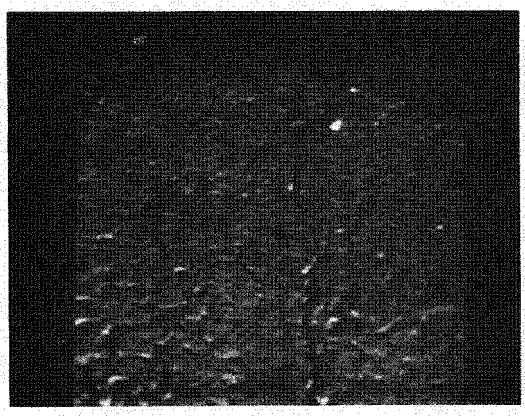

Photomicrograph of
Scanned Area

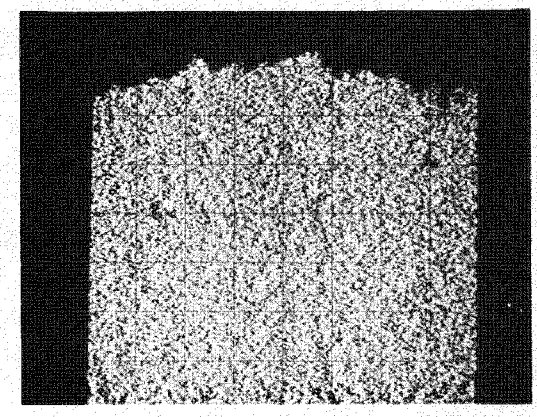

Calcium Scan

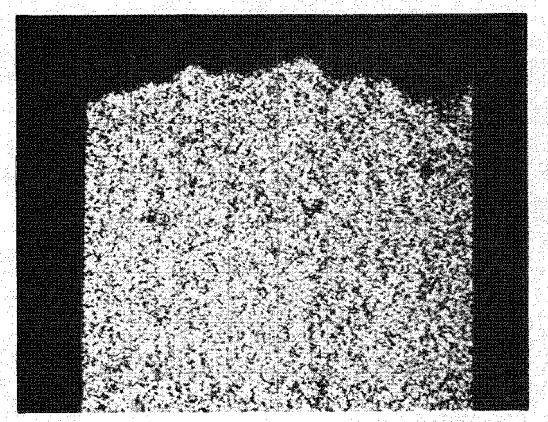

Sulfur Scan

Figure 3-55. Electron Microprobe Scans of Lowellvile Limestone From Run 116, Edge Section (X225)

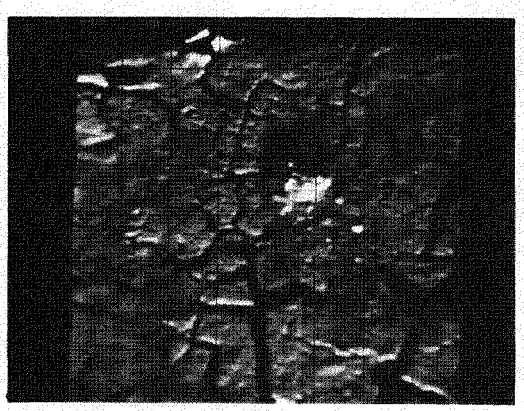

Photomicrograph of
Scanned Area

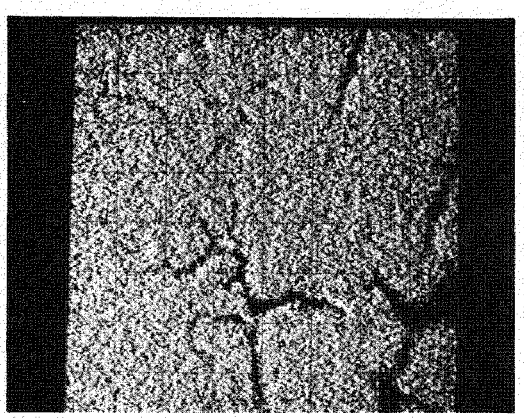

Calcium Scan

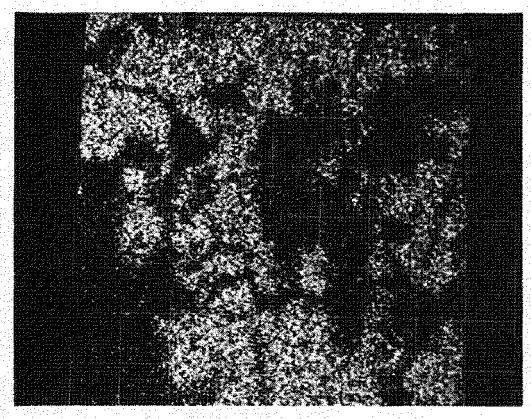

Sulfur Scan

Figure 3-56. Electron Microprobe Scans of Lowellville Limestone From Run 116, Center Section (X225)

Figure 3-57. Sulfated Particle of Lowellville Limestone From Run 141 (X50)

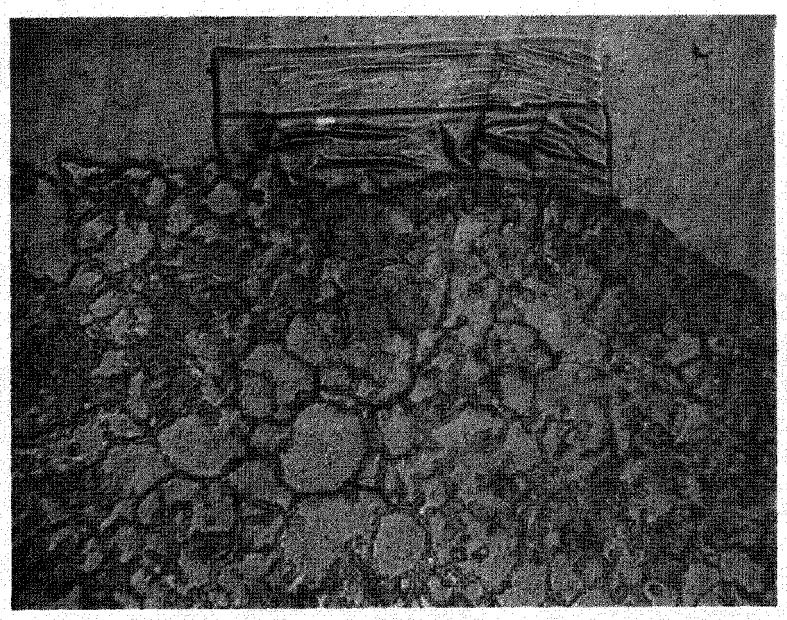

Edge
Section

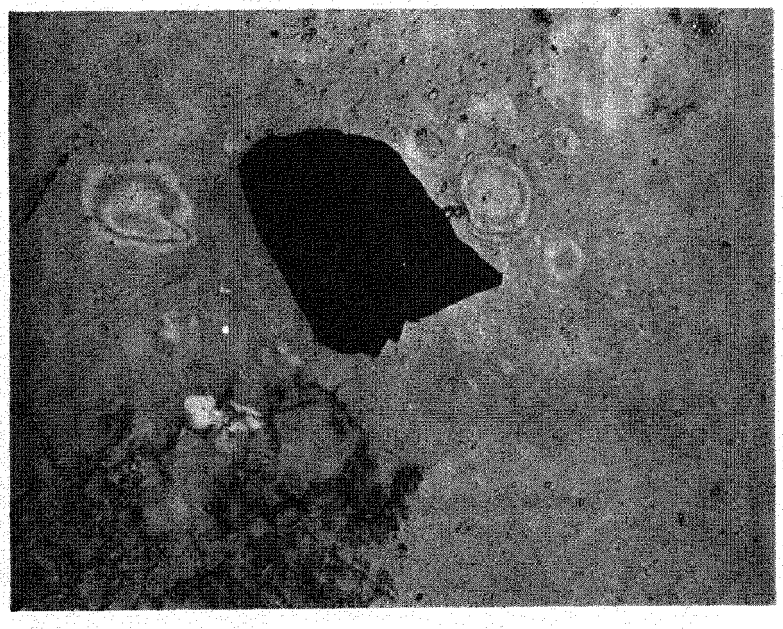

Center
Section

Figure 3-58. Sections of Particles From Run 141 Used for Electron Microprobe Scans (X200)

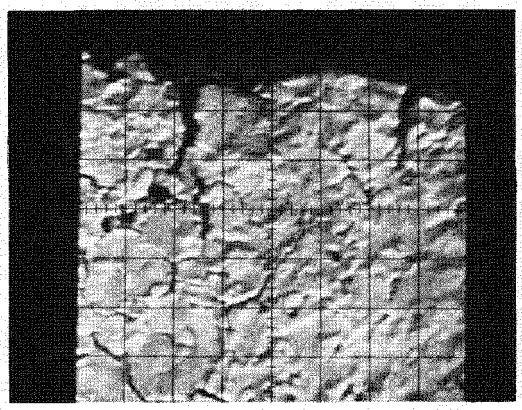

Photomicrograph of
Scanned Area

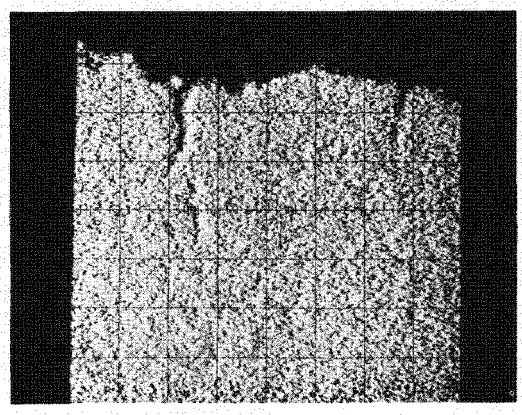

Calcium Scan

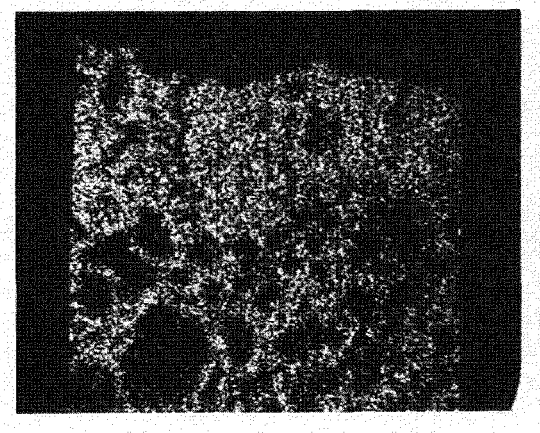

Sulfur Scan

Figure 3-59. Electron Microprobe Scans of Lowellville Limestone From Run 141, Edge Section (X225)

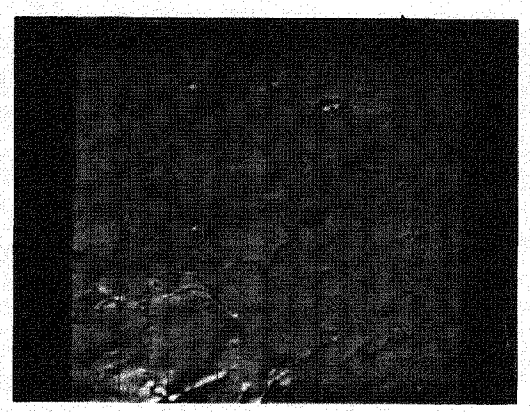

Photomicrograph of
Scanned Area

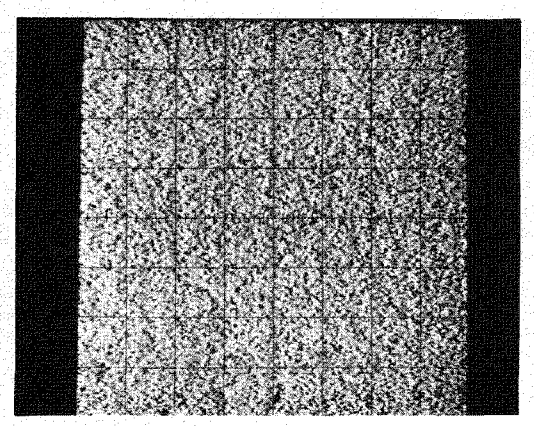

Calcium Scan

Sulfur Scan

Figure 3-60. Electron Microprobe Scans of Lowellville Limestone From Run 141, Center Section (X225)

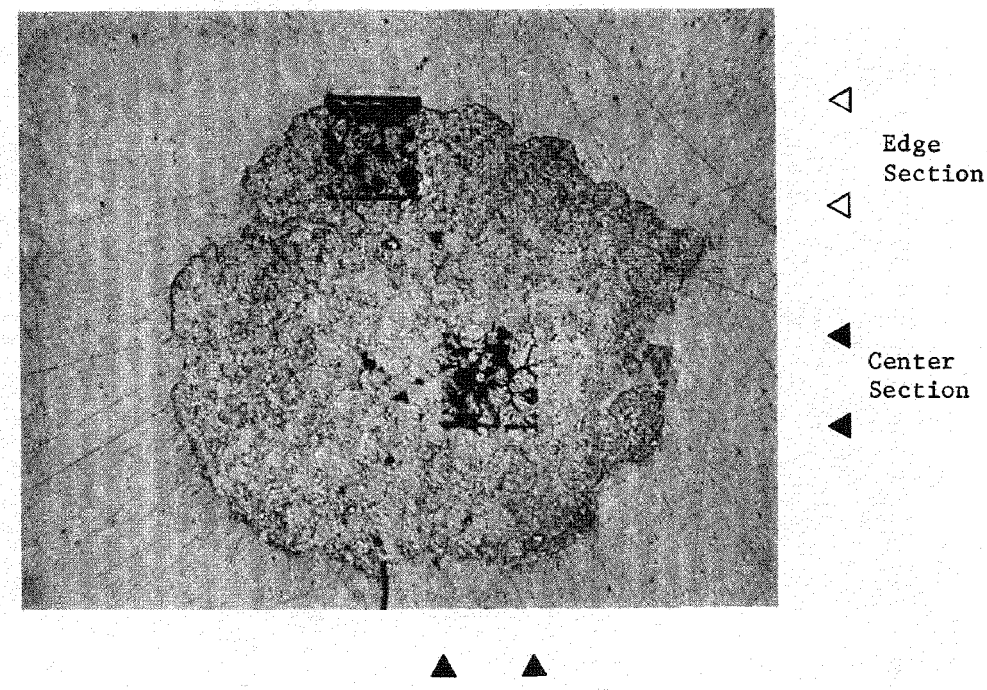

Figure 3-61. Sulfated Particle of Dolomite 1337 From Run 115 (X50)

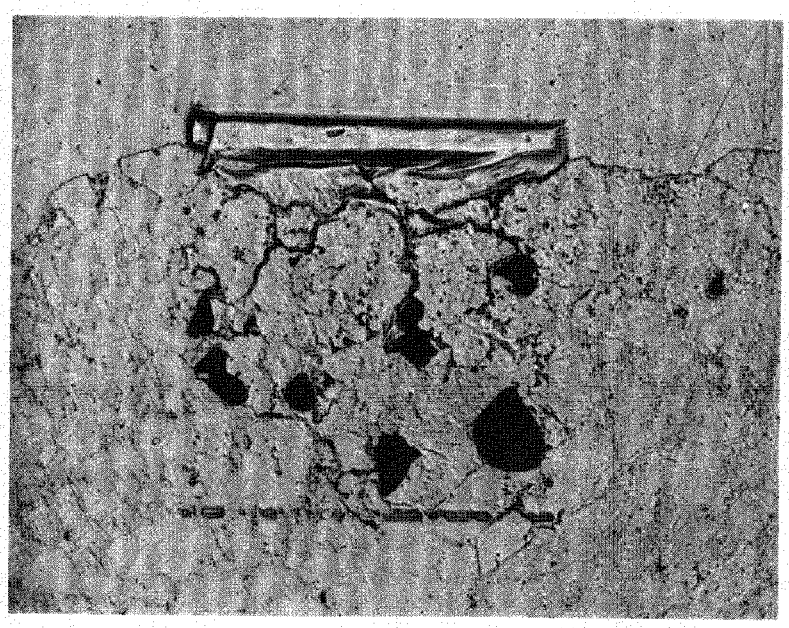

Edge Section

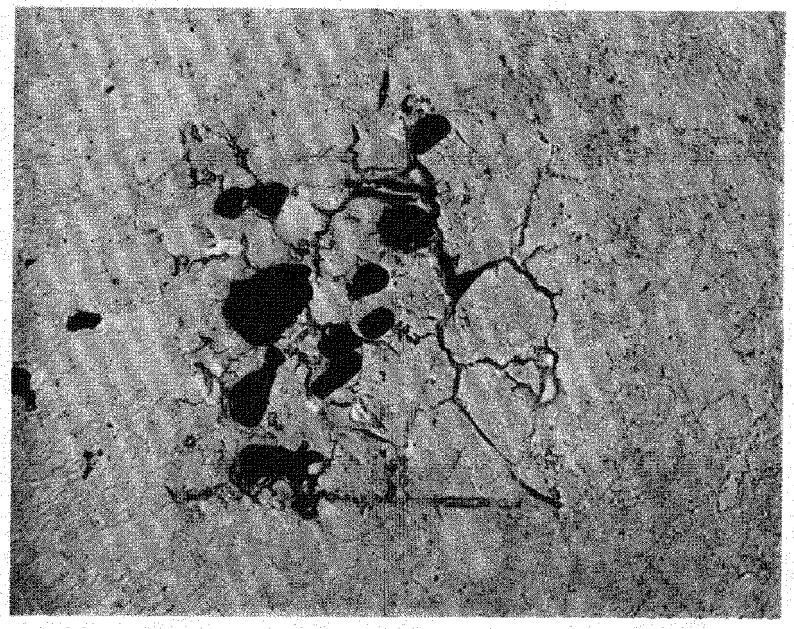

Center Section

Figure 3-62. Sections of Particle From Run 115 Used For Electron Microprobe Scans (X200)

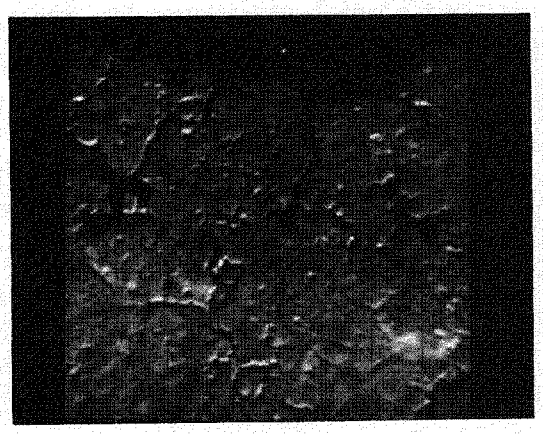

Photomicrograph of Scanned Area

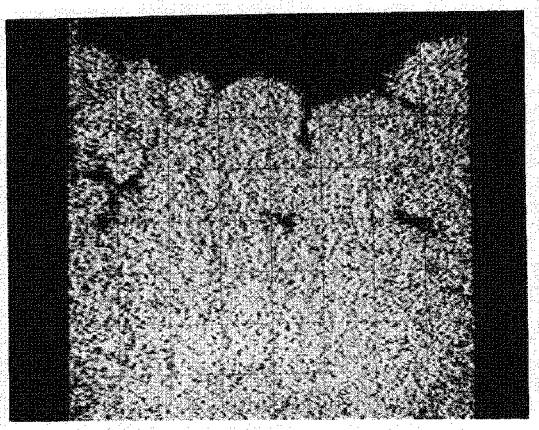

Calcium Scan

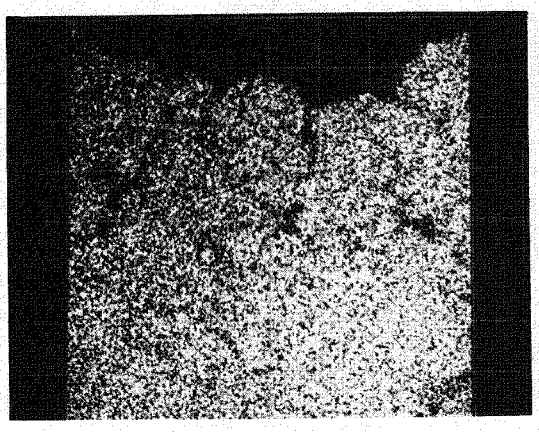

Magnesium Scan

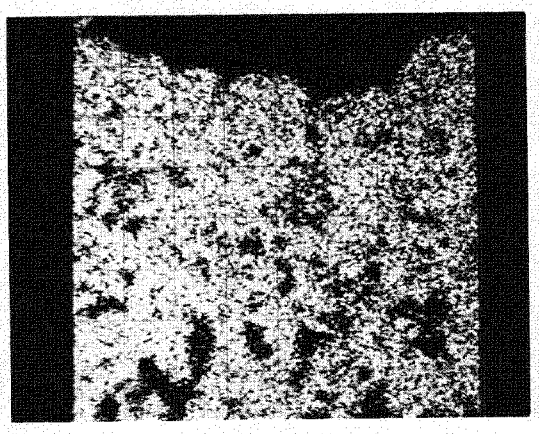

Sulfur Scan

Figure 3-63. Electron Microprobe of Dolomite 1337 From Run 115, Edge Section (X225)

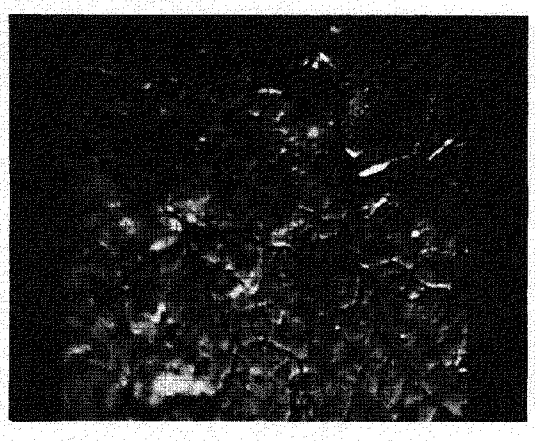

Photomicrograph of Scanned Area

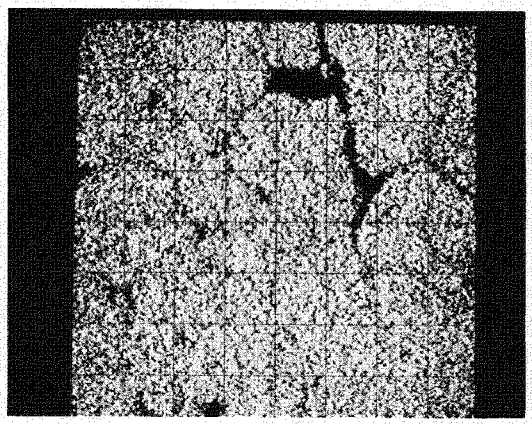

Calcium Scan

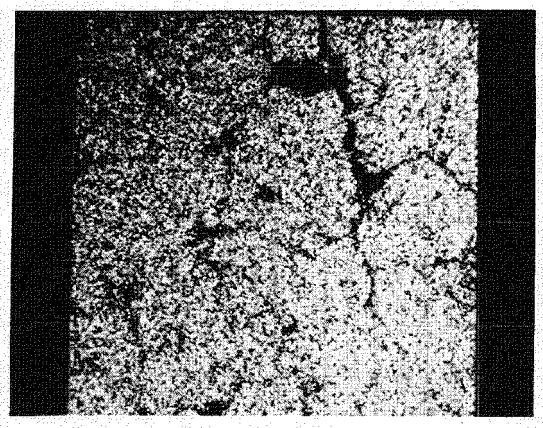

Magnesium Scan

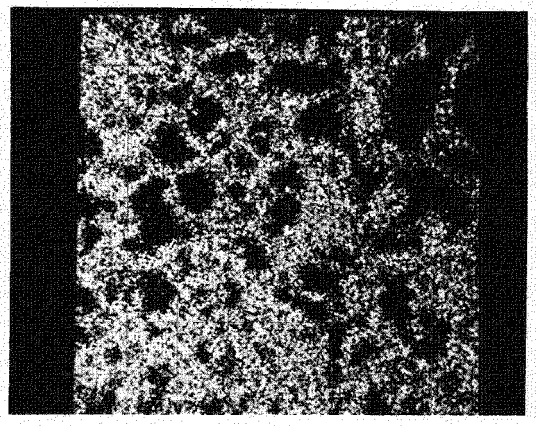

Sulfur Scan

Figure 3-64. Electron Microprobe Scans of Dolomite 1337 From Run 115, Center Section (X225)

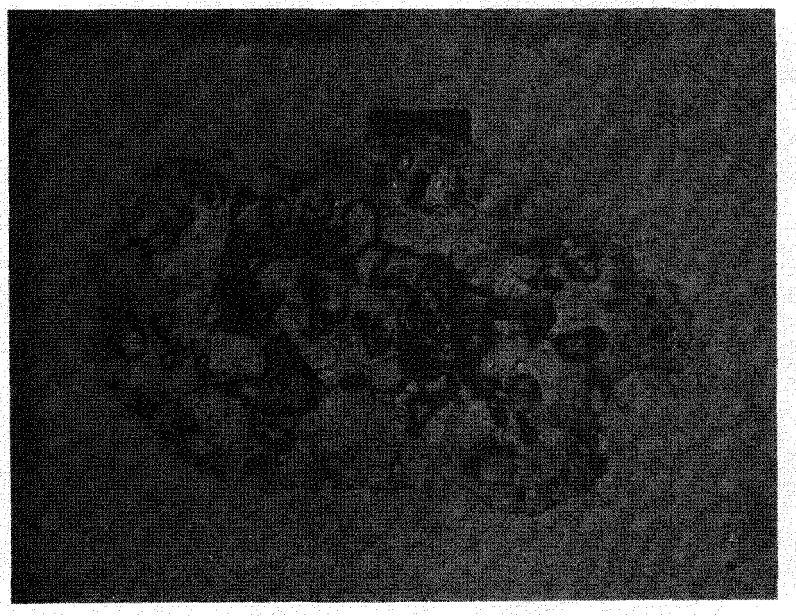

Figure 3-65. Sulfated Particle of Dolomite 1337 From Run 117 (X50)

Edge
Section

Center
Section

Figure 3-66. Sections of Particle From Run 117 Used For Electron Microprobe Scans (X200)

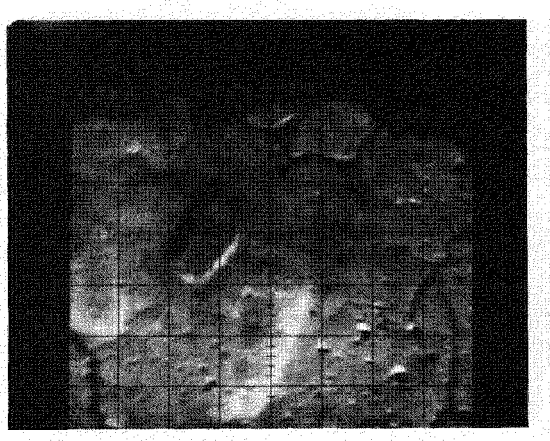

Photomicrograph of Scanned Area

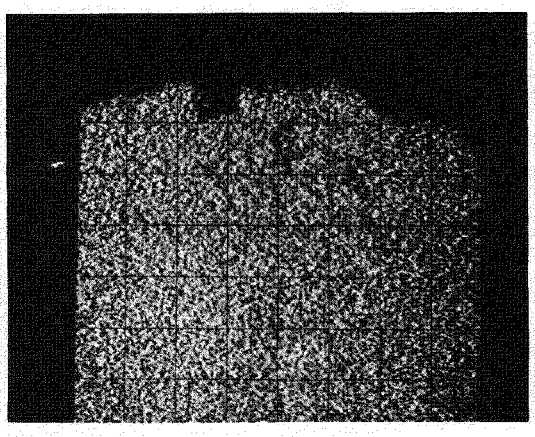

Calcium Scan

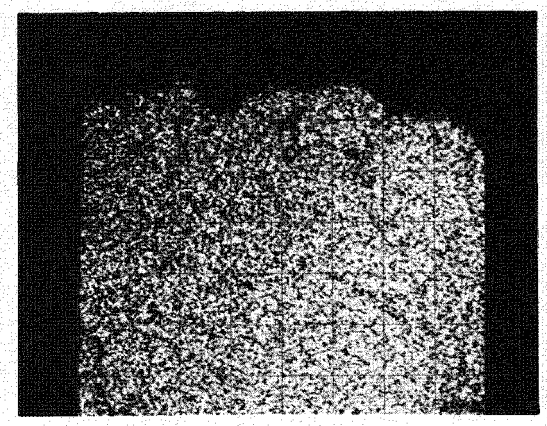

Magnesium Scan

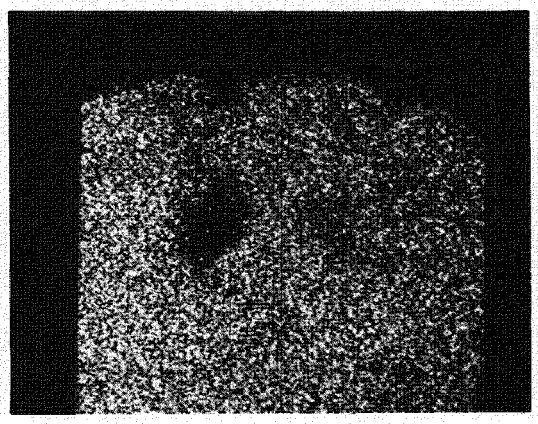

Sulfur Scan

Figure 3-67. Electron Microprobe Scans of Dolomite 1337 From Run 117, Edge Section (X225)

Photomicrograph of Scanned Area

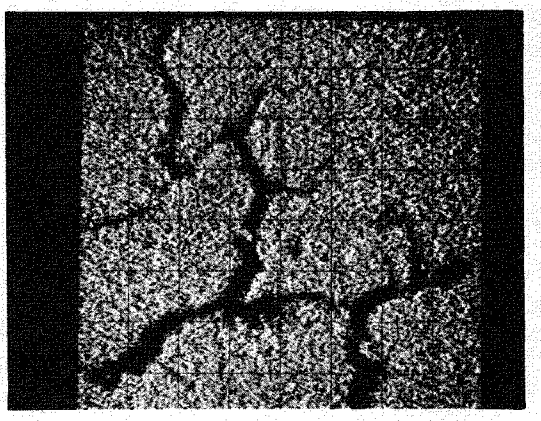

Calcium Scan

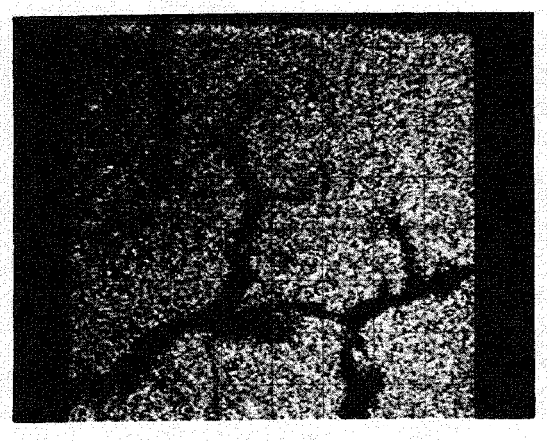

Magnesium Scan

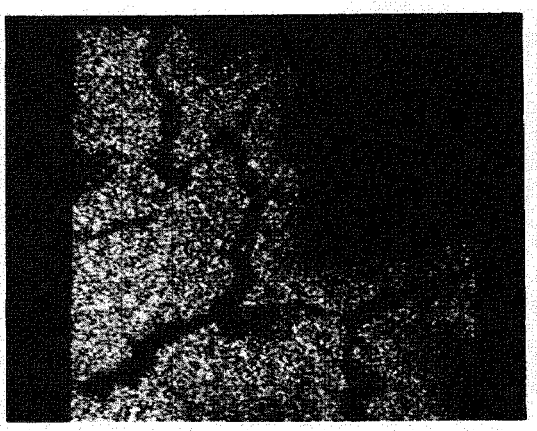

Sulfur Scan

Figure 3-68. Electron Microprobe Scans of Dolomite 1337 From Run 117, Center Section (X225)

Section 4

APPLICATION OF CONTROLLED CALCINATION TO A FLUID BED COMBUSTOR

4.1 GENERAL CONSIDERATIONS

The basic result of the experimental work reported is that control of calcination conditions leads to superior utilization of limestone in desulfurization. The impact of improved sorbent utilization on the over-all afbc system is advantageous in that it reduces sorbent consumption and the production of waste material, or spent sorbent. The negative impact of improved utilization lies in additional costs incurred in adding a controlled calcination step to the system, and in any added complexity of process control encountered as a result of this additional process step.

The decrease in sorbent consumption and spent sorbent production is illustrated in Figure 4.1 for the Lowellville limestone. If mean sorbent utilization is doubled from 20 to 40%, then sorbent consumption is halved - a direct saving of 380,000 tons per annum or $\$3.1 \times 10^6$ at \$8 per ton, for a 600 MW plant using a 4% S coal. Capital costs associated with limestone storage and handling facilities would also be somewhat reduced. The sorbent waste disposal costs are unknown at this stage. However higher sorbent utilization in sulfation means that there is less calcium oxide to be ultimately exposed to a weathering process, in the spent sorbent.

The disadvantages of a controlled calcination treatment lie in the equipment required and additional operating restrictions imposed. The process can be considered on three levels - purchase of precalcined material; calcination in a separate unit adjacent to the fluid bed combustor, and calcination in a special compartment in or configuration of, the afbc unit.

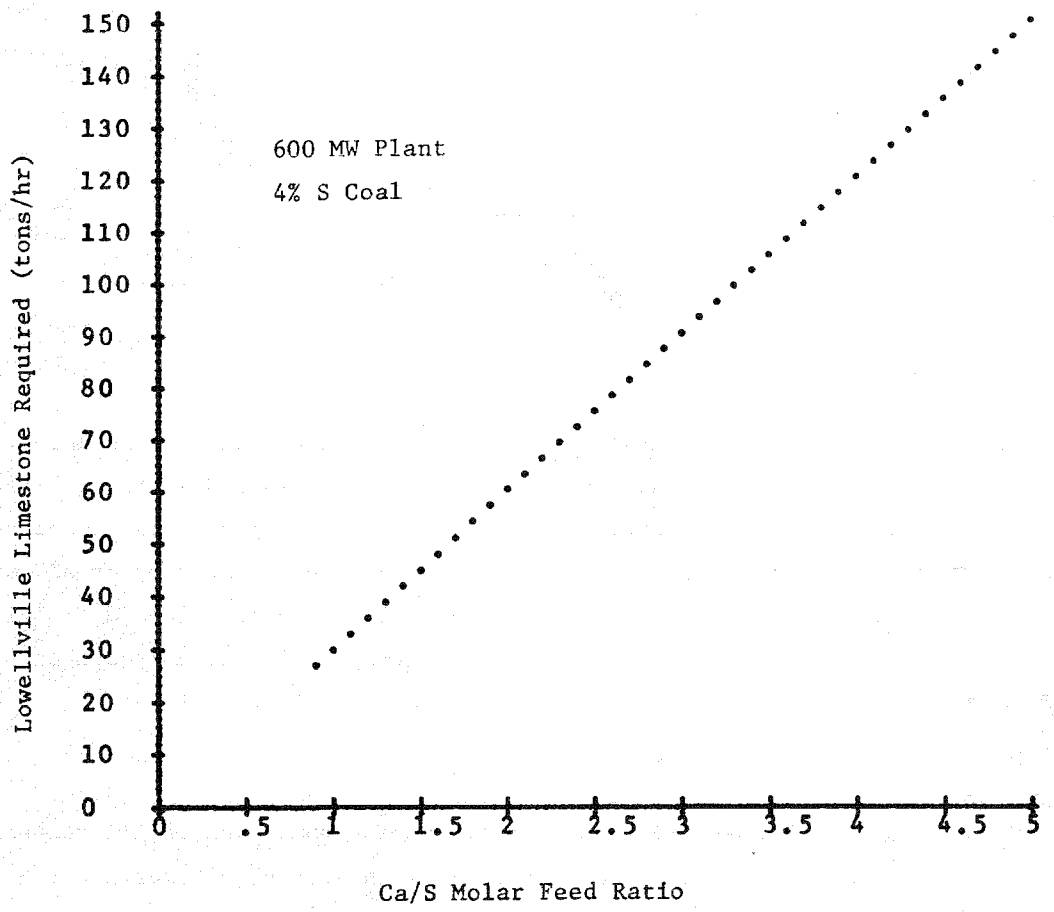

Figure 4.1. Consumption of Limestone Sorbent

4.2 PURCHASE OF PRECALCINED MATERIAL

A rotary kiln uses 1 lb of coal to produce 3.37 lbs of lime, i.e., to calcine 6.02 lbs of limestone. This is equivalent to consumption of 3.7% of the coal feed to the boiler. The lime must then be reheated on introduction to the boiler module, requiring an additional 1% of the coal. The difference between "in situ" calcination and purchase of precalcined material involves an energy penalty of about 3% of the coal feed, plus the added economic penalty of handling at the lime plant. Since lime costs are in the region of $30 per ton, or roughly four times the cost of limestone per unit of calcium this option is generally unattractive. The impact of delayed calcination by CO_2 on the rotary calciner has not been assessed, but both plant modifications and cost increases would be involved.

4.3 PRECALCINATION AT THE POWER PLANT

It is desirable to carry out the precalcination at the plant site if it proves feasible to feed the hot lime to the boiler, recover the heat from the calciner effluent gases, and recycle the carbon dioxide generated in the precalciner to control the calcination.

Two alternative methods of preparing precalcined material at the power plant site are:

(1) To build a fluid bed calciner (or alternative design if it provides improved integration) capable of feeding the entire plant.

(2) To have a separate calcination zone as part of each boiler module.

In either case, the essential feature of the process is to build up the carbon dioxide partial pressure in the calciner, so that the sorbent is calcined in ∿0.6 atm of CO_2 at about 900°C. The CO_2 required can come from three sources:

(a) The coal required to heat the limestone to reaction temperature and drive the endothermic calcination reaction (2-1/4% of the coal feed to the power plant)

(b) From the limestone itself as it calcines

(c) From the calciner effluent, or the plant stack gas, or a recycled CO_2 recovery unit.

The calciner size is governed by the residence time required for the slow calcination reaction (1-2 hours). For a 30 MW modular unit of a fluid bed combustor operating under the conditions outlined in Table 4-1, precalciner bed dimensions of 110 cubic feet are required. Since the coal firing rate is 230 kg/hr (510 lb/hr), the air supply for complete coal combustion is 7.62×10^6 litres/hr, or 2.1×10^3 litres/second. At a minimum fluidizing velocity of 90 cm/sec, the cross-section area of the bed inlet would be 2.3×10^4 cm^2, or a 5' x 5' square bed. The bed height would be 135 cm or 4.4 ft, and the maximum effluent CO_2 concentration would be 46%. This concentration is limited by the thermal requirements of the reactor. If air preheat and solids preheat are used, then less coal and air are required, and the CO_2 target of >60% CO_2 can be attained.

Table 4-1a

30 MWe FLUID BED BOILER MODULE - PRECALCINER OUTLINE

COAL:	12,000 Btu/lb 4% S
LIMESTONE:	Pure $CaCO_3$
SULFUR REMOVAL:	90% SO_2 trapped at Ca/S = 1.8
COAL FEED TO BOILER:	22,460 lb/hr
LIMESTONE FEED REQUIRED:	5,000 lb/hr
SORBENT RESIDENCE TIME IN PRECALCINER:	2 hrs
PRECALCINER EFFLUENT:	∿46% CO_2
PRECALCINER BED HEIGHT:	∿4 ft
PRECALCINER COAL FEED:	511 lb coal
PRECALCINER VOLUME:	111 cu. ft
PRECALCINER SUPERFICIAL INLET AIR VELOCITY:	3 ft/sec
PRECALCINER TEMPERATURE:	850-900°C

Table 4-1b

600 MWe PRECALCINER FOR FLUID BED COMBUSTION

LIMESTONE FEED:	60,000 lb/hr
COAL FEED:	10,220 lb/hr
PRECALCINER VOLUME:	2,220 cu. ft
CIRCULAR VESSEL:	20 ft diameter
BED HEIGHT:	10 ft
SUPERFICIAL INLET AIR VELOCITY	4.8 ft/sec

If recycle of the calciner effluent from one module is used to fluidize the next module by blending it with air, the ratio of air to effluent can apparently be used to control the rate of calcination. Increasing the CO_2 concentration through the bed will lower the rate of calcination. However a detailed heat and mass balance of the system is required to determine which factors control the calcination operation, since the decrease in calcination rate will be offset by a rise in temperature of the bed. The rate of heat supply (from coal combustion) may be the controlling factor.

An alternative method of providing the partial pressure of carbon dioxide required is to pressurize the stack gas, and calcine the sorbent in a pressurized unit. This would allow a wide range of CO_2 partial pressures in the fluidizing gas (by blending with air) to permit control of the calcination rate.

It should be noted that calcination rates measured under high partial pressures of CO_2 were slower than predicted here. If calcination is slower in such a precalciner, then the temperature will rise until the rate has sufficiently accelerated to absorb the heat input to the system. The question which must be answered is whether the temperature would rise to a point where sintering and deactivation of the sorbent occurs.

The over-all impact of controlled calcination should be to reduce energy losses associated with the use of limestone as a desulfurizing agent. Assuming that heat recovery from both solid and gaseous effluent streams is 90% efficient, then reduction of the Ca/S mole ratio from 3.6/1 to 1.8/1 saves the heat of calcination of limestone equivalent to 0.9% of the total coal feed in the system. In either case, the heat gained by the sulfation reaction is the same.

4.4 CONCLUSIONS

In considering conceptual options for applying the precalcination technique to an atmospheric pressure fluidized bed combustor no fundamental barriers to implementation of the process improvement have been identified. The process is technically feasible and apparently marginally superior in energy efficiency to a conventional once-through sorbent system.

The potential of the controlled calcination system should now be assessed in depth by comparing technical and economic performance projections for it and other sorbent utilization enhancement processes, including regenerative systems. Such a study would require detailed conceptual designs of commercial-scale systems using these processes. For the controlled calcination system, some further basic research should greatly reduce the margin of uncertainty in the over-all assessment. Four specific areas where fundamental design data could contribute greatly to the assessment are

- Determination of essential sorbent residence times in the precalciner (necessary for vessel sizing)
- Determination of the effect of controlled calcination on the attrition suffered by the sorbent both in the calciner, and under sulfating conditions
- Determination of the effect of sorbent residence time at temperatures on the activation or deactivation of the sorbent
- Determination of the improved sorbent utilization impact on regenerability of the sorbent.

REFERENCES

1. Keairns, D. L., et al., "Fluidized Bed Combustion Process Evaluation-Phase II-Pressurized Fluidized Bed Coal Combustion Development", Westinghouse Research Laboratories, EPA 650/2-75-027c, September 1975.

2. Mesko, J. E., S. Ehrlich and R. A. Gamble (PER, Inc.), "Multicell Fluidized Bed Boiler Design Construction and Test Program", August 1974 (OCR), PB 236 254.

3. Corman, J. C. and J. H. Eskesen, "Energy Conversion Alternatives Study (ECAS)", General Electric Phase 1 Final Report, Volume III, Part 2, NASA CR 134948.

4. Archer, D. H., D. L. Keairns, J. R. Hamm, R. A. Newby and W. C. Yang, "Evaluation of the Fluidized Bed Combustion Process", U. S. National Technical Information Service Report No. APTD-1165, 1972.

5. Strom, S., Personal Communication.

6. Borgwardt, R. H. and R. D. Harvey, Env. Sci. Tech., 6, 350, 1972.

7. Hatfield, J. D., Y. K. Kim, R. C. Mullins, and G. H. McClellan, "Investigation of the Reactivities of Limestone to Remove Sulfur Dioxide from Flue Gas", Air Pollution Control Office, Tennessee Valley Authority, 1971.

8. Avco Corporation, "A Survey of Metal Oxides as Sorbents for Oxides of Sulfur", 1969, PB 185190.

9. Benito, D. and A. W. Searcy, JCS Faraday Trans. I, 2145, 1974.

10. Zawadski, J. and Bretsnajder, S., Trans. Faraday Soc., 34, 951 (1938).

11. Cremer, E. and W. Nitsch, Z. Elektrochem, 66, 697-708 (1962).

12. Ruth, L. A., "Reaction of Hydrogen Sulfide with Half-Calcined Dolomite", Ph.D. Thesis, Dept. of Chemical Engineering, City College, City University of New York, 1972.

13. Coats, A. W. and J. P. Redfern, Nature 201, 68, 1964.

14. Ingraham, T. R. and P. Marier, Can. J. Chem. Engr. 41, 170, 1963.

15. Hills, A. W. D., Trans. Inst. Min. Metal, C, 76, 241, 1967.

16. Borgwardt, R. H., "Kinetics of the Reaction of SO_2 with Calcined Limestone", Environmental Science and Technology, Vol. 4, No. 1, January 1970, pp. 59-63.

17. Keairns, et al., "Evaluation of the Fluidized Bed Combustion Process", Vol. 1, Westinghouse Research Laboratories to EPA, December 1973, PB 211494.

18. Coutant, R. W., et al., "Investigation of the Reactivity of Limestone and Dolomite for Capturing SO_2 from Flue Gas", Battelle Memorial Institute, November 1970, PB 196749.

19. Barker, R., J. Appl. Chem. Biotechnol. 23, 733, 1973.

APPENDIX 1

CALCINATION

A1.1 THE RATE OF CALCINATION OF LIMESTONE

The rate of limestone calcination is a function of the temperature, particle size and gas atmosphere under which the reaction is conducted.

Assuming that the partial pressure of carbon dioxide evolved in the reaction does not suppress further reaction, the rate appears to be constant as a function of temperature. Reaction occurs at the interface between CaO and $CaCO_3$. If the area of this interface is reduced during reaction (as is the case with a spherical particle of $CaCO_3$), the decrease in rate is directly proportional to the reduction in surface area. In theory, the rate of reaction, if suitably adjusted for the geometric reduction in reaction interface, can be measured by gas evolution or weight loss measurements, and should be constant. By repeating measurements at different temperatures the activation energy and pre-exponential factor may be derived.

In practice, several other factors usually intervene to create a situation which has resulted in a chaotic assemblage of literature values to describe the kinetics of this reaction.

First of all, the reaction is strongly endothermic ($\Delta H \cong + 163$ kJ $mole^{-1}$), and if the sample is to react it may self-cool to temperatures which are much lower than the ambient temperature of the experiment, e.g., 100°C for 1 cm spheres. Reaction proceeds at a rate corresponding to the lower temperature which is governed by heat transfer from the surroundings balancing the enthalpy requirements of the reaction rate at the lower temperature.

Secondly the reaction is readily reversible. If the evolved carbon dioxide is not removed from the vicinity of the reaction interface, it lowers the observed rate of reaction. Removal of the evolved carbon dioxide requires rapid external

mass transfer from the particle surface, and rapid diffusion through the product layer of calcium oxide. At some particle size, this layer will eventually become so thick that diffusion of carbon dioxide away from the reaction interface is the rate controlling step.

Since our concern is with the time required to calcine limestone particles in a fluidized bed, and the extent to which calcination is hindered by the presence of carbon dioxide, we require

(1) estimates of the fastest possible rate of calcination as a function of temperature, and particle size

(2) estimates of the extent to which the local carbon dioxide partial pressure retards the calcination reaction.

Because of the high heat transfer rates in a fluidized bed coal combustor, and the relatively small particle sizes of limestone used, the reaction interface will be at a temperature very close to that measured in the fluidized bed. (The heat required for total calcination at a 3/1 Ca/S molar feed ratio for 4% sulfur in coal is about 2% of the heat released by coal combustion).

In order to calculate the rate of limestone calcination, the following assumptions have been made.

(1) The rate of calcination of a "spherical" limestone particle is well described by the equation

$$\frac{d\alpha}{dt} = k(1 - \alpha)^{2/3}$$

(2) k is inversely proportional to the surface area of the reacting sphere

(3) k varies with temperature according to the Arrhenius relation

$$k = Ae^{-\left\{E_a/RT\right\}}$$

(4) The effect of a particl pressure of carbon dioxide at the reaction interface lowers the rate of reaction by the factor

$$1 - P_{CO_2}/P_{eq}$$

where P_{eq} is the equilibrium partial pressure of carbon dioxide over calcium carbonate.

This factor may be derived from models of the reaction where either chemical reaction or mass transfer at the surface, or internal diffusion of CO_2 is controlling the rate. For mass transfer and diffusion, the driving forces are expressed by a ΔP term where

$$\Delta P = [P_{CO_2} \text{ (reaction interface)} - P_{CO_2} \text{ (gas outside particle)}]$$

If P_{CO_2} (reaction interface) = P_{CO_2} (equilibrium), then if the pressure of CO_2 in the gas outside the particle changes from zero to P_{CO_2},

$$\Delta P_1/\Delta P_2 = \frac{P_{CO_2} \text{ (equilibrium)}}{P_{CO_2} \text{ (equilibrium)} - P_{CO_2} \text{ (gas)}}$$

and

$$\Delta P_2 = \Delta P_1 \left\{ 1 - \frac{P_{CO_2} \text{ (gas)}}{P_{CO_2} \text{ (equilibrium)}} \right\}$$

If chemical reaction is rate controlling, and the rate of recarbonation is directly proportional to the pressure of CO_2

$$\text{rate} = k_f - k_{rev} P_{CO_2} \text{ (gas)}$$

where rate at P_{CO_2} (gas) = 0, is k_f

at equilibrium, $k_{rev} P_{CO_2} = k_f$

$$\therefore \text{rate} = k P_{eq} - k P_{CO_2} \text{ (gas)}$$

$$\therefore \frac{\text{rate in } P_{CO_2} \text{ (gas)}}{\text{rate in } N_2} = \frac{k_r P_{eq} - k_r P_{CO_2} \text{ (gas)}}{k_r P_{eq}}$$

$$= 1 - \left\{ \frac{P_{CO_2}}{P_{eq}} \right\}$$

(5) For the particle sizes with which we are concerned, (1,000 - 2,000 micron diameter), heat transfer to the limestone particles and across the shell of product lime is sufficiently rapid to prevent significant temperature differences (>10°C) developing between the reaction interface, and the bulk of the fluidized bed.

The values of k at a given temperature, and A and E_a over a range of temperatures are determined from isothermal weight loss measurements, or weight loss measurements taken while the sample is heated at a constant rate.

In the latter case, the data are plotted after the method of Coats and Redfern in the form $F(\alpha)$ vs $1/T$, where

$$F(\alpha) = - \ln \frac{1 - (1-\alpha)^{1-n}}{(1-n)\ T^2}$$

This form may be derived using the rate equation for calcination

$$\frac{d\alpha}{dt} = k\ (1-\alpha)^n$$

where

$$k = A\ e^{-E_a/RT}$$

so

$$d\alpha = A\ e^{-E_a/RT}\ (1-\alpha)^n\ dt$$

If the constant rate of heating is taken as

$$B = dT/dt$$

$$d\alpha = \frac{A}{B}\ e^{-E_a/RT}\ (1-\alpha)^n\ dT$$

Integration gives

$$\int_0^{\alpha} \frac{d\alpha}{(1-\alpha)^n} = \frac{A}{B} \int_0^{T} e^{-E_a/RT}\, dT$$

The right side is solved by making the substitution $\mu = E_a/RT$ (13)

$$\frac{1 - (1-\alpha)^{1-n}}{1-n} = \frac{AR\,T^2}{BE_a}\left(1 - \frac{2RT}{E_a}\right) e^{-E_a/RT}$$

Taking logs for $n \neq 1$ gives

$$\ln\left[\frac{1 - (1-\alpha)^{1-n}}{T^2\,(1-n)}\right] = \ln\left[\frac{AR}{BE_a}\left(1 - \frac{2RT}{E_a}\right)\right] - \frac{E_a}{RT}$$

The slope of this line yields the activation energy (slope = $-E_a/R$), and the intercept may be used to deduce an average value of A.

$$\text{intercept} = \ell n \frac{AR}{BE_a}\left\{1 - \frac{2RT}{E_a}\right\}$$

Justification for Using Non-Isothermal Parameters

The non-isothermal A and E_a parameters provide a simple means of estimating the rate of reaction at any given temperature. The utility of the method must be balanced against the general suspicion of the method based on the wide variety of results it has produced from data taken under different physical conditions.

In Table A-1, the isothermal rate constants obtained by direct TG measurement are compared with the predictions based on non-isothermal parameters. The agreement is excellent at lower temperatures, but divergence is evident at higher temperatures.

Table Al

T°C	Isothermal Data (sec^{-1})	Predicted by Non-isothermal Data (sec^{-1})
550	1.11×10^{-5}	1.06×10^{-5}
646	1.49×10^{-4}	1.38×10^{-4}
750	1.73×10^{-3}	1.29×10^{-3}
875	1.73×10^{-2}	1.11×10^{-2}

The initial rate of calcination of limestone 1359 (495 micron diameter particles)

The recent isothermal data of Searcy, applied to the case of a 490 micron sphere, is compared in Figure A-1 with the non-isothermal data line. The TG data predicts a lower rate than Searcy's data at higher temperatures: however, Searcy's data extends only up to 740°C.

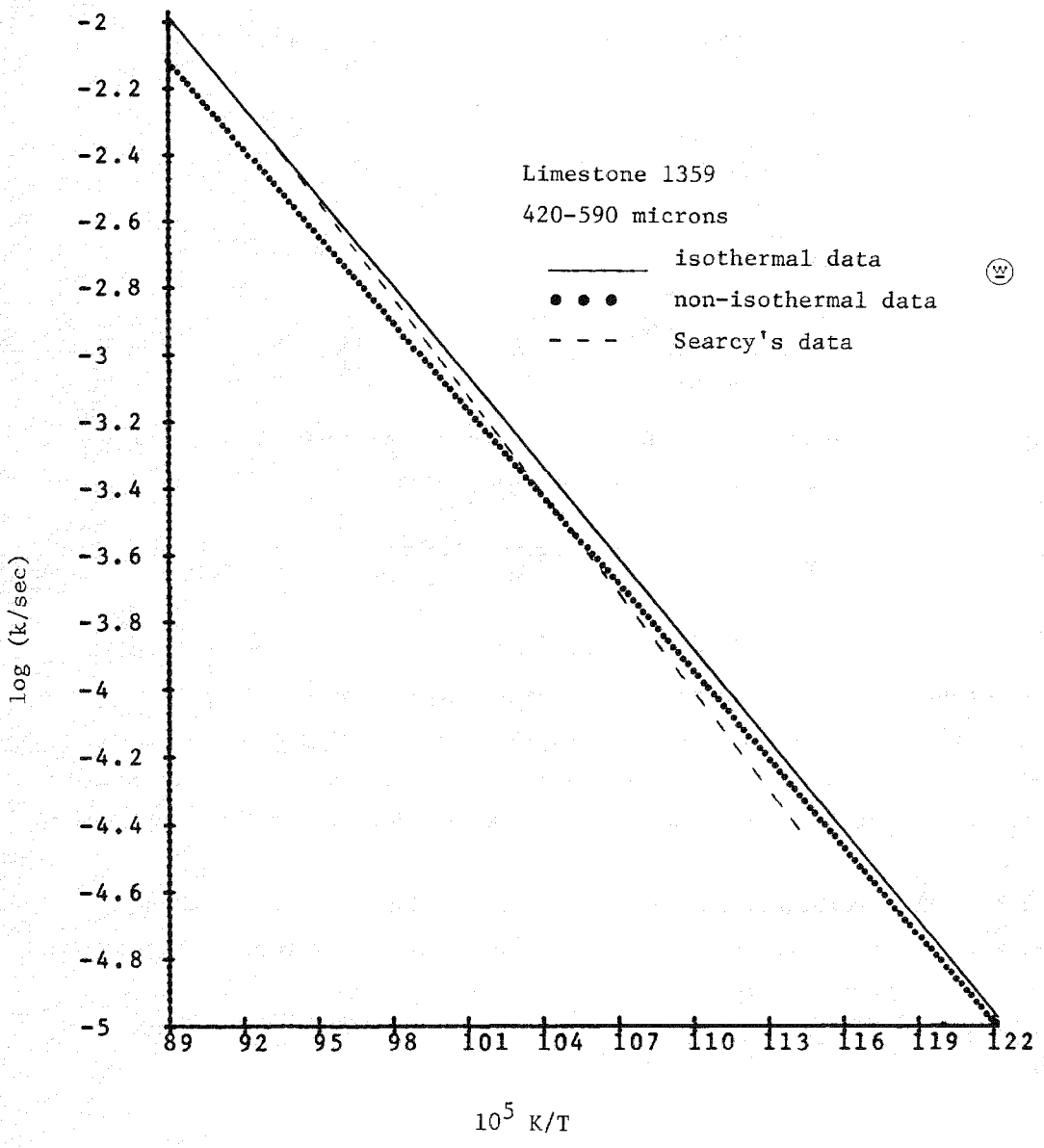

Figure A-1. The Initial Rate of Limestone Calcination, $k(sec^{-1})$, as a Function of Temperature

A1.2 SORBENT CALCINATION TIME

The fraction of limestone calcined at a given time can be calculated using the Arrhenius equation

$$k = Ae^{\left\{-E_a/RT\right\}}$$

and the equation for the rate of a 2/3 order reaction

$$\frac{d\alpha}{dt} = k\ (1-\alpha)^{2/3}$$

correcting the rate constant for the mean CO_2 pressure. So

$$\frac{d\alpha}{dt} = k\ (1-\alpha)^{2/3} \left\{1 - \frac{P_{CO_2}}{P_{eq}}\right\}$$

or

$$\frac{d\alpha}{dt} = Ae^{-E_a/RT}\ (1-\alpha)^{2/3} \left\{1 - \frac{P_{CO_2}}{P_{eq}}\right\}$$

Rearranging and integrating, we find

$$\alpha = 1 - \left\{1 - \frac{Qt}{3}^{3}\right\}$$

where

$$Q = Ae^{-E_a/RT} \left\{1 - \frac{P_{CO_2}}{P_{eq}}\right\}$$

E_a and A can be found as described by Coats and Redfern,[13] using TGA data and plotting a function of the fraction reacted versus 1/T °K. The equilibrium pressure of CO_2 is found to be dependent only on temperature, and may be found using the equation

$$P_{eq} = e^{\left\{-\frac{1.90164 \times 10^4}{T} + 16.2971\right\}}$$

If we assume A is proportional to 1/r, we may find the fraction reacted for different particle sizes as well as for different temperatures of calcination and pressures of CO_2.

With complete mixing of solids in a fluidized bed the residence time distribution of solids in the bed is given by

$$E(t) = \frac{1}{\bar{t}} e \left\{ - \frac{t}{\bar{t}} \right\}$$

where $\bar{t}$ = the mean residence time of solids in the bed and E(t) dt is the fraction of solids leaving the bed between t and t + dt. Thus, the percent calcination is equal to the sum of the following products: the fraction of particles leaving the bed in a given time interval and the percent calcination at that time, i.e.

$$\% \text{ calcination total} = \sum_{t=0}^{t=T} \int_{t}^{t+dt} E(t)\, dt \ (\% \text{ calcined at } T=t+dt)$$

where T = time at which all particles have left bed or when

$$\int_{o}^{t} E(t)\, dt = 1 \ (0.99)$$

So % calcination of spent sorbent =

$$\sum_{t=0}^{t=T} \left\{ e^{\left\{ - \frac{t}{\bar{t}} \right\}} - e^{\left\{ - \frac{(t+dt)}{\bar{t}} \right\}} \right\} \left\{ 1 - \left\{ 1 - Q(t+dt)/3 \right\}^{3} \right\}$$

Using dt = 0.1 hours the following values were obtained.

Retention time (hr)	Radius (μm)	Temperature °C	% Calcination of Spent Sorbent
25	3175	775	91.14
25	1587.5	775	95.04
25	3175	765	87.37
25	1587.5	765	92.98
25	3175	755	79.68

Retention time (hr)	Radius (μm)	Temperature °C	% Calcination of Spent Sorbent
25	1587.5	755	88.62
25	793.75	755	93.67
25	3175	745	56.82
25	1587.5	745	73.16
25	793.75	745	84.57
25	396.87	745	91.42
16.7	3175	775	87.61
16.7	3175	765	82.40
16.7	1587.5	765	90.21
16.7	3175	755	72.28
16.7	1587.5	755	84.05
16.7	793.75	755	91.16
16.7	3175	745	46.04
16.7	1587.5	745	64.22
16.7	793.75	745	78.64
16.7	396.87	745	88.00
16.7	198.44	745	93.37

Appendix 2

THE EFFECT OF CALCINATION CONDITIONS ON ACTIVITY OF CaO

A literature review on CaO products formed from calcination of $CaCO_3$ is summarized in Table A2.1. Conditions of calcination investigated include temperature, retention time, heating rate, and impurities in the stone.

Although porosity, specific surface area, and reactivity are closely related, care must be taken in comparing results when different methods are used as gauges of activity. As Murray speculated;[1] "two stones can have the same percent porosity, but if one has pore diameters of 1000 Å and the other 40 Å, then the internal surface area of the stone with the larger pores will be only 4% of the internal surface area of the stone with the smaller pores."

The literature supports the following general conclusions:

(1) Higher temperatures of calcination produce more dense, less reactive CaO.

(2) Higher heating rates before and during calcination produce stones of lower porosity and less reactivity.

(3) Long retention times, (heating after complete decomposition of $CaCO_3$), always cause sintering, in air or vacuum.

(4) Impurities increase the sintering of the stone, because of their low Tammann temperatures which permit diffusion into line cracks and fissures.

(5) Sodium, unlike other impurities, may increase lime reactivity by decreasing shrinkage particularly in stones prone to high shrinkage.

(6) There is disagreement as to the relative importance of temperature and heating rate on lime reactivity. Temperature is probably the more important factor until heating rates get extremely high.

(7) Calcination atmosphere has been shown to affect the structure of CaO.[6] Decomposition in vacuo rather than in N_2 or air produces a calcine with high internal surface area.

Table A2

REVIEW OF LITERATURE ON CALCINATION OF $CaCO_3$

Source of Information	Conditions of Calcination	Effect on Product CaO	Experimental Method Used
Murray,[2] Fischer	Temperatures of calcination	Higher temperatures cause lower porosity and reactivity. The effect is more pronounced when retention times are short.	Material-pure calcite (840-2000 μm) $\text{Porosity} = 100\left[\frac{D_{He} - D_{Hg}}{D_{He}}\right]$ D_{He} = density by He displacement D_{Hg} = density by Hg displacement
(2)	Retention time	An optimum time can be found for each temperature. If the retention time is too long, the porosity decreases, but if it is too short, the porosity even more greatly decreases.	
(2)	Rate of heating before and during calcination	Too fast - low porosity. It is hypothesized that this effect is greater than either temperature or retention time effects.	
Murray[3]	NaCl or Na_2CO_3	Lowers shrinkage of limes that are prone to high shrinkage.	Limes soaked in 10% solns for 16 hours before calcination. $\text{Shrinkage} = \frac{100\left[\frac{100}{D_s} - \frac{100-L}{D_L}\right]}{100/D_s}$ D_s = density of stone D_L = density of quicklime L = loss on ignition of stone
Glasson[4]	Impurities (1) NaCl	(a) Small amounts (0.01%) do not effect CaO at 1472°F, but slightly increase lime activity at 1652°F. (b) Larger amounts increasingly accelerate sintering at 1472, 1652, and 1832°F.	Samples of B.D.H. "Analar" $CaCO_3$ were mixed with known amounts of impurities.
	(2) $CaSO_4$	(a) At 1472°F: lime activity reduced when up to 10% added; when 20% is added, activity of CaO slightly increased (not as active as 0%); from 50-100% activity is again reduced. (b) Above 1472 lime surface diffusion becomes important and lime sintering is promoted.	The activity or sintering reported is based on specific surface measurements determined by BET procedure from nitrogen isotherms recorded at -183°C on an electrical sorption balance or vacuum micro-balance and by average crystallite sizes determined from x-ray powder photographs.

Table A2 (Cont)

Source of Information	Conditions of Calcination	Effect on Product CaO	Experimental Method Used
	(3) PO_4^{-3}	(a) Little effect at 1472, 1652, or 1832°F. (b) At 1652°F some activation of CaO occurs at 20% PO_4^{-3}	
	(4) Fe_2O_3	Additions progressively increase lime sintering.	
	(5) Alumina	(a) Little effect below 1832°F. (b) At 2012°F, small amounts (<5%) increase sintering of CaO.	
	(6) Silica	(a) Little effect below 1832°F. (b) At 2012°F, 10% enhance sintering.	
Fischer[5]	Temperature of calcination	(a) If temperature is <1750°F the density is small and unaffected by other factors. (b) (1750-2200°F) as the temperature increases more dense CaO is formed. (c) (>2200°F) a decrease in density results as temperature increases.	Material - highly pure calcite (840-2000 μm) density. 2.7 g/cc porosity 0.7%. Bulk density of CaO used as reactivity criterion.
Fischer[5]	Heating rate during calcination	(a) Higher heating rates increases CaO density. (b) A larger % change in heating rate than % change in temperature is required to increase CaO density. (c) A given change in heating rate is more effective to change CaO density at higher heating rates than at lower rates.	
Fischer[5]	Heating rate after calcination	Usually uneffective in changing CaO density but densification may occur with increased heating rate in impure samples.	
Fischer[5]	Retention time	The density of CaO increases with increased retention times.	
Beruto/ Searcy[6]	Calcination atmosphere	The reactivity of CaO formed by decomposition in vacuo is higher than CaO formed in air or nitrogen.	Reactivity with water as determined by: 1) Grinding in air for 10 minutes. 2) 3 minute exposure to water vapor steam at 140°C.

A2.1 REFERENCES

1. Boynton, Robert S., Chemistry and Technology of Lime and Limestone, Interscience Publishers (New York, 1966), p.146.
2. Murray, J. A., H. C. Fischer, and D. W. Sabean, Proc. ASTM, (1950), p. 1263.
3. Murray, J. A., H. C. Fischer, and L. S. Dolnick, J. Am. Ceram., Soc., 37, 7 (1954), pp. 323-328.
4. Glasson, D. R., J. Appl. Chem. (London, 1967), 17, pp. 91-96.
5. Fischer, H. C., J. Am. Ceram. Soc., 38, 7 (1955), pp. 245-251.
6. Beruto, D. and A. W. Searcy, Nature, Vol. 263 (1976) pp. 221-222.

Appendix 3

SULFATION DATA

Table A3-1

SULFATION AT 815°C IN 4% O_2, 0.5% SO_2 AND N_2

Calcines Prepared on the TGA

Run No.	Stone	Size (U. S. Mesh)	Calcination Temperature (°C)	$\%CO_2$	Flow Rate (ml/min.)	% Sulf. (*)
74	1359	16/18	Nonisothermal up to 815	0	200	10.2
75	Greer	16/18	Nonisothermal up to 815	0	200	16
76	1359	35/40	Nonisothermal up to 815	0	200	13
78	Greer	35/40	Nonisothermal up to 815	0	200	27
84	1359	16/18	Nonisothermal up to 815	0	200	11.3
85	1359	16/18	Nonisothermal up to 815	15	100	12
86	Greer	16/18	Nonisothermal up to 815	15	100	28
87	Greer	16/18	Isothermal at 900	60	200	55
89	1359	16/18	Nonisothermal up to 815	0	200	11.4
91	Greer	16/18	Isothermal at 815	15	100	18
93	Greer	16/18	Isothermal at 900	15	200	62
110	Greer	16/18	Isothermal at 900	60	200	55
114	Lowellville	16/18	Nonisothermal up to 815	0	200	17
115	1337	16/18	Nonisothermal up to 815	0	200	51
116	Lowellville	16/18	Isothermal at 900	60	200	40
117	1337	16/18	Isothermal at 900	60	200	85
119	Greer	16/18	1) Nonisothermal up to 815 2) Held at 900 for 130 min.	0	200	40
141	Lowellville	16/18	Nonisothermal up to 815	15	200	24.8
142	1337	16/18	Nonisothermal up to 815	15	200	80
143	1359	16/18	Isothermal at 815	15'	200	10.7
144	Lowellville	16/18	Isothermal at 815	15	200	23
145	Lowellville	16/18	Nonisothermal up to 900	60	200	33
147	Lowellville	16/18	Nonisothermal up to 935	100	200	47
148	Lowellville	16/18	Nonisothermal up to 750	5	200	28
149	Lowellville	16/18	Nonisothermal up to 900	15	200	17.8
150	Lowellville	16/18	Nonisothermal up to 900	38	200	26
161	Lowellville	16/18	Nonisothermal up to 900	0	200	15.5
162	Lowellville	16/18	Nonisothermal up to 900	80	200	42
163	1359	16/18	Isothermal at 815	0	200	9
165	1359	16/18	1) Held at 815 for 1 hour 2) Isothermal at 815	0	200	7.7
166	1359	16/18	Isothermal at 815	0	200	10
168	1359	16/18	1) Held at 815 for 1 hour 2) Isothermal at 815	0	200	8
177	Lowellville	16/18	Nonisothermal up to 750	5	200	16.2
178	1359	16/18	Isothermal at 815	15'	200	9.2
180	1359	16/18	Nonisothermal up to 900	80	200	47
181	1359	16/18	Nonisothermal up to 900	60	200	37.3
182	1359	16/18	Nonisothermal up to 900	15	200	5.6
184	Lowellville	16/18	1) Held at 815 for 2 hours 2) Isothermal at 815	15	200	20.2
185	1359	16/18	Nonisothermal up to 900	0	200	9.1
186	Lowellville	16/18	Isothermal at 815	15'	200	42
187	Lowellville	16/18	Isothermal at 815	15'	200	20.2

*Extent of sulfation obtained when rate falls below 0.1% Ca/min.
'CO_2 concentration was varied from 15-0%.

Table A3-2

SULFATIONS AT 815°C IN 4% O_2, 0.5% SO_2 AND N_2

Calcines Prepared in the Fluid Bed

Run No.	Stone	Size U. S. Mesh	Calcination Temperature (°C)	Calcination Time min.	Calcination % CO_2	Velocity (cm/sec)	% Sulf*
80(E-0-1)	1359	14/18	815	120	15	53	12
81(E-0-2)	1359	14/18	815	120	0	53	6
82(E-0-6)	Greer	14/18	815	124	15	130	42
83(E-0-6)	Greer	14/18	815	124	15	130	38
92(E-0-3)	Greer	14/18	815	120	15	57	44
111(E-0-3)	Greer	14/18	815	120	15	57	42
133(E-0-10)	Greer	14/18	815	240	15	81	56
134(E-0-11)	Lowellville	14/18	900	90	60	81	3
135(E-0-12)	1337	14/18	900	82	60	81	100
136(E-0-10)	Greer	14/18	815	240	15	81	55
138(E-0-8)	1337	14/18	815	240	15	81	>80
139(E-0-7)	Lowellville	14/18	815	240	15	81	30
140(E-0-9)	1359	14/18	815	240	15	81	12
146(E-0-8)	1337	14/18	815	240	15	81	98
151(E-0-14)	Greer	14/18	815	240	0	81	29
152(E-0-15)	1337	14/18	900	82	15	81	86
153(E-0-13)	1359(E-0-2)	14/18	900	60	0	81	10
155(E-0-17)	1359	14/18	900	120	15	81	29
156(E-0-16)	Greer	14/18	900	120	15	81	50
157(E-0-18)	Greer	14/18	900	120	15	81	57
158(E-0-19)	Lowellville (E-0-11)	14/18	900	180	0	81	25
159(E-0-20)	Greer	14/18	900	120	60	81	47
160(E-0-21)	1359	14/18	900	120	60	81	26
169(E-0-18)	Greer	14/18	900	120	15	81	>54

*Extent of sulfation obtained when the rate falls below 0.1% Ca/min.

Table A3-3

HIGH TEMPERATURE SULFATIONS IN .4% O_2, 0.5% SO_2 AND N_2 AT 200 ML/MIN

Run No.	Stone	Sulfation Temperature (°C)	% Sulf*
188	Greer (E-0-18)	855	62
189	Greer (E-0-14)	855	24.7
190	Greer (E-0-14)	895	21.6
191	Greer (E-0-18)	895	>67

*Extent of sulfation obtained when the rate falls below 0.1% Ca/min.

Table A3-4

SULFATIONS IN 4% O_2, 0.5% SO_2, 12% CO_2, AND N_2 AT 815°C

Run No.	Stone	% Sulf*
175	Greer (E-0-10)	56
194	Greer (E-0-3)	50

*Extent of sulfation obtained when the rate falls below 0.1% Ca/min.

Table A3-5

SULFATIONS AT 815°C IN 4% O_2 AND VARIED SO_2 CONCENTRATIONS IN N_2

Calcines Prepared in the TGA

Run No.	Stone	Calcination	% SO_2	% Sulf*
167	1359	Nonisothermal up to 815 in N_2	0.3	6
170	1359	Nonisothermal up to 815 in N_2	0.1	4.2
171	1359	Nonisothermal up to 815 in N_2	0.05	4.3

Calcines Prepared in the Fluid Bed

Run No.	Stone	% SO_2	% Sulf*
172	Greer (E-0-18)	0.1	31.2
173	1359 (E-0-17)	0.1	7.5
174	1359 (E-0-17)	0.05	12.9
192	1359 (E-0-17)	0.5[1]	11.7
193	1359 (E-0-17)	0.5[1]	11.8
179	1359 (E-o-17)	0.5[2]	8.8

1 Sulfation interrupted after 9 min, held at 815 in N_2 for 130 minutes.
2 Sorbent held at 815 in N_2 for 200 minutes before sulfation.

*Sulfation extent obtained when sorbent can no longer maintain 90% desulfurization in a fluid bed.

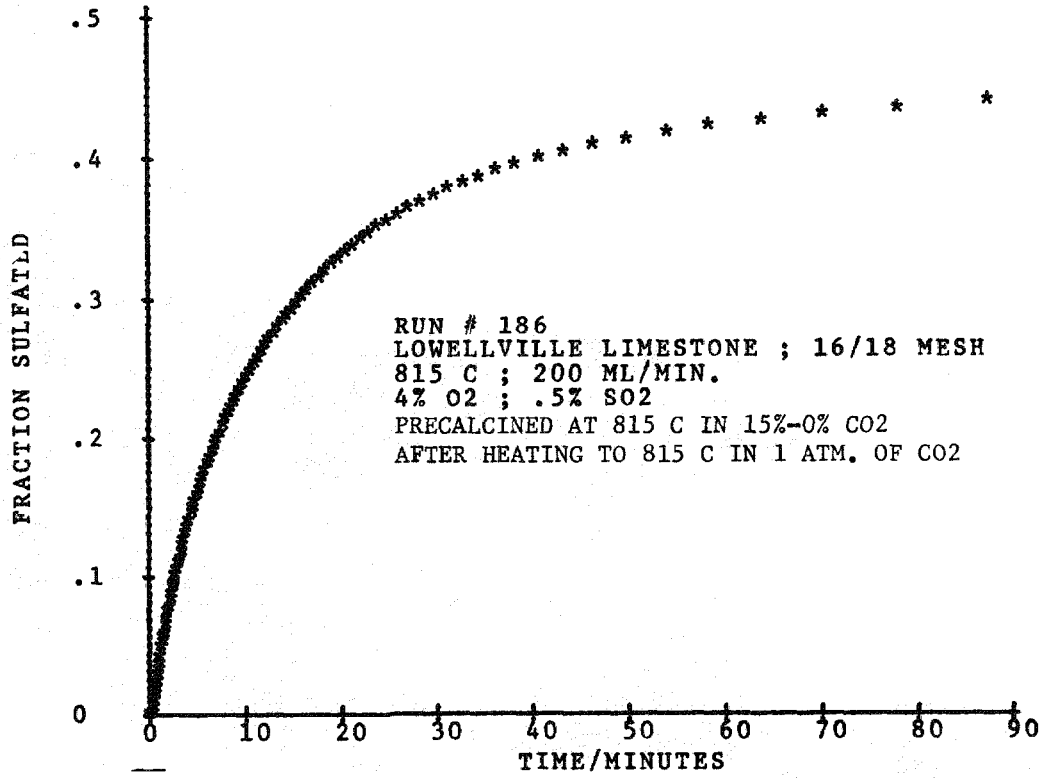

Figure A-2. Sample of Sulfation Data

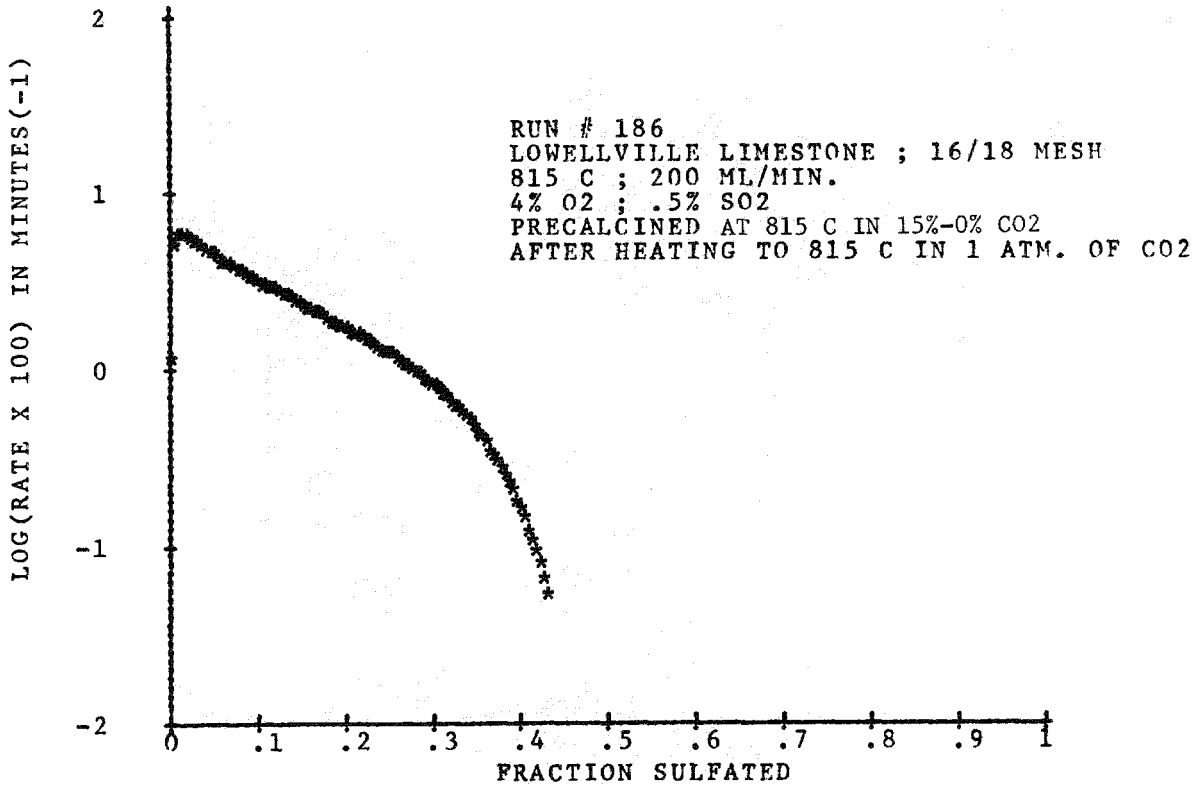

Figure A-3. Sample of Rate Data

Appendix 4

POROSITY DATA

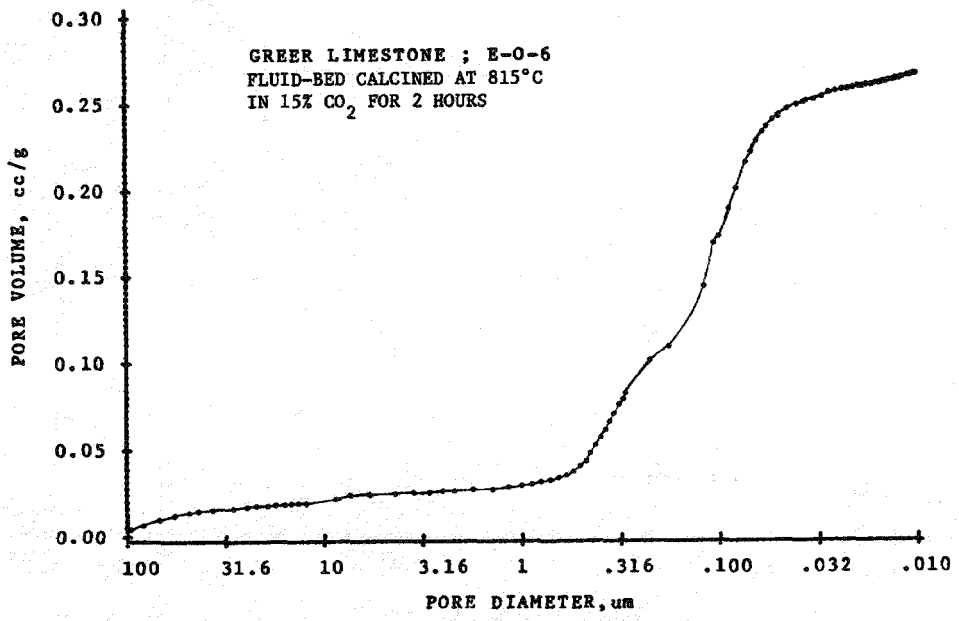

Figure A-4. Sample of Porosimetry Data

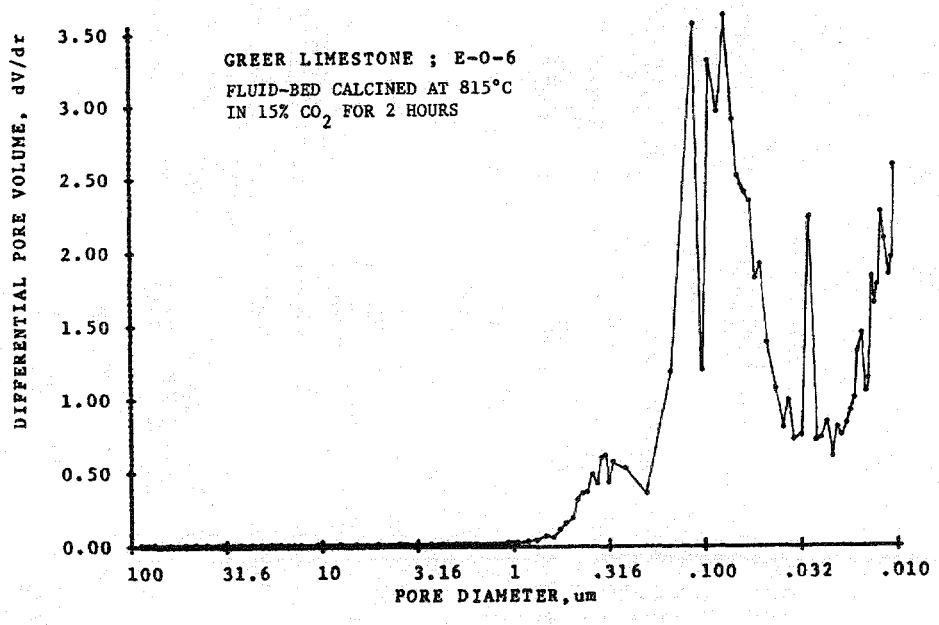

Figure A-5. Sample of Differential Pore Volume Distribution Data

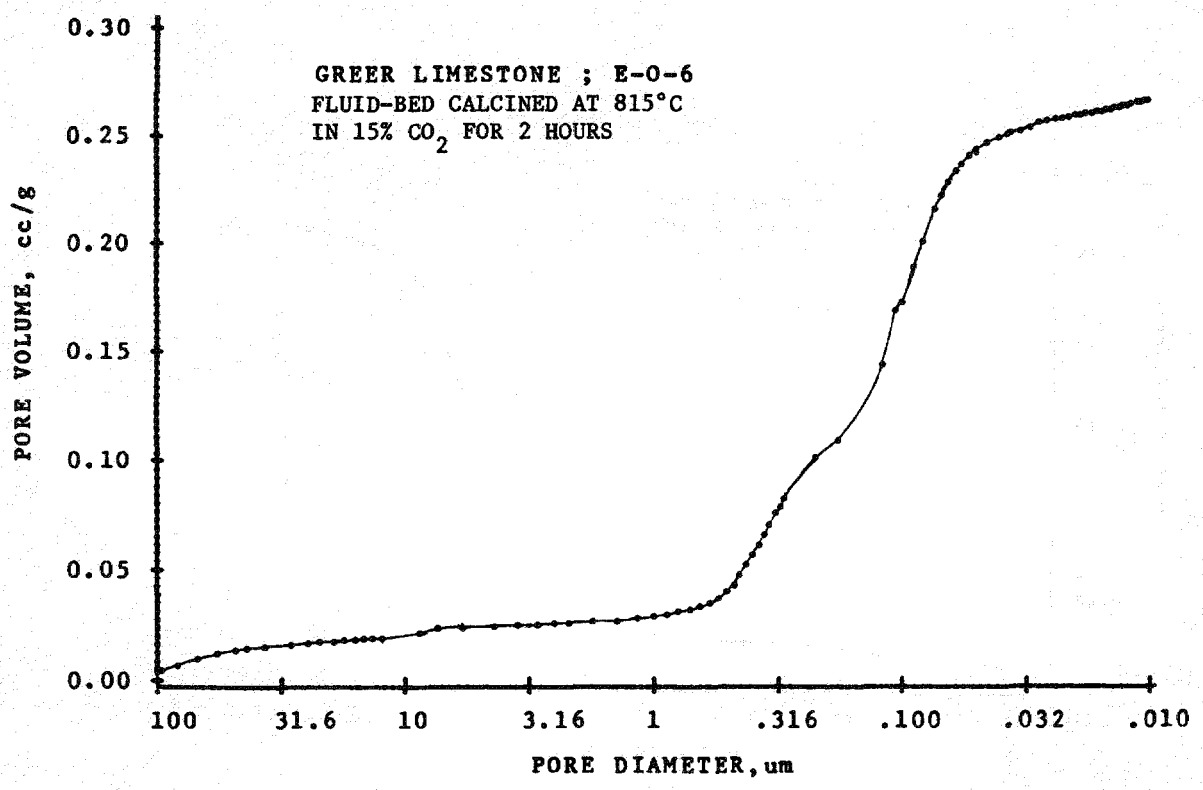

Figure A-4. Sample of Porosimetry Data

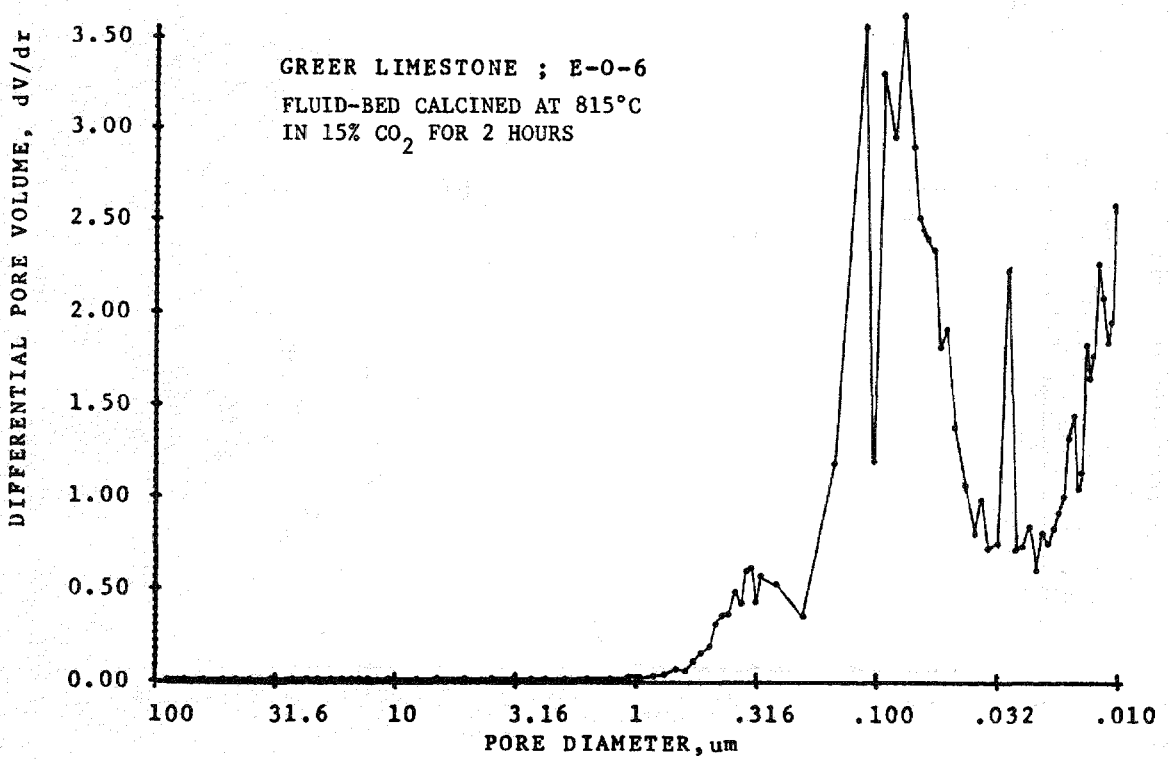

Figure A-5. Sample of Differential Pore Volume Distribution Data